SOYSOMES AND OTHER FUNCTIONAL BIOMATERIALS FROM SUCROSE SOYATE

DERIVATIVES

A Dissertation
Submitted to the Graduate Faculty
of the
North Dakota State University
of Agriculture and Applied Science

By

Ruvimbo Pearl Wright

In Partial Fulfillment of the Requirements
for the Degree of
DOCTOR OF PHILOSOPHY

Major Department:
Coatings and Polymeric Materials

July 2019

Fargo, North Dakota

North Dakota State University
Graduate School

Title

Soysomes and Other Functional Biomaterials from Sucrose Soyate
Derivatives

By

Ruvimbo Pearl Wright

The Supervisory Committee certifies that this ***disquisition*** complies with North Dakota

State University's regulations and meets the accepted standards for the degree of

DOCTOR OF PHILOSOPHY

SUPERVISORY COMMITTEE:

Dr. Mohiuddin A. Quadir

Chair

Dr. Dean C. Webster

Dr. Andriy Voronov

Dr. Mukund Sibi

Approved:

07/25/2019	Dr. Dean Webster
Date	Department Chair

ABSTRACT

Biomaterials serve as interventional tools in medicine to treat, improve or replace diseased tissues, organs or function of the body. Although several polymeric biomaterials already exist, they often present challenges, at material level, such as non-biodegradability, degradation into acidic by-products or tissue incompatibility, or at functional level such as failure to sustain prolonged release of therapeutic payload for a desired period. Research has been focused on investigating new polymeric candidates to address these problems of current systems. The use of renewable resources to generate smart polymers for biomedical and pharmaceutical purposes presents a new and exciting avenue for biomaterials. As part of these efforts, a new set of biomaterials were developed from plant-derived high molecular weight (~3.0 kDa) compounds. The advantages of biobased materials include availability for large-scale synthesis, facile post-synthetic modification, biocompatibility, improvement of functional properties and affordability. In this project we used sucrose soyates, i.e. octa-esters obtained from conjugation of sucrose molecules and multiple soybean oil fatty acid chains, to prepare three groups of functional biomaterials namely: a). self-assembled soy-based nano-constructs, b). blended soy-based free-standing films and c). Three-dimensional cross-linked soy-based soft matrices. Here, we will discuss the fabrication and physical, chemical and mechanical characterization of these biomaterials prepared from soy-based compounds, as well as, the assessment of their functional performance in biological environment.

ACKNOWLEDGEMENTS

unlimited access to your HPLC instrument, Janet Krom and Diana Kowalski thank you for always granting me access to your department's DLS instrument.

To my family and friends, none of this would be possible without your love, support and encouragement. To my mother, Sibusisiwe Chitemere, and siblings, Gari, Dolly and Flora, a special thank you for supporting and inspiring my best decisions.

To my husband, Richard Wright, thank you for being my best audience and pillar of strength.

Thanks, and praise to God for the strength to pull through.

My immense gratitude also goes to all the faculty, staff and students of Department of Coatings and Polymeric Materials who had shared their knowledge, experiences, time and friendship through my graduate studies.

DEDICATION

I dedicate this dissertation to my family and friends. Clarsen Mhuru, you always believed in me.

Gwinyai Dzimano, Janet Ostercamp, Dolly and Remi Oseni thank you for investing in my

education.

TABLE OF CONTENTS

LIST OF TABLES

LIST OF FIGURES

LIST OF ABBREVIATIONS

ACN ....Acetonitrile

ACT...Acetone

EtOH ....Ethanol

FA ....Fatty Acids

IPA ....Isopropyl Alcohol

LA ....Linoleic Acid

LNA ....Linolenic Acid

PA ....Palmitic Acid

AFM...Atomic Force Microscopy

ATR-IR ....Attenuated Total Reflectance-Infrared

BA..Butyric Acid

BLI...Kier Benzene-Likeliness Index

CA..Citric Acid

CAC ....Critical Aggregation Concentration

DA..Decanoic Acid

DCC ....N, N'-Dicyclohexylcarbodiimide

DLS...Dynamic Light Scattering

DMF...N′, N-Dimethylformamide

DMSO ....Dimethyl Sulfoxide

Dox...Doxorubicin Hydrochloride

DSC..Differential Scanning Calorimetry

EG ....Ethylene Glycol

ESS...Epoxidized Sucrose Soyate

HA..Sodium Hyaluronate

CHAPTER 1. GENERAL INTRODUCTION

Overview

Biomaterials are any substances synthetic or natural that used in contact with biological systems for treatment, augmentation, or replacement of any tissue, organ or function of the body.[1] Biomaterials can be metallic, ceramic, and polymeric in nature or in composite form. However, it is vital that these materials are biocompatible, i.e. able to function in the body in a safe and reliable manner with an appropriate host.[2-5] Areas of applications for biomaterials span a wide range from medical devices, implants and accessories, to medical equipment. Table 1.1 summarizes types of biomaterials and areas of application.

Table 1.1. Examples of Biomaterials and Applications

Biomaterials applications	Uses of Biomaterials	Types of biomaterials
Cardiovascular implants	Heart valves, stents, pacemakers vascular grafts	Polymers (such as polyamides, polyesters, polyurethanes, polyolefins)
Tissue engineering and Regenerative medicine	Heart, tissue constructs, bone grafts, skin grafts	
Orthopedics	Prosthetic knee, hip joint	
Extracorporeal applications	Dialyzers, plasmapheresis	Metals and their alloys (such as steel, titanium alloys, cobalt alloys)
Dental	Dental implants, orthodontic materials filling (restorative) materials, prostheses	Ceramics (such as zirconia, alumina)
Ophthalmological	Contact lenses, intraocular lenses	Composites
Neural implants	Cochlear implants	
Healthcare accessories	Catheters, gloves, glucose monitoring biosensors	
Drug Delivery Systems	Matrices, implants, coatings, transdermal patches	
Diagnostics	Cell culture substrates, blood protein assays	
Wound healing and General surgery	Sutures, bio-adhesives, blood substitutes stables, fracture fixtures, staples	

The biomaterial field is continually growing and estimated to reach a global market worth of USD 150 billion by 2021.[6] Polymeric biomaterials are an interesting subset; projected to contribute highest annual sales over upcoming years. However, there are challenges brought forth by the current polymers from which biomaterials are generated such as design complexity or complicated synthetic pathways, limited functionality, non -responsiveness to biological cues, slow or non-biodegradability, biocompatibility limitations and lack of affordability. Therefore, traction has grown toward investigating to new candidates that could yield new properties, form or enhanced function. Hence, plant-oil derivatives have emerged as prospective ideal candidates to generate biomaterials, as will be discussed in the following section.

Plant-oil Derivatives as New Platform for Biomaterials

The use of renewable resources has gained tremendous appeal in recent years due to the paradigm shift from reliance on finite petrochemical resource to exploring alternative, sustainable, bio-based feedstocks[7-11]. Particularly, plant-oils such as soy, linseed, palm, and sunflower oils, are an attractive resource to obtain chemical building blocks suitable to generate new materials amenable for use in biomedical and pharmaceutical. Plant-oil derivatives are obtainable via facile synthetic processes, have tunable properties, multi-functionality, versatility, inherent biodegradability and potential to improve performance properties of materials.[12, 13]

The main constituents of plant oils are triglycerides – esters of glycerol with three long-chain fatty acids (Figure 1.1). The fatty acids are the major component accounting for 95% of the total weight of the triglycerides and their compositions varies depending on the source of oil. [17-19] These oils serve as precursors for monomers used to generate a library of biobased macromolecules including polyurethanes, polyesters, polyethers and polyolefins. For example, polyglycerol sebacate derived from vegetable oil has found applications in soft tissue

2

engineering.[20-22] Polyester anhydrides obtained from sebacic and ricinoleic acid has been

successfully utilized as drug carriers for localized antitumor agent delivery.[23-27]
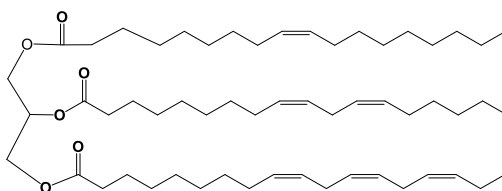
Figure 1.1. Generalized structure of plant oil triglyceride

Santin et al developed a new class of bioactive and biodegradable bone filler, for

reconstruction of bone defects from a powdered version of soybeans. This soy-based bone filler

showed reduced immunogenicity in comparison to conventional bone-fillers.[16] Soy proteins have

also been used to make thermosetting biomaterials ideal for short-term or temporary implants

due to adhesive and surface-active properties as well as ease of processability.[3] Miao et al have

extensively studied soybean oil derivatives such as acrylate resin obtained from epoxidized

soybean oil used to prepare scaffolds for supporting growing human bone marrow mesenchymal

stem cells (hMSCs); and also developed polyurethanes synthesized from polyol derived from

epoxidized soybean oil and lactic acid. [28,29] The functionalizability of these soy-derivatives is

limited to the three fatty acid chains of the soybean oil triglycerides. Using multifunctional

soybean oil derivatives such as sucrose soyates present as fascinating prospective candidates to

prepare new biomaterials.

Sucrose soyates, are a class of highly substituted sucrose esters of soybean oil fatty acids.

This class of macromolecules first gained popularity in developed by in the 1960s, marked by

commercialization of Olestra® from P&G [30, 31]. Olestra was a fat substitute, which quickly failed

on the market due unwanted side effects. Nonetheless, it was reported to be non-toxic to non-

rodent species even after long-term consumption, showing potential for other applications.[32, 33]

Later, P&G went on to introduce a new family of sucrose esters commercialized under brand

name SEFOSE from which can be further modified to introduce functionality.[34-36] Using in situ

peracid method an epoxidized version of sucrose soyate can be synthesized, epoxidized sucrose

soyate (ESS) and via alcoholysis, ring opening reaction, secondary hydroxyls can be created on

the fatty acid chains (Figure 1.2.). Methoxylated sucrose soyate polyol (MSSP) is obtained when

methanol is used for the ring opening reaction. These sucrose soyates comprise a statistical

mixture of fatty acids and have already been used in several applications such as plastics,

solvents, adhesives and lubricants[37-40]
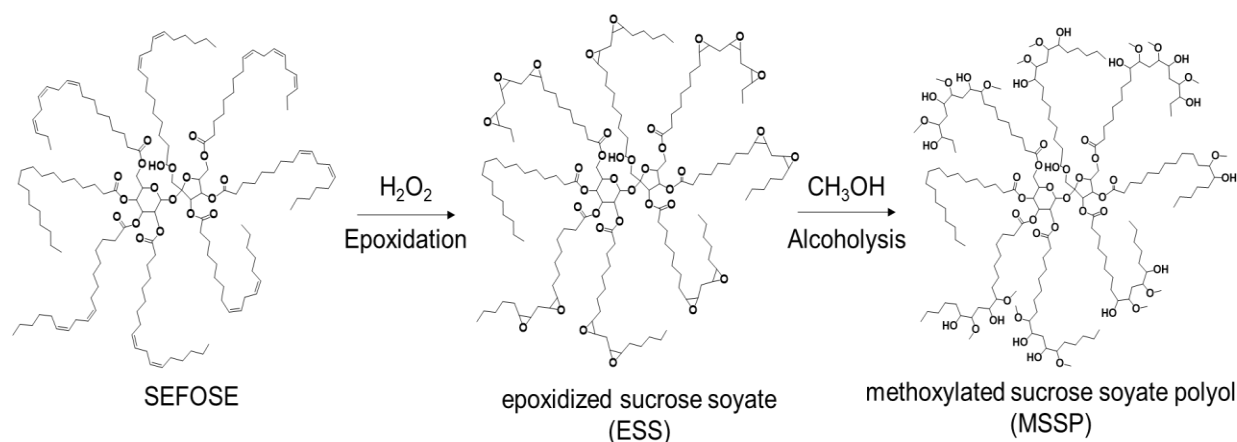
Figure 1.2. Schematic illustration of idealized structures of sucrose esters of soybean oil obtained from the subsequent functionalization of SEFOSE

Owing to their high functionality and biobased content, structural diversity, ease of

production, affordability, and commercial abundance, these soybean oil-derivatives offer the

promise of functional benefits for use as biomaterials. Additionally, these plant-oil derivatives

are inherently lipidic in nature hence offer the promise of increased compatibility and

solubilization of hydrophobic compounds which is most applicable in delivery applications.

Polymeric Biomaterials as Delivery Systems

Biomaterials technology breakthroughs have led to transformation in the method or

processes of administering pharmaceutical agents to achieve therapeutic effect. Traditional

routes of drug administration (oral and parenteral) can only effectively transport the active

payload in the form of a solution or emulsion. These methods cannot target specific site and

expose the cargo to degradation or rapid clearance from the body before achieving therapeutic

effect. Additionally, many of the potent and effective drugs developed for complex diseases such

as cancer tend to be hydrophobic and cannot be administered in a simple aqueous solution.

Hence limiting the route by which the drug may be delivered in order to achieve sufficient

bioavailability. Such challenges combined with the need for controlled and targeted drug

delivery as well as less solubility-restrictive system has driven research to develop many

innovative technologies.

There are several biomaterial platforms for drug delivery from nanoscale tools to

microscopic systems that have been developed such as nanoparticles, coatings, matrixes or

implants. A few examples will be discussed in the following subsections.

Nanostructured Polymeric Biomaterials

New horizons in nanomedicine, have placed polymeric biomaterials at the frontiers of

nanotechnology specialized in highly specific medical interventions at the molecular scale. Over

recent decades, the focus has been development of nanoscale drug delivery systems targeted at

cancer treatment.[41] The common goal within the nanomedicine research community is to design

these nanomaterials with specific particle size and surface properties in order to achieve

controlled or targeted release of active pharmaceutical agent.

In general, nanoparticles are ultra-dispersed supramolecular structures or solid particles

within the 10nm-1000nm size range. However, for usefulness in biological systems, size range

narrows to facilitate cell penetration and uptake, avoid renal clearance or avoid inciting

immunogenic response.[42-44] The loaded cargo can be dissolved, entrapped, encapsulated within

cavity surround by polymer or physically or chemically conjugated to the polymer matrix. Several types of nanostructured systems exist of various forms, sizes and shapes depending on their composition and method of synthesis. Examples of nanocarrier systems include dendritic polymers, polymer drug conjugates, polyplexes, polymeric micelles liposomes and other lipid-based systems. Polymers that have been studied for nanocarriers systems include poly (ethylene glycol)-*b*-poly (lactic-*co*-glycolic acid) (PEG -PLGA) [45-47], PEG-*b*-poly (aspartate) [48] and PEG-*b*-poly (propargyl L-glutamate[49]. Recently, nanoparticles prepared from plant proteins such as zein, animal proteins such as albumin and gelatin, and complex carbohydrates such as chitosan, and hyaluronic acids have been successfully used for designing drug nanocarriers.[50, 51] Drug delivery systems are enabling the repurposing of drugs with high potency yet limited solubility or toxicity to be efficiently delivered to targeted sites. Lipid-based nanoparticles show a lot of promise is this respect.

Lipid-based nanoparticles were developed to enhance dissolution, bioavailability and biodistribution of hydrophobic active therapeutic cargo. They are composed of lipids or their derivatives and are typically non-toxic. A wide array of lipid-based nanocarriers used in pharmaceutical formulations from liposomes to innovations such as solid lipid nanoparticles (SLN) nanostructured lipid carriers (NLC) (Figure 1.3.).
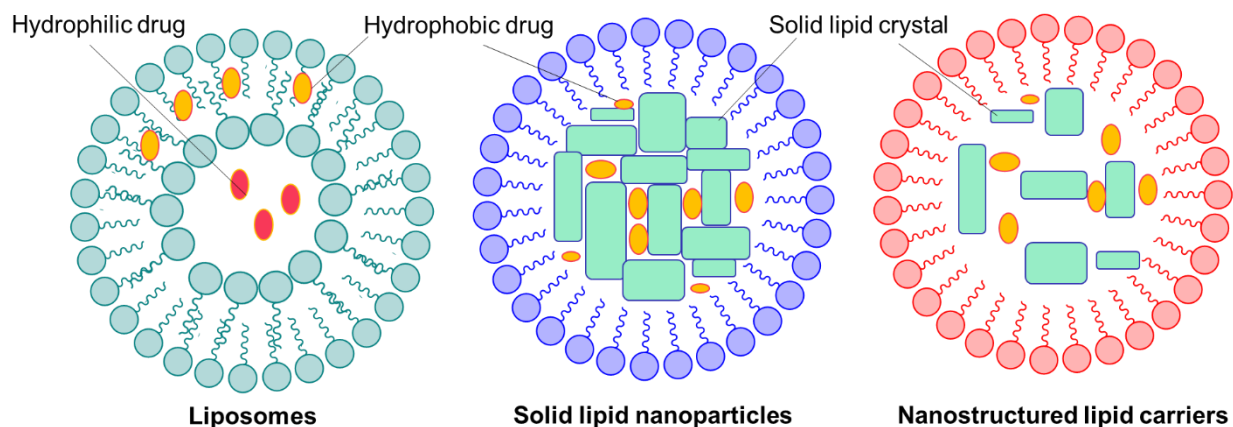
Figure 1.3. Different types of lipid-based nanocarriers. Liposomes formed from phospholipids, solid lipid nanoparticles composed of mixture of solid lipids in the core and nanostructured lipid carriers composed of a mixture of solid and liquid lipids

Liposomes are spherical vesicles composed of one or more natural or synthetic phospholipid bilayers, which were first described by Bangham et al.[52, 53] The lipid bilayers self-assemble in a fashion that can harbor lipophilic drugs within the lipid bilayers while encapsulating hydrophilic guest molecules in the inner aqueous core. The diameter of the lipid vesicles may vary between about 20 nm and a few micrometers depending on method of preparation and number of bilayers. Chemical modifications including PEGylation or incorporation of additives can render the liposomes more sterically stable or reduce uptake rate allowing for more controlled drug release.[54-56]Additionally liposomes have been reported to not only increase solubility of poorly-water soluble drugs, protect drugs from degradation but also reduce toxicity and side effects. However, several limitations remain like low encapsulation efficiency, rapid 'burst' release or leakage of drug, poor long-term storage stability and difficulties in scaling up.[57-60]

Advances research in lipid-based systems led to the emergence of SLN and NLC. These innovative nanocarrier systems were designed to be physical stability, shield loaded drugs from degradation, eliminate manufacture and design complexity, introduce affordable formulation

materials, reduce systemic toxicity, offer controlled and targeted release and have the capacity to solubilize and transport both hydrophobic and hydrophilic active payload. [61-67] SLN are solid particles prepared from functional lipids and stabilized by surfactants. SLN are typically formulated with highly purified triglycerides, fatty acids, complex glyceride mixtures or even waxes which serve as the primary carrier component.[65, 67]

NLC are a matrix-type nanocarrier system composed of mixture of multiple solid and lipids. This gives them the added advantage of higher active loading due to increased solvency from the liquid component. Additionally, modulation of the liquid component allows for customized release pattern.[67, 68] Covalent conjugation of drug to the lipids is sometimes used to achieve even higher drug loading, reported to reach over 30%.[62, 63]

Functional lipids have long played a major role in pharmaceutical formulations as excipients, solubility enhancers, and processing aids. They remain relevant area of interest for development of innovative drug delivery platforms aimed at continually improving drug solubility, bioavailability and biodistribution not only at nanoscale but also at larger scale.

Coating Systems/Film-based Biomaterials

Polymeric films have been investigated for use as drug delivery vehicles. Polymeric films are particularly appealing for application requiring a flexible, drug-eluting material. [70, 71] For example for buccal drug delivery, films offer benefits such as controlled release and extended residence time of the released payload by reducing the rate at which the cargo is washed away by saliva. [72] The basic criteria for such films are biocompatibility, flexibility and comfort. Swelling characteristics of the films should be limited while bio-adhesive strength should be adequate to retain film in the oral cavity for targeted duration.

Free-films are attractive as flexible, implantable applications such as post-surgical care, where localized delivery is necessary in order to sufficiently treat the affected area, minimize risk of infection or recurrence.[72, 73] Advances in cancer research have investigated use of polymer films to deliver anti-cancer therapeutics. Films composed of a waxy, hydrophobic polymer, poly (glycerol monostearate-co-ε-caprolactone) were reported to prolong release, improved drug stability, and reduce the systemic toxicity of anti-cancer drugs, such as paclitaxel (PTX) and hydroxycamptothecin.[72, 74, 75]

Lipidic films or coatings systems offer other advantages as well such as structural stability and improving biocompatibility.[76] Lipidic materials show a lot of promise as flexible drug-eluting platform; however, when longer, extended release is required a larger depot type system is ideal.

Three-dimensional Delivery Systems

3D-polymeric biomaterials have had heavy presence in regenerative medicine tissue engineering and drug delivery applications, as well.[77-82] These materials are employed, ideally, for localized drug delivery but can also be used for systemic delivery. As depot-type formulations, they function as slow release systems, maintaining a high local concentration of the payload in the surrounding environment over an extended period. These extended release dosage forms increase the lifetime of an active formulation and reduce fluctuations in bioavailable concentrations. These systems are implantable; therefore, they also eliminate reliance on patient compliance to maintain required dosage frequency.

Polymer matrices are composed hydrophilic or hydrophobic polymers matrix and drug are mixed into the formulation. The capacity of the matrix to swell or the erosion of polymer network and diffusion of the cargo controls release of the cargo. Most of them are based on

alginates, chitosan, cellulose derivatives (hydroxyethyl cellulose and hydroxypropyl methylcellulose), and cross-linked homopolymer and co-polymers of acrylic acid.[83-89]

On the other hand, hydrophobic matrixes are prepared from water insoluble materials such as lipids, waxes, or fatty acids such as Carnauba wax, beeswax, micro crystalline wax, candelilla wax, and paraffin waxes.[90-96] They are engaged to achieve sustained release due to the increased retardation in rate of diffusion of encapsulated cargo out of the polymer network. They are based on natural materials; therefore, are highly affordable and environmentally-friendly material candidates to generate controlled-release platforms.

A lot of attention has been paid to lipid-based matrixes due to the promise of superior performance. Advantages of these systems include the ability to load and release both hydrophilic and hydrophobic compounds, biocompatibility, lower immunogenicity, improved stability of the drug, degradation to biocompatible end-products unlike many synthetic polymers[97, 98]. Characteristics of the matrix influence the loading and release kinetics i.e. porosity of the structure, dissolution properties, polymer erosion, and diffusion characteristics. Loading is achieved in various ways, dispersing or dissolving drug within a rate-controlling polymer matrix (monolithic), enclosed drug within polymer coatings (drug reservoir) or synthesizing polymer-drug conjugates in matrix form. Release may be erosion-controlled, diffusion controlled, or a combination thereof, as depicted in Figure 1.4.
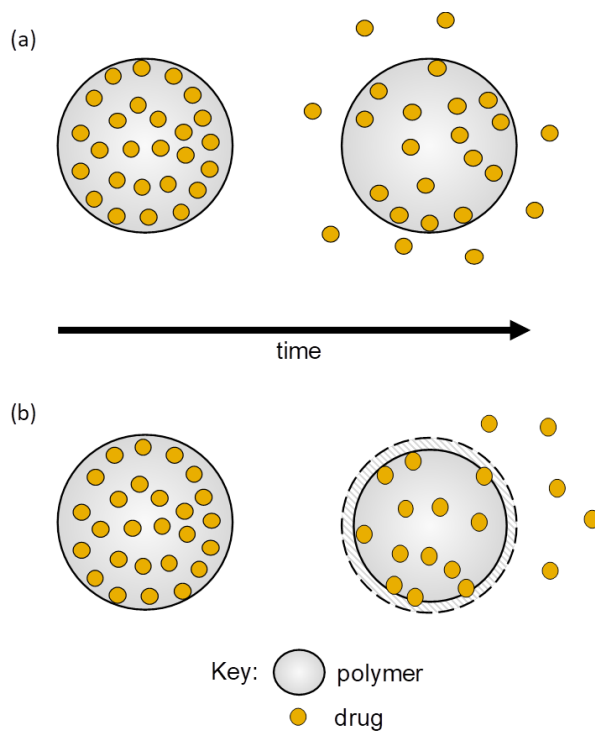
Figure 1.4. Illustration of two possible mechanisms of drug release from polymer matrix over time (a). Diffusion-controlled release and (b). Erosion-controlled release

The matrices are prepared from solid or liquid lipids or related materials such as fatty acids and triglycerides. Many of the currently FDA-approved hydrophobic matrix-formers such as beeswax, carnauba wax, and phospholipids, possess complex chemical structures and exhibit batch-to-batch variations depending on the source and method of extraction. A new avenue of pursuit is semi-synthetic bio-based lipid-like materials, which offer the benefit of batch-to-batch uniformity, affordability, biodegradability, low toxicity, accessibility, and facile preparation. Particular interest is growing directed at plant oil derivatives as viable source for chemicals amenable to prepare various biomaterials including polymer-drug matrixes.[7, 8, 99].

Limitation of Current Polymeric Biomaterials

Currently, most polymeric biomaterials are generated from either synthetic or naturally occurring polymers. Synthetic polymers are typically designed to offer durability. Examples include poly(ethylene glycol) (PEG), poly (methylmethacrylate), poly(lactic-co-glycolic) acid

(PLGA), PLA and poly (ε-caprolactone) (PCL).[46, 47, 100-111] On the other hand, natural polymers are attractive due to their structure, morphology and chemistry that can be easily manipulated to substitute or mimic biological systems.[112-115] Some of the commonly used natural polymers include cellulose, chitin, collagen, gelatin, fibrin.

These polymers are already influencing medicine and have been successfully translated into clinical use. However, they have several limitations as discussed below:

- High cost or unaffordability. Only a few polymer candidates have FDA approval for use resulting in higher cost to synthesize the polymer and manufacture the biomaterials. Most of these conventional polymers have mono-functionality, which limits versatility or potential applications.

- Design and synthetic complexity. Many of the current polymers are mono-functional, which limits versatility and potential applications. Complex synthetic pathways are often required to prepare the target polymers, leading to extensive purification processes, poor reproducibility

- Low biodegradation. Many synthetic polymers are either non-or low-degrading. Those that biodegrade often require special condition to degrade or degrade into toxic materials such as acidic by-products from PLA or PLGA.

- Low biocompatibility. Non-responsiveness toward biological cues or invoking an undesirable immune response limits biocompatibility. The immune system constantly surveilles for any potentially harmful exogenous materials and upon detection of foreign substance attacks as a quick defense. For effective performance, polymeric biomaterials should be able to bypass this system. Though deemed, as biocompatible petrochemical

derived polymers are not always easily metabolically cleared from the body, which can trigger health complications.

- Requirement of safe-by-design approach. The polymer candidates need to be safe to humans. The FDA provides a database of materials classified as GRAS (generally regarded as safe) which can be used as candidates for the formation of biomaterials. This limits the library of useable polymers and can also drive up the cost of current systems.

- Functional limitations. For example, low solubilization and transport of therapeutic agents. In recent years, pharmaceutical research community has intensely focused on repurposing and combining potent yet toxic drug candidates for cancer treatment. Many of these drug candidates have limited solubility and stability; therefore, increased encapsulation efficiency is required. However, many of the current polymer candidates exhibit poor loading, are unable to sustain release over prolonged periods, nor can they enhance stability of drug.

- Batch-to-batch variation and unreliability. Biopolymers or natural polymers are a seemingly attractive sustainable resource for generating biomaterials due to their potential to substitute or mimic biological systems. However, biopolymers are often complex, heterogeneous and present batch-to-batch variability.

All these problems can culminate in failed performance of biomaterial or undesirable side effects. Therefore, there is a need for the introduction of better performing and safer biomaterials. Hence, the emergence of plant-derived building blocks as an abundant, renewable feedstock for starting materials to synthesize customizable molecules amenable for biomedical applications.

Research Scope

As representative biobased macromolecules, sucrose soyate derivatives have been extensively studied as a new platform for developing functional materials amenable for biomedical and pharmaceutical applications. Such Biobased feedstock have been mainly applied to coatings applications and little attention has been focused on studying their potential as biomaterials. This current work aims at formulating, designing and characterizing functional biomaterials prepared from ESS and MSSP.

Sucrose soyates offer versatility due to multivalent functionality. Tunability and ease of synthesis of these biobased large molecules allows for modification introducing functionality, which diversifies the range of applications. The hydroxyls present in MSSP or epoxy groups in ESS enable cross-linking capacity and potential for self-assembly behavior. The biomaterials were designed to investigate properties from mesoscale to nanoscale (Figure 1.5.).

MSSP is expected to self-assemble into nanoparticles due to solvent shifting enabling development of a new biobased nanocarrier system. The versatility of these sucrose soyates, allows incorporating of MSSP in formulation of flexible, cargo-eluting thermoplastic composite films. Finally, the epoxy groups in ESS are cross-linked to development of 3D lipid-based matrix useful for molecular transport.
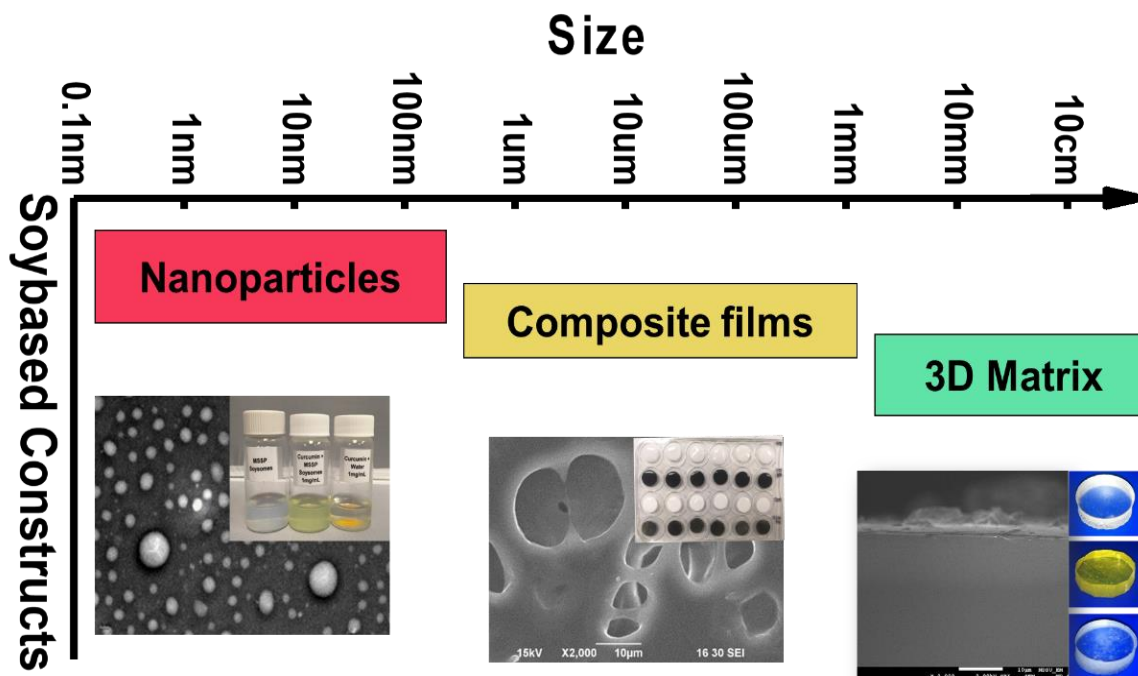
Figure 1.5. Examples of soy-based biomaterials prepared from epoxidized sucrose soyate (ESS) and methoxylated sucrose soyate polyol (MSSP)

References

1.   Williams, D. F., The Williams dictionary of biomaterials. Liverpool University Press: 1999.

2.   Peppas, N. A.; Langer, R., New challenges in biomaterials. Science 1994, 263 (5154), 1715-1720.

3.   Raquez, J.-M.; Deléglise, M.; Lacrampe, M.-F.; Krawczak, P., Thermosetting (bio) materials derived from renewable resources: a critical review. Prog. Polym. Sci. 2010, 35 (4), 487-509.

4.   Ratner, B. D.; Hoffman, A. S.; Schoen, F. J.; Lemons, J. E., Biomaterials science: an introduction to materials in medicine. 2nd ed.; Academic press: 2004.

5.   Nair, L. S.; Laurencin, C. T., Biodegradable polymers as biomaterials. Prog. Polym. Sci. 2007, 32 (8-9), 762-798.

6.	Biomaterials Market by Type of Materials (Metallic, Ceramic, Polymers, Natural) & Application (Cardiovascular, Orthopedic, Dental, Plastic Surgery, Wound Healing, Neurology, Tissue Engineering, Ophthalmology) - Global Forecast to 2021. https://www.marketsandmarkets.com/Market-Reports/biomaterials-393.html.

7.	Zhang, C.; Garrison, T. F.; Madbouly, S. A.; Kessler, M. R., Recent Advances in Vegetable Oil-Based Polymers and Their Composites. Prog. Polym. Sci. 2017.

8.	Miao, S.; Wang, P.; Su, Z.; Zhang, S., Vegetable-oil-based polymers as future polymeric biomaterials. Acta Biomater. 2014, 10 (4), 1692-1704.

9.	Alam, M.; Akram, D.; Sharmin, E.; Zafar, F.; Ahmad, S., Vegetable oil based eco-friendly coating materials: A review article. Arabian J. Chem. 2014, 7 (4), 469-479.

10.	Lligadas, G.; Ronda, J. C.; Galia, M.; Cádiz, V., Plant oils as platform chemicals for polyurethane synthesis: current state-of-the-art. Biomacromolecules 2010, 11 (11), 2825-2835.

11.	Alagi, P.; Ghorpade, R.; Jang, J. H.; Patil, C.; Jirimali, H.; Gite, V.; Hong, S. C., Functional soybean oil-based polyols as sustainable feedstocks for polyurethane coatings. Ind. Crops Prod. 2018, 113, 249-258.

12.	Lligadas, G.; Ronda, J. C.; Galià, M.; Cádiz, V., Poly (ether urethane) networks from renewable resources as candidate biomaterials: synthesis and characterization. Biomacromolecules 2007, 8 (2), 686-692.

13.	Lamba, N. K., Polyurethanes in biomedical applications. Routledge: 2017.

14.	Lasprilla, A. J.; Martinez, G. A.; Lunelli, B. H.; Jardini, A. L.; Maciel Filho, R., Poly-lactic acid synthesis for application in biomedical devices—A review. Biotechnol. Adv. 2012, 30 (1), 321-328.

15.   Gupta, B.; Revagade, N.; Hilborn, J., Poly (lactic acid) fiber: An overview. Prog. Polym. Sci. 2007, 32 (4), 455-482.

16.   Santin, M.; Morris, C.; Standen, G.; Nicolais, L.; Ambrosio, L., A new class of bioactive and biodegradable soybean-based bone fillers. Biomacromolecules 2007, 8 (9), 2706-2711.

17.   Meier, M. A.; Metzger, J. O.; Schubert, U. S., Plant oil renewable resources as green alternatives in polymer science. Chem. Soc. Rev. 2007, 36 (11), 1788-1802.

18.   Güner, F. S.; Yağcı, Y.; Erciyes, A. T., Polymers from triglyceride oils. Prog. Polym. Sci. 2006, 31 (7), 633-670.

19.   Lligadas, G.; Ronda, J. C.; Galia, M.; Cadiz, V., Renewable polymeric materials from vegetable oils: a perspective. Mater. Today 2013, 16 (9), 337-343.

20.   Motlagh, D.; Yang, J.; Lui, K. Y.; Webb, A. R.; Ameer, G. A., Hemocompatibility evaluation of poly (glycerol-sebacate) in vitro for vascular tissue engineering. Biomaterials 2006, 27 (24), 4315-4324.

21.   Redenti, S.; Neeley, W. L.; Rompani, S.; Saigal, S.; Yang, J.; Klassen, H.; Langer, R.; Young, M. J., Engineering retinal progenitor cell and scrollable poly (glycerol-sebacate) composites for expansion and subretinal transplantation. Biomaterials 2009, 30 (20), 3405-3414.

22.   Sundback, C. A.; Shyu, J. Y.; Wang, Y.; Faquin, W. C.; Langer, R. S.; Vacanti, J. P.; Hadlock, T. A., Biocompatibility analysis of poly (glycerol sebacate) as a nerve guide material. Biomaterials 2005, 26 (27), 5454-5464.

23. Shikanov, A.; Shikanov, S.; Vaisman, B.; Golenser, J.; Domb, A. J., Paclitaxel tumor biodistribution and efficacy after intratumoral injection of a biodegradable extended release implant. Int. J. Pharm. 2008, 358 (1-2), 114-120.

24. Teomim, D.; Domb, A. J., Fatty acid terminated polyanhydrides. J. Polym. Sci., Part A: Polym. Chem. 1999, 37 (16), 3337-3344.

25. Teomim, D.; Domb, A. J., Nonlinear fatty acid terminated polyanhydrides. Biomacromolecules 2001, 2 (1), 37-44.

26. Shikanov, S.; Shikanov, A.; Gofrit, O.; Nyska, A.; Corn, B.; Domb, A. J., Intratumoral Delivery of Paclitaxel for Treatment of Orthotopic Prostate Cancer. J. Pharm. Sci. 2009, 98 (3), 1005-1014.

27. Krasko, M. Y.; Golenser, J.; Nyska, A.; Nyska, M.; Brin, Y. S.; Domb, A. J., Gentamicin extended release from an injectable polymeric implant. J. Controlled Release 2007, 117 (1), 90-96.

28. Miao, S.; Zhu, W.; Castro, N. J.; Nowicki, M.; Zhou, X.; Cui, H.; Fisher, J. P.; Zhang, L. G., Sci. Rep. 2016, 6, 27226.

29. Miao, S.; Zhang, S.; Su, Z.; Wang, P., Journal of Polymer Science Part A: Polymer Chemistry 2010, 48 (1), 243-250.

30. Eckey, E. W.; Alderson, R. O., Plastic glyceride fat and process for preparing it. Google Patents: 1963.

31. Myhre, D. V., Process for the preparation of fatty acid esters of sugar glycosides. Google Patents: 1971.

32. Miller, K.; Wood, F.; Stuard, S.; Alden, C., A 20-month olestra feeding study in dogs. Food and chemical toxicology 1991, 29 (7), 427-435.

33. Rogers, S. A., No More Heartburn: Stop the Pain in 30 Days--Naturally!: The Safe, Effective Way to Prevent and Heal Chronic Gastrointestinal Disorders. Kensington Books: 2000.

34. Carter, J. D.; Burt, E. M., Hair Care Composition Comprising Metathesized Unsaturated Polyol Esters. Google Patents: 2013.

35. Pan, X.; Sengupta, P.; Webster, D. C., Novel biobased epoxy compounds: epoxidized sucrose esters of fatty acids. Green Chem. 2011, 13 (4), 965-975.

36. Pan, X.; Webster, D. C., New biobased high functionality polyols and their use in polyurethane coatings. ChemSusChem 2012, 5 (2), 419-429.

37. Nelson, T. J.; Bultema, L.; Eidenschink, N.; Webster, D. C., Bio-based high functionality polyols and their use in 1K polyurethane coatings. J. Renewable Mater. 2013, 1 (2), 141-153.

38. Guo, A.; Demydov, D.; Zhang, W.; Petrovic, Z. S., Polyols and polyurethanes from hydroformylation of soybean oil. J. Polym. Environ. 2002, 10 (1), 49-52.

39. Kumari, A.; Yadav, S. K.; Yadav, S. C., Biodegradable polymeric nanoparticles based drug delivery systems. Colloids Surf., B 2010, 75 (1), 1-18.

40. Guo, B.; Chen, Y.; Lei, Y.; Zhang, L.; Zhou, W. Y.; Rabie, A. B. M.; Zhao, J., Biobased poly (propylene sebacate) as shape memory polymer with tunable switching temperature for potential biomedical applications. Biomacromolecules 2011, 12 (4), 1312-1321.

41. Mohanty, A.; Misra, M.; Drzal, L., Sustainable bio-composites from renewable resources: opportunities and challenges in the green materials world. J. Polym. Environ. 2002, 10 (1), 19-26.

42. Hammond, P. T., Nano tools pave the way to new solutions in infectious disease. ACS Infect. Dis. 2017, 3 (8), 554-558

43. Davis, M. E.; Chen, Z.; Shin, D. M., Nanoparticle therapeutics: an emerging treatment modality for cancer. In Nanoscience And Technology: A Collection of Reviews from Nature Journals, World Scientific: 2010; pp 239-250.

44. Mohanraj, V.; Chen, Y., Nanoparticles-a review. Trop. J. Pharm. Res. 2006, 5 (1), 561-573.

45. Couvreur, P., Nanoparticles in drug delivery: past, present and future. Adv. Drug Delivery Rev. 2013, 65 (1), 21-23.

46. Farokhzad, O. C.; Jon, S.; Khademhosseini, A.; Tran, T.-N. T.; LaVan, D. A.; Langer, R., Nanoparticle-aptamer bioconjugates. Cancer Res 2004, 64 (21), 7668-7672.

47. Farokhzad, O. C.; Cheng, J.; Teply, B. A.; Sherifi, I.; Jon, S.; Kantoff, P. W.; Richie, J. P.; Langer, R., Targeted nanoparticle-aptamer bioconjugates for cancer chemotherapy in vivo. Proc. Natl. Acad. Sci. U. S. A. 2006, 103 (16), 6315-6320.

48. Cheng, J.; Teply, B. A.; Sherifi, I.; Sung, J.; Luther, G.; Gu, F. X.; Levy-Nissenbaum, E.; Radovic-Moreno, A. F.; Langer, R.; Farokhzad, O. C., Formulation of functionalized PLGA–PEG nanoparticles for in vivo targeted drug delivery. Biomaterials 2007, 28 (5), 869-876.

49. Nakanishi, T.; Fukushima, S.; Okamoto, K.; Suzuki, M.; Matsumura, Y.; Yokoyama, M.; Okano, T.; Sakurai, Y.; Kataoka, K., Development of the polymer micelle carrier system for doxorubicin. J. Controlled Release 2001, 74 (1-3), 295-302.

50. Zhao, X.; Poon, Z.; Engler, A. C.; Bonner, D. K.; Hammond, P. T., Enhanced stability of polymeric micelles based on postfunctionalized poly (ethylene glycol)-b-poly (γ-

propargyl L-glutamate): the substituent effect. Biomacromolecules 2012, 13 (5), 1315-1322.

51.   Weissmueller, N. T.; Lu, H. D.; Hurley, A.; Prud'homme, R. K., Nanocarriers from GRAS zein proteins to encapsulate hydrophobic actives. Biomacromolecules 2016, 17 (11), 3828-3837.

52.   Anitha, A.; Deepagan, V.; Rani, V. D.; Menon, D.; Nair, S.; Jayakumar, R., Preparation, characterization, in vitro drug release and biological studies of curcumin loaded dextran sulphate–chitosan nanoparticles. Carbohydr. Polym. 2011, 84 (3), 1158-1164.

53.   Bangham, A. D.; Horne, R., Negative staining of phospholipids and their structural modification by surface-active agents as observed in the electron microscope. J. Mol. Biol. 1964, 8 (5), 660-IN10.

54.   Antonietti, M.; Förster, S., Vesicles and liposomes: a self-assembly principle beyond lipids. Adv. Mater. 2003, 15 (16), 1323-1333.

55.   Martins, S.; Sarmento, B.; Ferreira, D. C.; Souto, E. B., Lipid-based colloidal carriers for peptide and protein delivery–liposomes versus lipid nanoparticles. Int. J. Nanomed. 2007, 2 (4), 595.

55.   Gabizon, A.; Catane, R.; Uziely, B.; Kaufman, B.; Safra, T.; Cohen, R.; Martin, F.; Huang, A.; Barenholz, Y., Prolonged circulation time and enhanced accumulation in malignant exudates of doxorubicin encapsulated in polyethylene-glycol coated liposomes. Cancer Res 1994, 54 (4), 987-992.

56.   Chuang, S.-Y.; Lin, C.-H.; Huang, T.-H.; Fang, J.-Y., Lipid-based nanoparticles as a potential delivery approach in the treatment of rheumatoid arthritis. Nanomaterials 2018, 8 (1), 42.

57.   Sharma, A.; Sharma, U. S., Liposomes in drug delivery: progress and limitations. Int. J. Pharm. 1997, 154 (2), 123-140.

58.   Lian, T.; Ho, R. J., Trends and developments in liposome drug delivery systems. J. Pharm. Sci. 2001, 90 (6), 667-680.

59.   Gregoriadis, G., Engineering liposomes for drug delivery: progress and problems. Trends Biotechnol. 1995, 13 (12), 527-537.

60.   Čerpnjak, K.; Zvonar, A.; Gašperlin, M.; Vrečer, F., Lipid-based systems as a promising approach for enhancing the bioavailability of poorly water-soluble drugs. Acta Pharm. 2013, 63 (4), 427-445.

61.   Müller, R. H.; Radtke, M.; Wissing, S. A., Solid lipid nanoparticles (SLN) and nanostructured lipid carriers (NLC) in cosmetic and dermatological preparations. Adv. Drug Delivery Rev. 2002, 54, S131-S155.

62.   Olbrich, C.; Gessner, A.; Kayser, O.; Müller, R. H., Lipid-drug-conjugate (LDC) nanoparticles as novel carrier system for the hydrophilic antitrypanosomal drug diminazenediaceturate. J. Drug Targeting 2002, 10 (5), 387-396.

63.   Olbrich, C.; Gessner, A.; Schröder, W.; Kayser, O.; Müller, R. H., Lipid–drug conjugate nanoparticles of the hydrophilic drug diminazene—cytotoxicity testing and mouse serum adsorption. J. Controlled Release 2004, 96 (3), 425-435.

64. Heiati, H.; Phillips, N. C.; Tawashi, R., Evidence for phospholipid bilayer formation in solid lipid nanoparticles formulated with phospholipid and triglyceride. Pharm. Res. 1996, 13 (9), 1406-1410.

65. Bunjes, H.; Westesen, K.; Koch, M. H., Crystallization tendency and polymorphic transitions in triglyceride nanoparticles. Int. J. Pharm. 1996, 129 (1-2), 159-173.

66. Schwarz, C.; Mehnert, W.; Lucks, J.; Müller, R., Solid lipid nanoparticles (SLN) for controlled drug delivery. I. Production, characterization and sterilization. J. Controlled Release 1994, 30 (1), 83-96.

67. Wissing, S.; Kayser, O.; Müller, R., Solid lipid nanoparticles for parenteral drug delivery. Adv. Drug Delivery Rev. 2004, 56 (9), 1257-1272.

68. Tillotson, J., K, Lipid-Based Delivery – Advanced Lipid-Based Drug Delivery Systems: Solid Lipid Nanoparticles & Nanostructured Lipid Carriers. Drug Dev. Delivery 2018.

69. Tiwari, R.; Pathak, K., Nanostructured lipid carrier versus solid lipid nanoparticles of simvastatin: comparative analysis of characteristics, pharmacokinetics and tissue uptake. Int. J. Pharm. 2011, 415 (1-2), 232-243.

70. Peh, K. K.; Wong, C. F., Polymeric films as vehicle for buccal delivery: swelling, mechanical, and bio-adhesive properties. J Pharm Pharm Sci 1999, 2 (2), 53-61.

71. Wolinsky, J. B.; Colson, Y. L.; Grinstaff, M. W., Local drug delivery strategies for cancer treatment: gels, nanoparticles, polymeric films, rods, and wafers. J. Controlled Release 2012, 159 (1), 14-26.

72. Liu, R.; Wolinsky, J. B.; Walpole, J.; Southard, E.; Chirieac, L. R.; Grinstaff, M. W.; Colson, Y. L., Prevention of local tumor recurrence following surgery using low-dose chemotherapeutic polymer films. Ann Surg Oncol. 2010, 17 (4), 1203-1213.

73.   Luo, Y.; Kirker, K. R.; Prestwich, G. D., Cross-linked hyaluronic acid hydrogel films: new biomaterials for drug delivery. J. Controlled Release 2000, 69 (1), 169-184.

74.   Wolinsky, J. B.; Liu, R.; Walpole, J.; Chirieac, L. R.; Colson, Y. L.; Grinstaff, M. W., Prevention of in vivo lung tumor growth by prolonged local delivery of hydroxycamptothecin using poly (ester-carbonate)-collagen composites. J. Controlled Release 2010, 144 (3), 280-287.

75.   Hartmann, J. T.; Lipp, H.-P., Camptothecin and podophyllotoxin derivatives. Drug Safety 2006, 29 (3), 209-230.

76.   Westedt, U.; Wittmar, M.; Hellwig, M.; Hanefeld, P.; Greiner, A.; Schaper, A. K.; Kissel, T., Paclitaxel releasing films consisting of poly (vinyl alcohol)-graft-poly (lactide-co-glycolide) and their potential as biodegradable stent coatings. J. Controlled Release 2006, 111 (1-2), 235-246.

77.   Lee, K. Y.; Mooney, D. J., Hydrogels for tissue engineering. Chem. Rev. 2001, 101 (7), 1869-1880.

78.   Thomson, R. C.; Wake, M. C.; Yaszemski, M. J.; Mikos, A. G., Biodegradable polymer scaffolds to regenerate organs. Biopolymers Ii 1995, 122, 245-274.

79.   Seliktar, D.; Dikovsky, D.; Napadensky, E., Bioprinting and Tissue Engineering: Recent Advances and Future Perspectives. Isr. J. Chem. 2013, 53 (9-10), 795-804.

80.   Do, A. V.; Khorsand, B.; Geary, S. M.; Salem, A. K., 3D Printing of Scaffolds for Tissue Regeneration Applications. Adv. Healthcare Mater. 2015, 4 (12), 1742-1762.

81.   Liu, X.; Ma, P. X., Polymeric scaffolds for bone tissue engineering. Ann. Biomed. Eng. 2004, 32 (3), 477-486.

82. Rezwan, K.; Chen, Q.; Blaker, J.; Boccaccini, A. R., Biodegradable and bioactive porous polymer/inorganic composite scaffolds for bone tissue engineering. Biomaterials 2006, 27 (18), 3413-3431.

83. Chandran, S.; Asghar, L. F.; Mantha, N., Design and evaluation of ethyl cellulose based matrix tablets of ibuprofen with pH modulated release kinetics. Indian J. Pharm. Sci. 2008, 70 (5), 596.

84. Tiwari, S. B.; Murthy, T. K.; Pai, M. R.; Mehta, P. R.; Chowdary, P. B., Controlled release formulation of tramadol hydrochloride using hydrophilic and hydrophobic matrix system. AAPS PharmSciTech 2003, 4 (3), 18-23.

85. Jeong, B.; Bae, Y. H.; Kim, S. W., Drug release from biodegradable injectable thermosensitive hydrogel of PEG–PLGA–PEG triblock copolymers. J. Controlled Release 2000, 63 (1), 155-163.

86. Siepmann, J.; Peppas, N., Modeling of drug release from delivery systems based on hydroxypropyl methylcellulose (HPMC). Adv. Drug Delivery Rev. 2012, 64, 163-174.

87. Tahara, K.; Yamamoto, K.; Nishihata, T., Overall mechanism behind matrix sustained release (SR) tablets prepared with hydroxypropyl methylcellulose 2910. J. Controlled Release 1995, 35 (1), 59-66.

88. Rowley, J. A.; Madlambayan, G.; Mooney, D. J., Alginate hydrogels as synthetic extracellular matrix materials. Biomaterials 1999, 20 (1), 45-53.

89. Ruel-Gariépy, E.; Shive, M.; Bichara, A.; Berrada, M.; Le Garrec, D.; Chenite, A.; Leroux, J.-C, A thermosensitive chitosan-based hydrogel for the local delivery of paclitaxel. Eur. J. Pharm. Biopharm. 2004, 57 (1), 53-63.

90. Reza, M. S.; Quadir, M. A.; Haider, S. S., Comparative evaluation of plastic, hydrophobic and hydrophilic polymers as matrices for controlled-release drug delivery. J Pharm Pharm Sci 2003, 6 (2), 282-91.

91. Quadir, M.; Reza, M.; Haider, S., Effect of polyethylene glycols on release of diclofenac sodium from directly compressed carnauba wax matrix tablets. Journal-Bangladesh Academy of Sciences 2002, 26 (1), 1-8.

92. Madureira, A. R.; Campos, D. A.; Fonte, P.; Nunes, S.; Reis, F.; Gomes, A. M.; Sarmento, B.; Pintado, M. M., Characterization of solid lipid nanoparticles produced with carnauba wax for rosmarinic acid oral delivery. RSC Adv. 2015, 5 (29), 22665-22673.

93. De, C.; Vervaet, C.; Görtz, J.; Remon, J. P.; Berlo, J., Bioavailability of ibuprofen from matrix mini-tablets based on a mixture of starch and microcrystalline wax. Int. J. Pharm. 2000, 208 (1-2), 81-86.

94. Kheradmandnia, S.; Vasheghani-Farahani, E.; Nosrati, M.; Atyabi, F., Preparation and characterization of ketoprofen-loaded solid lipid nanoparticles made from beeswax and carnauba wax. Nanomedicine: Nanotechnology, Biology and Medicine 2010, 6 (6), 753-759.

95. Attama, A.; Schicke, B.; Müller-Goymann, C., Further characterization of theobroma oil–beeswax admixtures as lipid matrices for improved drug delivery systems. Eur. J. Pharm. Biopharm. 2006, 64 (3), 294-306.

96. Toro-Vazquez, J.; Morales-Rueda, J.; Dibildox-Alvarado, E.; Charó-Alonso, M.; Alonzo-Macias, M.; González-Chávez, M., Thermal and textural properties of organogels developed by candelilla wax in safflower oil. J. Am. Oil Chem. Soc. 2007, 84 (11), 989-1000.

97. Humberstone, A. J.; Charman, W. N., Lipid-based vehicles for the oral delivery of poorly water soluble drugs. Adv. Drug Delivery Rev. 1997, 25 (1), 103-128.

98. Shogren, R. L.; Petrovic, Z.; Liu, Z.; Erhan, S. Z., Biodegradation behavior of some vegetable oil-based polymers. J. Polym. Environ. 2004, 12 (3), 173-178.

99. Miao, S.; Sun, L.; Wang, P.; Liu, R.; Su, Z.; Zhang, S., Soybean oil-based polyurethane networks as candidate biomaterials: Synthesis and biocompatibility. Eur. J. Lipid Sci. Technol. 2012, 114 (10), 1165-1174.

100. Chen, H.; Kim, S.; He, W.; Wang, H.; Low, P. S.; Park, K.; Cheng, J.-X., Fast release of lipophilic agents from circulating PEG-PDLLA micelles revealed by in vivo forster resonance energy transfer imaging. Langmuir 2008, 24 (10), 5213-5217.

101. Tibbitt, M. W.; Rodell, C. B.; Burdick, J. A.; Anseth, K. S., Progress in material design for biomedical applications. Proc. Natl. Acad. Sci. U. S. A. 2015, 112 (47), 14444-14451.

102. Li, C., Poly (L-glutamic acid)–anticancer drug conjugates. Adv. Drug Delivery Rev. 2002, 54 (5), 695-713.

103. Kitchell, J. P.; Wise, D. L., [32] Poly (lactic/glycolic acid) biodegradable drug—polymer matrix systems. Methods Enzymol., Elsevier: 1985; 112, 436-448.

104. Khorasani, M.; Mirzadeh, H.; Irani, S., Plasma surface modification of poly (L-lactic acid) and poly (lactic-co-glycolic acid) films for improvement of nerve cells adhesion. Radiat. Phys. Chem. 2008, 77 (3), 280-287.

105. Perez, C.; Sanchez, A.; Putnam, D.; Ting, D.; Langer, R.; Alonso, M., Poly (lactic acid)-poly (ethylene glycol) nanoparticles as new carriers for the delivery of plasmid DNA. J. Controlled Release 2001, 75 (1-2), 211-224.

106. Richmond, R.; Macfarlane, T.; McCord, J., An evaluation of the surface changes in PMMA biomaterial formulations as a result of toothbrush/dentifrice abrasion. Dent. Mater. 2004, 20 (2), 124-132.

107. Kim, S. B.; Kim, Y. J.; Yoon, T. L.; Park, S. A.; Cho, I. H.; Kim, E. J.; Kim, I. A.; Shin, J.-W., The characteristics of a hydroxyapatite–chitosan–PMMA bone cement. Biomaterials 2004, 25 (26), 5715-5723.

108. Kurtz, S. M.; Devine, J. N., PEEK biomaterials in trauma, orthopedic, and spinal implants. Biomaterials 2007, 28 (32), 4845-4869.

109. Williams, D.; McNamara, A.; Turner, R., Potential of polyetheretherketone (PEEK) and carbon-fibre-reinforced PEEK in medical applications. J. Mater. Sci. Lett. 1987, 6 (2), 188-190.

110. Toth, J. M.; Wang, M.; Estes, B. T.; Scifert, J. L.; Seim III, H. B.; Turner, A. S., Polyetheretherketone as a biomaterial for spinal applications. Biomaterials 2006, 27 (3), 324-334.

111. Guan, J.; Wagner, W. R., Synthesis, characterization and cytocompatibility of polyurethaneurea elastomers with designed elastase sensitivity. Biomacromolecules 2005, 6 (5), 2833-2842.

112. Velema, J.; Kaplan, D., Biopolymer-based biomaterials as scaffolds for tissue engineering. Tissue Eng. I Springer: 2006; 187-238.

113. Kadokawa, J.-i., Precision polysaccharide synthesis catalyzed by enzymes. Chem. Rev. 2011, 111 (7), 4308-4345.

114. Arya, M. H.; Reis, R.; Boesel, V. C., Material properties of biodegradable polymers. Biodegrad. Polym. Ind. Appl. 2005, 336.

115.   Martino, M.; Perri, T.; Tamburro, A. M., Biopolymers and biomaterials based on

elastomeric proteins. Macromol. Biosci. 2002, 2 (7), 319-328.

CHAPTER 2. STUDY OF SELF-ASSEMBLY BEHAVIOR OF SOY-BASED MACROMOLECULES[12]

Abstract

A new class of lipid-based nano-constructs was generated from plant-oil derived macromolecules. Lipid based nanoparticulate systems have applications in the areas of pharmaceutical sciences, nutritional sciences, and in cosmetic industries; particularly to improve stability, transport and functional properties of the encapsulated content. Soybean oil derivatives such as MSSP present an interesting class of biobased materials from which lipidic nanoassemblies amenable for biomedical purposes may be fabricated. Using a facile nanoprecipitation technique, it was demonstrated that upon solvent shifting (Ouzo effect), MSSP forms self-assembled structure with a size range within 70-150nm and narrow polydispersity index (PDI). Soysomes exhibited long-term storage stability in the absence of any stabilizers or surfactants. Without the aid of surfactants or stabilizers, these MSSP nanoparticles termed "soysomes" were found to be stable in water for an extended period, withstanding the destabilizing effect of time, temperature, and pH. Understanding the mechanistic properties of Soysomes could open exciting avenues for use of renewable resources to generate smart

---

[1] This chapter contains some material adapted with permission from Chitemere, R. P.; Stafslien, S.; Rasulev, B.; Webster, D. C.; Quadir, M., Soysome: A surfactant-free, fully biobased, self-assembled platform for nanoscale drug delivery applications. ACS Appl. Bio Mater. 2018, 1 (6), 1830-1841. Copyright 2018 American Chemical Society.

[2] Some material in this chapter was co-authored by Ruvimbo Chitemere (Wright), Bhaktiyor Rasulev, Dean Webster and Mohiuddin Quadir. Ruvimbo Chitemere (Wright) had primary responsibility for sample formulation, conducting experiments, materials characterization and data interpretation. Ruvimbo Chitemere (Wright) was the primary developer of the conclusions that are advanced here. Ruvimbo Chitemere (Wright) also drafted and revised all versions of this chapter.), Bhaktiyor Rasulev conducted the computational studies. Dean Webster and Mohiuddin Quadir conceived and designed the experiments. Mohiuddin Quadir served as proofreader and corresponding author.

colloidal materials amenable towards multifarious applications. In this work, the physico-chemical factors governing self-assembly behavior of soy-based nanoparticles were investigated.

Introduction

Over recent decades nanomaterials have been the focus to advance medical interventions Research has intensely targeted improving the solubility of poorly water-soluble drug candidates which are highly potent and are promising pharmaceutical formulation with the potential achieve desired therapeutic effect, particularly to treat cancer and other complex disease conditions.[1-8] However, the transport of such hydrophobic compounds remains a challenge. Current polymers used as vehicles for drug delivery systems present several challenges such as low loading capacity, low bioavailability achievable, inability to sustain release over prolonged periods, poor stability and non-degradation or degradation into toxic by-products. Researchers in nanoscience continually develop new tools to address these challenges.

Although, nano-biomaterials have already gained tremendous research interest, only a few polymers are FDA approved, thus reliance on these can be costly, making manufacturing economically unviable. The need for designing and developing new and better polymers remains. To this end, large biobased molecules, particularly plant oil derivatives have become fascinating new avenue for developing new innovative materials with an enhanced form or function for application in pharmaceutics, medicine or agriculture.[9-13]

Particularly interest is focused on sucrose octa-esters of soybean oils such as MSSP and ESS. Sucrose esters of plant oils are synthesized from sucrose molecules conjugates to fatty acid chains from the plant oil. In the early 2000s, Procter & Gamble (P&G) introduced the first of this class of macromolecules, SEFOSE and commercialized it for applications in lubricant and coatings industries. [14,15] MSSP and ESS have previously been used to fabricate high

31

performance, durable biobased coatings, matrices, shape-memory composites and hybrid materials.[16-19] Historically, several biomaterials translated to clinical use were originally designed other non-related applications. For example, materials used for artificial hearts were originally based on commercial-grade polyurethanes and the first dialysis tubing was fabricated from cellulose acetate, which is used to make various plastic components in automotive industry.[20]

Nanocarriers from lipids or their derivatives has a long-standing history in drug delivery technology. Family of lipid-based colloidal systems includes liposomes, solid lipid nanocarriers, nanostructured lipid carriers and lipid drug nano-conjugates. Such lipid –based delivery systems offer the promise of improved solubility of poorly water-soluble active pharmaceutical agents and other hydrophobic compounds, increased stability of the encapsulated cargo, enhanced bioavailability and biodistribution. Lipidic nanocarriers address many of the challenges of hydrophilic nanoparticle systems; however, still have limitations including poor storage stability or need for surfactants in the formulation. Therefore, designing a new lipid-based system from large biobased molecules with tunable properties such as sucrose soyates presents an exciting prospect of customizable, stable, lipid-based nanocarriers systems applicable as a delivery platform.

Design complexity of the nanocarriers systems results in difficulties in large-scale production. Several techniques have been developed to prepare nanoparticles and encapsulation of any cargo. Some of the most commonly, employed methods include solvent diffusion[15], solvent displacement, emulsion, salting out, solvent evaporation, interfacial deposition, polymerization, ionic gelation and nanoprecipitation.[7, 21-27] Nanoprecipitation method was established by Fessi et al as facile technique to produce polymeric nanoparticles[28, 29]. It has since

then been used to synthesize several polymeric nanoparticles as well as encapsulate hydrophobic drugs within the nanoparticles[22, 30-36]

Briefly, the polymer is dissolved in a water-miscible organic solvent and added dropwise to an aqueous phase, under moderate stirring, leading to precipitation of polymer forming colloidal particles. Removal of the organic solvent results in polymeric nanoparticles suspended in water. Nanoprecipitation is a facile method that may be undertaken to eliminate complicated preparatory methods for nanocarriers.

In this work, the self-assembly behavior of sucrose octa-ester, MSSP was investigated. MSSP is expected to form stable nanoparticles upon solvent shifting during nanoprecipitation process. Systematic study was carried out to evaluate the characteristics, performance and viability of sucrose ester, MSSP as a potential new platform for biomaterials.

Experimental

Materials

MSSP, M_n 3442 g/mol (characterized by gel permeation chromatography with THF as an eluent) has been synthesized earlier by Nelson et al.[16] PEG–PLGA M_n for PEG = 5 kDa, M_n for PLGA = 25 kDa (lactide: glycolide ratio = 50:50), pyrene, oleic acid (OA), linoleic acid (LA), linolenic acid (LNA), acetonitrile (ACN), tetrahydrofuran (THF), acetone (ACT), inhibitor-free anhydrous grade N',N-dimethylformamide (99.8%) (DMF), ethanol (EtOH), dimethyl sulfoxide (DMSO), isopropyl alcohol (IPA) and 1-octanol were purchased from Millipore Sigma. Ethylene glycol (EG) was acquired from BDH Chemicals. Phosphate buffer saline (PBS) tablets (10 mM) were purchased from VWR (Solon, OH, USA), which was used to prepare PBS pH 7.4.

Preparation of Soy-based Nanoassemblies

Soysomes were prepared by the nanoprecipitation method[7, 34, 37, 38]. A specified

concentration of MSSP was dissolved in a water-miscible organic solvent and stirred for 30 min.

To form nanoparticles, the MSSP solution was added dropwise to water, a nonsolvent for MSSP,

using a syringe pump at a 0.2 mL/min infusion rate. The resulting soysomes suspension was

stirred at room temperature for 15 h and then dialyzed against water for 24 h using benzoylated

dialysis tubing molecular weight cut-off (MWCO)1200 (Sigma-Aldrich). The soysomes were

purified by filtration using a 0.45 μm PES syringe filter (VWR). Organic solvents that were used

as the nonselective media for nanoprecipitation were ACN, ACT, DMF, DMSO, EtOH, EG, IPA

and THF. The effect of solvent types on the self-assembly and resulting particle size was

evaluated. Polymer concentration in the organic solvent as well as the ratio of nonselective

(organic) to selective solvent (water) were also varied to optimize the process of

nanoprecipitation.

Fatty acids emulsions were prepared from oleic, linoleic and linolenic acid using similar

nanoprecipitation procedure. A specified concentration of each fatty acid (10mg/mL) was

dissolved in ethanol and stirred for 30 min. The fatty acid solution was titrated into water at

0.2mL/min addition rate. The resulting suspensions were stirred at room temperature for 15 h

and then dialyzed against water for 24 h. Fatty emulsions clogged the micro-filters immediately;

therefore, suspensions were analyzed without following the purification step.

Physicochemical Characterization of Nanoparticles

Evaluation of Soysomes Morphology by Transmission Electron Microscopy

A drop of the soysomes suspension was placed on a 300 mesh Formvar-carbon-coated

copper TEM grid (Electron Microscopy Sciences, Hatfield, Pennsylvania, USA) for 1 min and

wicked off. Phosphotungstic acid (0.1%), pH adjusted to 7–8, was dropped onto the grid, allowed to stand for 2 min, and then wicked off. After the grids were dry, images were obtained using a JEOL JEM-2100 LaB6 transmission electron microscope (JEOL USA, Peabody, MA) running at 200 kV.

Determination of Particle Size and Zeta Potential

The hydrodynamic diameter and particle size distribution of soysomes were measured by dynamic light scattering (DLS) using Malvern Zetasizer Nano-ZS90 (Malvern PANalytical, UK) at 25 °C after 60 s equilibration at a scattering angle of 90° using disposable polystyrene cuvettes. Three measurements were performed for each sample replicate (N=5), each with an average of 10 runs at 10s/run. The intensity-weighted mean value was recorded. The zeta potential was determined by DLS using the similar particle analyzer, Malvern Zetasizer Nano ZS90 (Malvern PANalytical, UK). Three measurements were performed for each sample replicate (N=5) for 10 runs each at 30s/run, after a 60 s equilibration period under automatic attenuation and automatic voltage.

Computational Analysis of Soysomes Structures

To investigate the MSSP–solvent interactions and stabilization of nanoparticles in corresponding solvents and build a predictive model, a computational analysis of MSSP structures, as well as solvent structures, was carried out. Various molecular features/descriptors were calculated per each solvent structure, after initial optimization. Molecular mechanics (MM) and quantum-mechanical (QM) calculations were performed using MM+ and PM3[39] methods within HyperChem software [HyperChem; Hypercube Inc., Gainesville, FL, USA]. The structures were built and used for QM calculations in two steps: (1) optimization of the molecular geometry and (2) calculation of various quantum chemical properties. The semi

35

empirical QM calculations were performed utilizing the efficient Parameterized Model 3 (PM3) method. PM3 (and its updated version, PM6) delivers results that are comparable to the density functional theory (DFT) level[40]. The following molecular properties were calculated for each structure: heat of formation (HF), dipole moment (μ), total energy (ET), electronic energy (EE), energy of the highest occupied molecular orbital (EHOMO), energy of the lowest unoccupied molecular orbital (ELUMO). In addition, a number of structural descriptors were generated by Dragon 6 software [Talete srl, Dragon (version 6.0), Milano, Italy]. A QSAR study was performed by the application of multiple linear regression (MLR) analysis, which is a commonly used statistical tool for which a dependent variable (y) is expressed as a linear combination of independent variables (e.g., physicochemical properties and/or structural features (x_1, x_2, ..., x_n)) with certain coefficients. In this study, a QSAR model was developed by selecting the most relevant independent variables (i.e., molecular descriptors) selected by a genetic algorithm (also known as GA-MLR modification)[41]. MLR models were developed using QSARINS software[42], and the results were compared to experimental data.

Construction of Phase Diagram and Determination of Ouzo Boundary

MSSP was dissolved in acetone and then added dropwise to the aqueous phase using a syringe pump. The mixture was kept under constant magnetic stirring (100rpm). After addition of the organic phase, the resulting colloidal suspension was visually inspected for change in turbidity. Mass fraction of each component: water (f_{water}), acetone ($f_{acetone}$) and the polymer, MSSP, (f_{MSSP}) was determined for each marked volume added. The volume of aqueous phase was kept constant. MSSP solution was titrated, identifying the cloud-point boundaries (binodal and spinodal), region where stable nanoparticle (ouzo region) form until the polymer precipitated. The binodal boundary was deduced from mass fraction of MSSP added at the onset

36

of turbidity, while the spinodal boundary was identified as the mass fraction after which super-saturation allows formation of emulsion or phase separation occurs. A phase diagram was constructed by plotting the mass fraction of the solvent, acetone against the mass fraction of the polymer, MSSP.

Evaluation of Soysomes Stability

Soysomes prepared according to the above-mentioned procedure were evaluated for particle size and polydispersity when subjected to varying temperatures and pH conditions. To control temperature, soysomes samples (2 mL) were placed in a bath at 37 and 80 °C, while a set of samples was allowed to sit at room temperature. In order to evaluate the effect of pH on the stability of soysomes, nanoparticles were prepared in 0.01 M PBS (pH 7.4), adjusted to pH 5.5 and to pH 12 by the addition of 0.01 N HCl or 0.1 N NaOH solution, respectively, and treated for 96 h. For long-term stability, soysomes were stored at 4 °C and the particle size of the nanoparticles were measured after a week and five months after the preparation.

Determination of Critical Aggregation Concentration (CAC)

Pyrene Method

Determination of CAC of MSSP was estimated by a fluorescence spectroscopic method using pyrene as a probe following a previously described procedure[43-45]. Briefly, 10 μL of 2.02 μg/mL (0.10 mM) pyrene solution in ACT was prepared in Eppendorf tubes, and the solvent was removed by evaporation overnight. To each of the tubes containing pyrene, a fixed volume (1 mL) of soysomes solution of varying concentrations ranging from 0.06 mg/mL (1.74×10^{-4} M) to 2.17 mg/mL (6.30×10^{-4} M) of MSSP equivalent was added to achieve a constant pyrene concentration 0.20 μg/mL (1×10^{-6} M) in each tube. Each Eppendorf tube was sonicated for 5 min (Branson 1800) and then allowed to stand for 3 h before the emission spectra were recorded. Fluorescence spectra of pyrene were recorded from 350 to 470 nm after excitation at 337 nm.

The slit width was set at 2 nm for both excitation and emission. The peak intensities at 373 and 383 nm were designated as I_1 and I_3, respectively, and the ratio of I_1 and I_3 was plotted against the MSSP concentration. The CAC was determined from the inflection point observed in this plot.

Cloud-Point Method

MSSP solution in organic solvent (ACT) was titrated against water forming a three-component system. Acetone was removed by evaporation and the turbidity of the resulting colloidal suspensions analyzed by transmittance using Varian Cary 5000 UV–vis-NIR spectrophotometer. A plot of the transmittance as a function of mass fraction of polymer was used to identify the cloud-point, i.e. concentration at which first stable colloidal structures are formed. Water was measured as the blank reference. The cloud-point was deduced as the inflection point due to drop in light transmittance.

Results and Discussion

Self-Assembly Behavior of Methoxylated Sucrose Soyate Polyol

A stable nano-particulate dispersion of MSSP, termed 'soysomes', was achieved in water through nanoprecipitation (solvent shifting) technique (Figure 2.1). The method requires miscibility between a solvent pair, with the polymer being completely soluble in the one (the solvent), but insoluble in the other (nonsolvent) [43]. In our work, we used water as the nonsolvent (aqueous phase) and selected a variety of organic solvents, ACT, ACN, DMF and THF based on their water miscibility[7, 22, 37, 44] and capacity to solubilize a broad spectrum of compounds. In a bid to improve the solvent system in the fabrication process, a series of "green solvents", EtOH, IPA, EG and DMSO were used for the nanoprecipitation of MSSP.[45] Complete solvent removal was achieved by dialysis resulting in solvent-free polymeric nanoparticles in water. The effect of solvent types, concentration and solvent ratio were evaluated and discussed in this section.
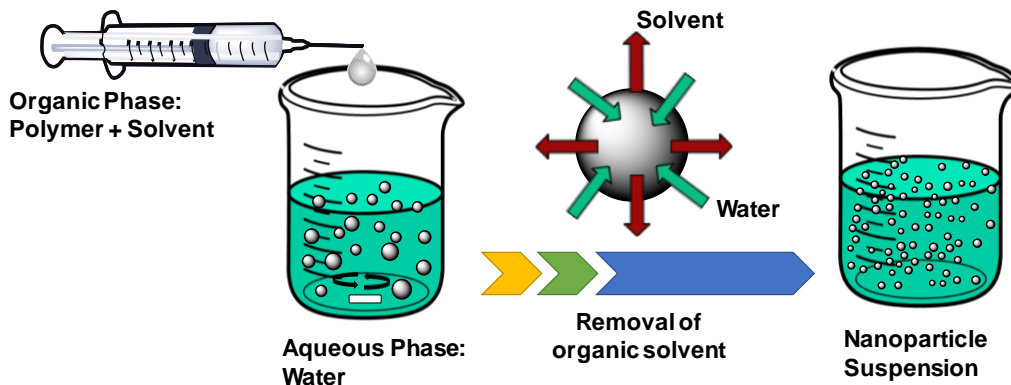
Figure 2.1. Representation of the nanoprecipitation technique to prepare Soysomes showing rapid dispersion of the organic solution in water followed by diffusion of solvent and water leading to particle nucleation. Solvent removal at the process resulting in an aqueous nano-suspension.

We have also established that the formation of soy-based nanoparticles (Soysomes) is a unique property of MSSP and not that of its constituent fatty acids by attempting to form nanoparticles from fatty acids of soybean oil alone under similar nanoprecipitation conditions. The typical fatty acid composition of soybean oil is 15.3 wt. % saturated fatty acids (11.3 wt. % palmitic acid and 3.6 wt. % stearic acid) and 25.6 wt. % monounsaturated fatty acids (24.9 wt. % OA) with 59.1 wt. % polyunsaturation (53.0 wt. % LA and 6.1 wt. % LNA).

OA, LA and LNA were selected as the representative fatty acids from which MSSP is synthesized. When these fatty acids were dissolved in ethanol and added water following the nanoprecipitation technique, rapid phase transition of fatty acids was observed, leading to the formation of an emulsion. Particle size analysis of the resulting emulsions (Figure 2.2.) shows the presence of larger particles with a high PDI > 0.4. LNA completely precipitated out of solution forming distinct oil and water phase, while OA and LA although formed emulsions, eventually demonstrated an uncontrolled size enlargement.
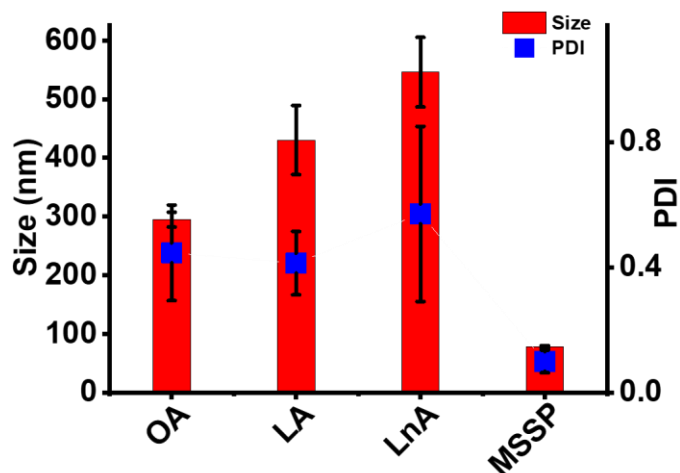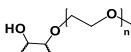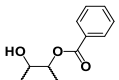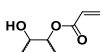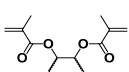
Figure 2.2. Particle size and PDI obtained from nanoprecipitation of fatty acids composing MSSP

Soysomes formation from other sucrose soyate derivatives was evaluated using a series of soy-based resins (Table 2.1). All resin were nanoprecipitated under similar conditions as MSSP, i.e. concentration of 10mg/mL in DMF at 1:3 DMF to water ratio. Propylated sucrose soyate polyol (PrSSP) and PEGylated sucrose soyate polyol are both formed from alcoholysis of ESS with propanol and PEG respectively. Both polyols self-assembled into soy-based nanostructures with particle size similar to MSSP and within range ideal for use in biological system (PrSSP: 93.84 ± 1.17 and PSSP: 84.57 ± 4.90 nm). Benzoylated sucrose soyate polyol (BASSP), obtained from reacting ESS with 10% benzoic acid, gave larger particles (205.50 ± 18.87nm) and difficult to filter through 0.45µm PES filter. The presence of acrylate group in the resin impeded soysome formation; acrylated sucrose soyate (ASSP) formed colloidal suspension briefly, which precipitated within an hour of formation. To evaluate the role of the hydroxyl group, sucrose soyates without any hydroxyl functionality were evaluated.

Dimethyl methacrylated sucrose soyate (DMESS) phase separated immediately without forming any nanoparticles while carbonated sucrose soyate was able to form large particles with poor stability; phase separating within 24 h. From Table 2.1, it is apparent that hydrophilic

moieties such as hydroxyl group are required to form nanoparticle size below 100nm. Presence

of aromatic group in sucrose soyate tends to increase the particle size of the resulting Soysomes.

Table 2.1. Evaluation of Soysomes Formation from Sucrose Soyate Derivatives

Sucrose Soyate	Structure	Forms Soysomes (-/+)	Particle Size (nm)
Methoxylated sucrose soyate polyol (MSSP)		+	75.11 ± 1.16
Propoxylated sucrose soyate polyol (PrSSP)		+	93.84 ± 1.17
PEGylated sucrose soyate polyol (PSSP)		+	84.57 ± 4.90
10% Benzoylated sucrose soyate polyol (BASSP)		+	205.50 ± 18.87
Acrylated sucrose soyate polyol (ASSP)		-	-
Dimethyl methacrylated sucrose soyate (DMESS)		-	-
Carbonate sucrose soyate (CSS)		+	176.33 ± 10.52

Factors Controlling Particle Size of Soysomes

To evaluate the size, shape, and polydispersity of soysomes, and optimize the processing

conditions, we characterized the size and morphology of the nanoparticles using TEM and DLS.

Soysomes were determined to exhibit spherical morphology as depicted in the TEM microgram

in Figure 2.3. (a).
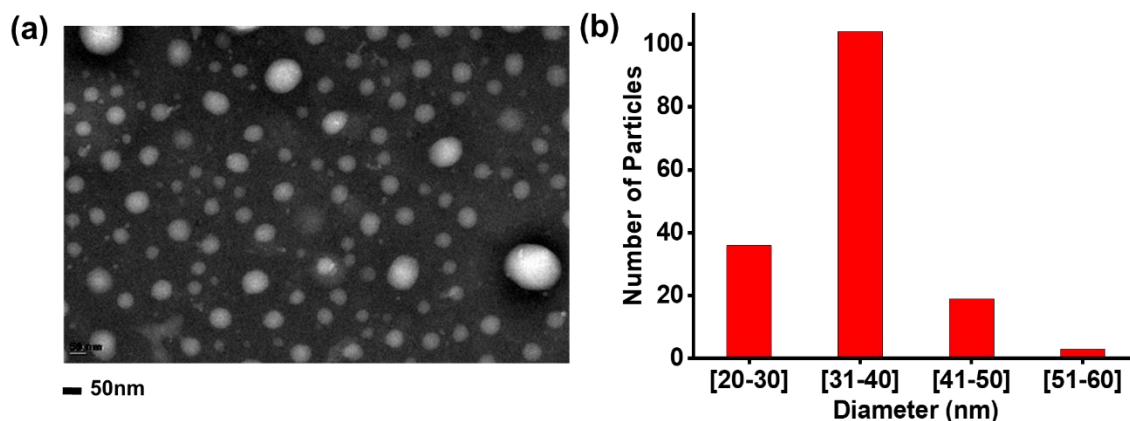
Figure 2.3. (a). TEM image of MSSP soysomes prepared with DMF as organic solvent with a scale bar of 50 nm and (b) histogram showing particle size distribution of MSSP Soysomes as determined by TEM

Furthermore, the TEM studies showed that, upon nanoprecipitation from organic to aqueous solvents, self-assembled constructs formed by MSSP are monodispersed and with majority of the nanoparticles within 31–40 nm size range (Figure 2.3. (b)). A spherical nanoparticle shape is typical, especially when the polymer solution is precipitated in a poor solvent, most likely to reduce interfacial tension[46, 47]

Hydrodynamic diameters (R_H) of Soysomes obtained from DLS analysis and reported in Table 2.2. were found to be within the range 100–200 nm, depending on the type of organic solvent, concentration of polymer and the ratio of organic solvents to water, the aqueous phase in which the nanoparticles were precipitated. The smaller particle size obtained from TEM in comparison to DLS-derived hydrodynamic diameter is most likely due to the dehydration of particles during the sample preparation for TEM. [48]

Table 2.2. Soysomes Particle Size and PDI Prepared from Four Different Solvents

Solvent	$\Delta\delta_{\text{solvent -water}}$	Particle Size (R_H), nm	PDI
DMF	31.14	137.63±1.70	0.078±0.009
ACT	35.74	180.03±6.39	0.058±0.019
THF	35.83	182.73±0.57	0.082±0.018
ACN	36.26	221.97±3.48	0.060±0.017

Particle size distribution has a similar distribution profile as that obtained from TEM. The Soysomes particles have a mono-modal and narrow distribution shown in Figure 2.4. This is supported by the very low PDI values (<0.09) observed for Soysomes regardless of solvent used in the preparative step. Soysomes prepared from THF were unstable and at high concentrations of MSSO or larger water to solvent ratios, MSSP precipitated out of solution forming a mixture of large particles and droplets of resin creaming at the air-water interface eventually leading to the formation of two phases. Due to this, THF was not used for subsequent testing.
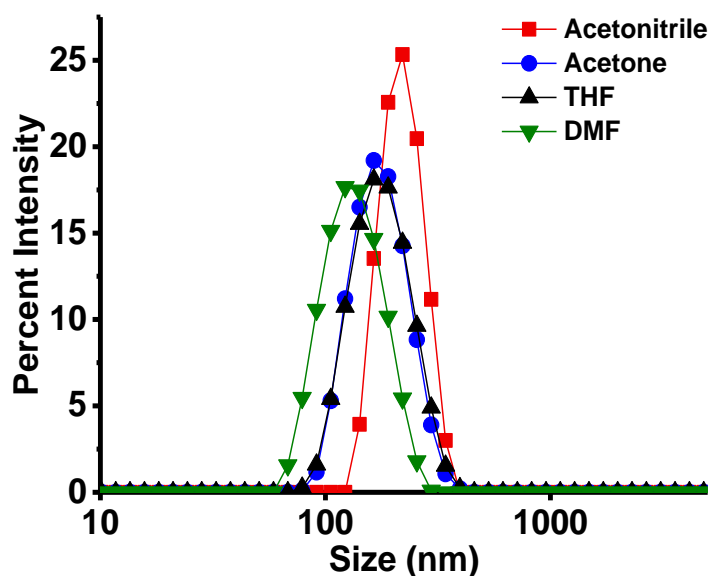
Figure 2.4. Soysomes particle size distribution profile as determined by DLS demonstrating monodisperse sample with various solvents

To investigate the influence of organic solvents on the final hydrodynamic particle size of Soysomes, we used four different solvents with varying miscibility in water as determined by comparing Hansen solubility parameters (δ) for both the solvent and water[32, 37]. The average particle size of Soysomes demonstrated solvent dependency (Figure 2.5.) when a fixed concentration of MSSP was used (10 mg/mL) during the nanoprecipitation process.

The general trend showed a decrease in mean nanoparticle size with the increase in miscibility of solvent with water. Soysomes prepared in DMF, which had the highest water

miscibility among the solvents tested in this experiment, yielded the smallest particles size (R_H = 98.48 ± 4.72 nm). This is presumably due to a more efficient solvent diffusion and polymer dispersion into water[22]. On the other hand, when ACN, which had the highest $\Delta\delta$, was used in Soysomes synthesis, it led to the formation of particles with the largest hydrodynamic diameter (212.03 ± 2.46 nm).
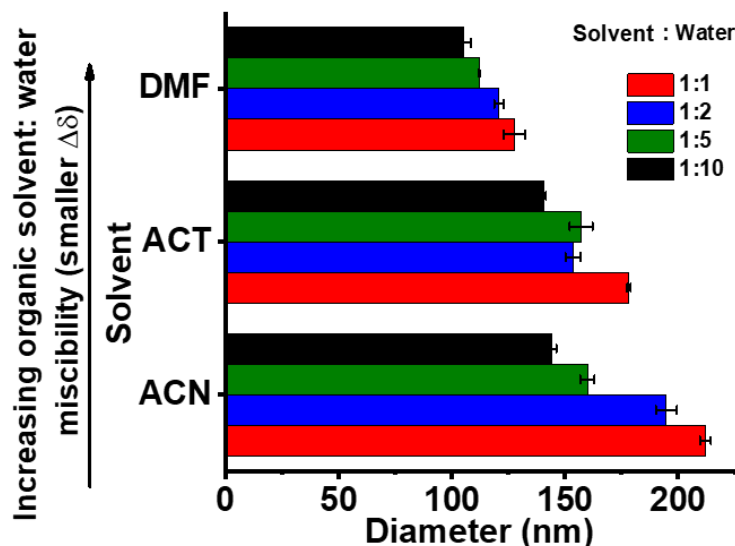
Figure 2.5. Soysomes particle size as a function of ratio of solvent–water (1:1, 1:2, 1:5, 1:10) at a constant MSSP concentration (10 mg/mL)

Previous studies have reported a correlation between the miscibility of organic solvents in water and the size of nanoparticles formed[28, 36]. When the difference of the solubility parameter ($\Delta\delta$) between the solvent and water is smaller, the miscibility of the solvent with water is higher[22, 28, 30, 32]. Solvents having a high affinity for water, which is evidenced by low solvent–water $\Delta\delta$ values, tend to promote an efficient solvent diffusion and rapid macromolecular precipitation into the aqueous phase, leading to the formation of smaller NPs. A similar phenomenon was observed in nanoparticle systems based on PEG-PLGA block copolymers, which have been widely used in preparation of drug delivery nanocarriers[33].

Water-solvent interaction plays a role in controlling particle size as well. As illustrated in Figure 2.5., the Soysomes particle size increased with increasing solvent to water ratios. At a 1:10 DMF to water ratio, Soysomes obtained from precipitating MSSP (at a concentration of 10 mg/mL) had the lowest diameter (87.47 ± 3.08 nm) compared to those prepared at a 1:1 ratio of DMF to water (99.53 ± 4.72 nm). These results showed that, by selecting the type and ratio of organic solvent to water, it would be possible to control the nanoparticle size for an optimal application outcome. Computational structural modeling (Figure 2.6. (a) and (b)) supports the difference in conformation of MSSP in different solvent environments, DMF and water respectively.
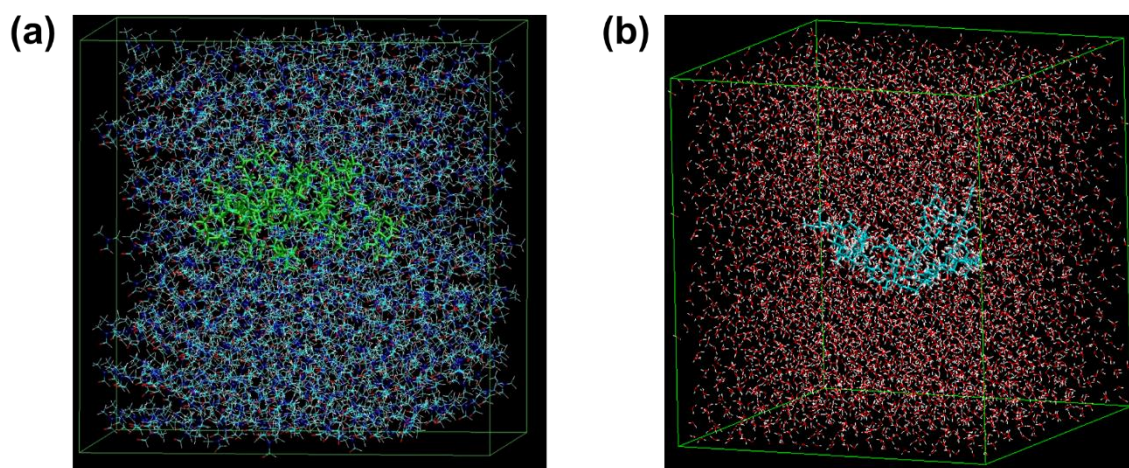
Figure 2.6. Computational structural model of a single molecule of MSSP in (a) DMF and (b) water

In addition to water–solvent interactions, factors such as the molecular volume as well as molar volume of the solvent and polymer–solvent interactions most likely played an important role in determining the size of nanoparticles. To demonstrate this, we have selected a set of green solvents for analyzing the prospect of preparing of MSSP nanoparticles (Figure 2.7.) in an eco-friendlier manner. We observed that nanoparticles with the smallest diameter were obtained when MSSP precipitated from DMSO (57.87 ± 2.09 nm), while nanoparticles with a

hydrodynamic diameter of 173.69 ± 7.49 nm were obtained when EG was used as the precipitating solvent. For this set of solvents, the solubility of MSSP in the respective solvent compensated for the solvent–water miscibility. For example, although EG possesses the highest water miscibility ($\Delta\delta_{\text{solvent–water}} = 17.11$), it produced significantly larger-diameter Soysomes in comparison to DMSO, which has a $\Delta\delta$ value of 32.22, but led to smaller nanoparticles. MSSP is easily solubilized in DMSO, which can be considered a good solvent for MSSP.
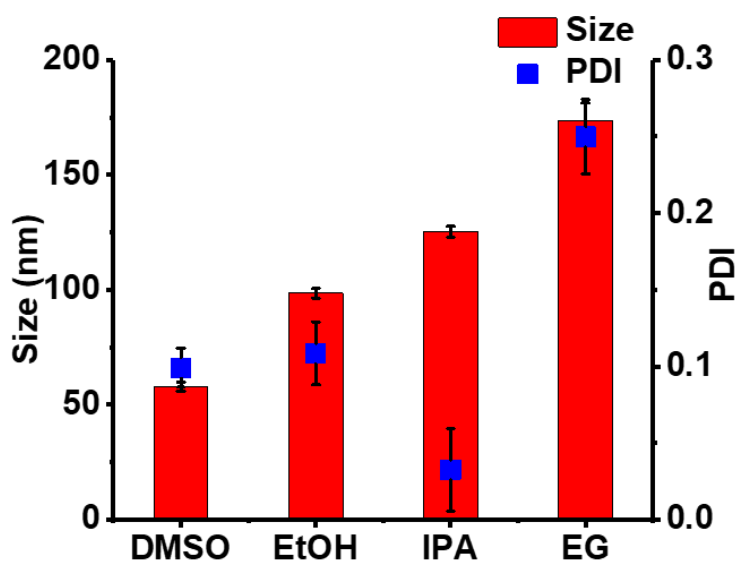
Figure 2.7. Particle size and PDI of Soysomes prepared from a set of green solvents

On the other hand, MSSP is much less soluble in EG, the "bad" solvent, as indicated by an increase in viscosity of the mixture as well as immediate turbidity observed when MSSP in EG solution is added to water. The organic solvent to water ratio also affected the particle size of Soysomes prepared from highly polar solvents such as DMF. Polymer concentration can be correlated to aggregation properties and hence the resulting particle size.

To investigate the relationship between the particle size of Soysomes and the feed concentration of MSSP, we prepared a series of MSSP solutions varying the concentration of the polymer from 1.0 mg/mL (2.9×10^{-4} M) to 10.0 mg/mL (2.9×10^{-3} M) in the organic phase (DMF and acetone) at a fixed solvent to water ratio. We found that the hydrodynamic diameter

of Soysomes was proportional to the initial polymer concentration regardless of the solvent type (Figure 2.8.).
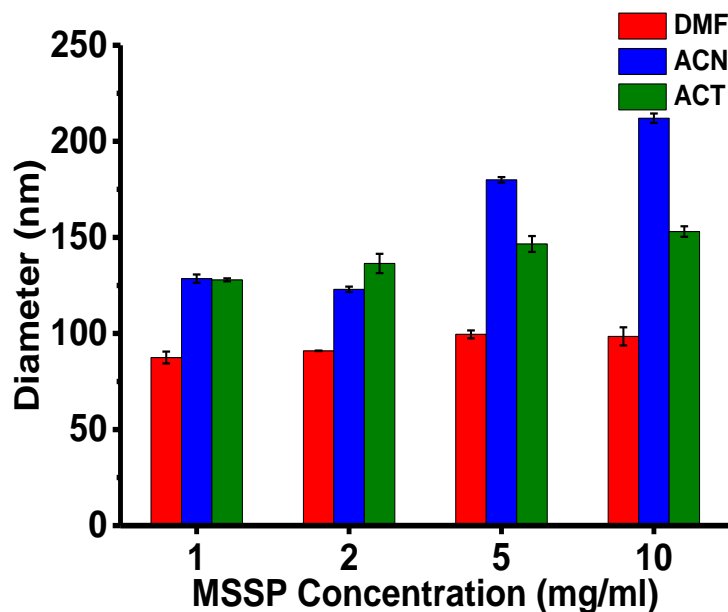
Figure 2.8. Effect of MSSP concentrations in the organic phase (1–10 mg/mL) on MSSP particle size, while keeping the solvent– water ratio fixed at 1:3

For example, with respect to DMF, the hydrodynamic diameter of Soysomes was doubled from 75.09 ± 0.97 nm to 147.97 ± 2.50 nm when the polymer concentration was increased 10-fold from 1 mg/mL to 10 mg/mL. This observation can be correlated with the increased mass of material per nanoparticle that is precipitated out of the organic solvent during the formation of the particles in an aqueous environment. We also observed that the preparative conditions critically influenced the size distribution of Soysomes. Filtration of nanoprecipitated Soysomes through a 0.45 µM PES filter reduced the particle size and improved the polydispersity in terms of PDI (Figure 2.9.).
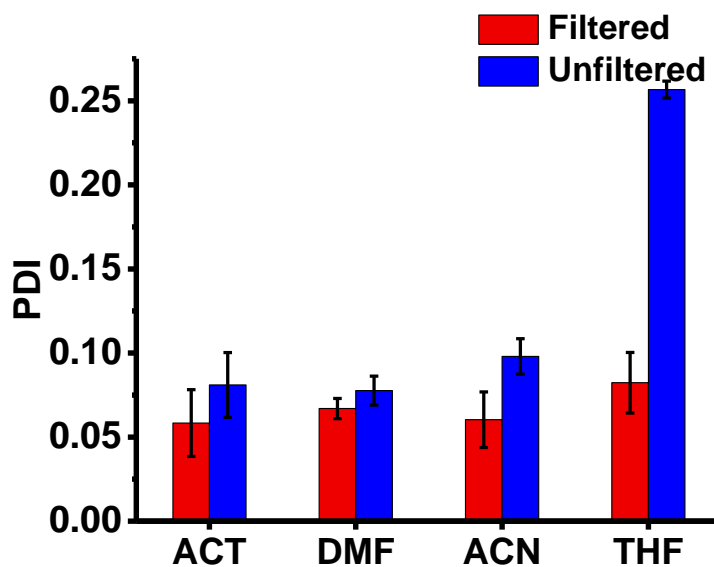
Figure 2.9. Evaluation of the effect of filtration on PDI of MSSP Soysomes prepared in water

The removal of organic solvent after nanoprecipitation was attempted using two different methods: dialysis, which entails a slow solvent exchange against water, and an evaporative method, where heat was applied near the boiling point of the respective solvent for 24 h, leaving only the Soysomes in an aqueous suspension. We observed that the dialysis-based purification method always yielded smaller particles compared to the evaporative method, possibly due to a slow and gradual phase transition of the dissolved MSSP occurring when the organic solvent was removed by dialysis (Figure 2.10.).
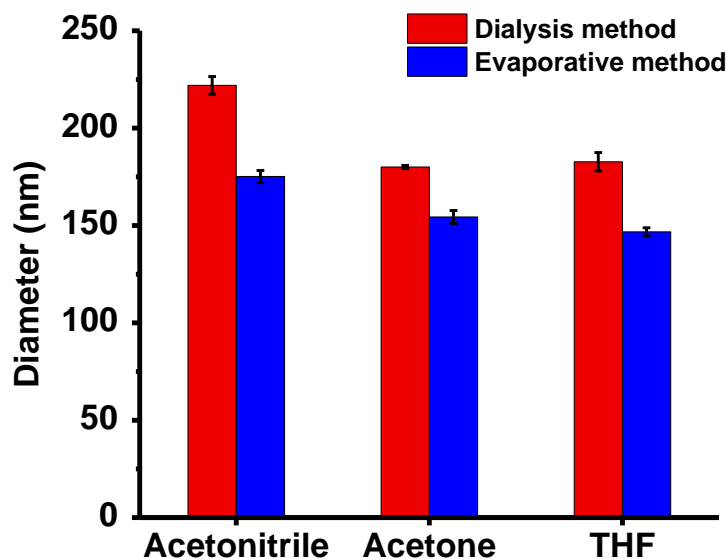
Figure 2.10. Effect of different solvent removal preparative methods (dialysis versus evaporation) on the particle size MSSP Soysomes

Computational Structure−Property Relationship Analysis between Solvent Type and Soysomes Particle Size

To understand the relationship between the particle size of Soysomes and organic solvents, we applied a cheminformatics approach, so-called quantitative structure–property relationship (QSPR). For this, we used the experimental data of the Soysomes particle sizes in each solvent (experimental end-point) and structural information on all solvent molecules, computationally derived. The optimized structures of solvent molecules (as described in the Materials and Methods section) were used to calculate a number of structure-related properties/descriptors. By applying the QSPR technique, we were able to develop a mathematical model for the relationship "solvent structure–Soysomes particle size", which shows a strong correlation with experimental values, $R^2 = 0.84$ (eq 2.1):

$$Soysome\ Size = 619.8(\pm239.1)\ x\ M_v - 67.4(\pm14.9)\ x\ BLI - 78.61 \qquad (2.1)$$

where $R^2 = 0.842$, $Q^2 = 0.689$, $CCC_{tr} = 0.914$, $RMSE_{tr} = 19.65$, $F = 13.32$, and $s = 24.85$.

The GA technique within QSPR has selected two main structural descriptors that are responsible for the relationship, M_v (mean atomic van der Waals volume) and Kier benzene-likeliness index (BLI). The M_v is related to the solvent molecule's volume size, and BLI represents a relative number of double bonds to total number of bonds in the molecule, i.e., indicates a higher electron density level in the structure. Both selected properties work synergistically to give a good correlation with experimental data and explain the phenomena (Figure 2.11.).
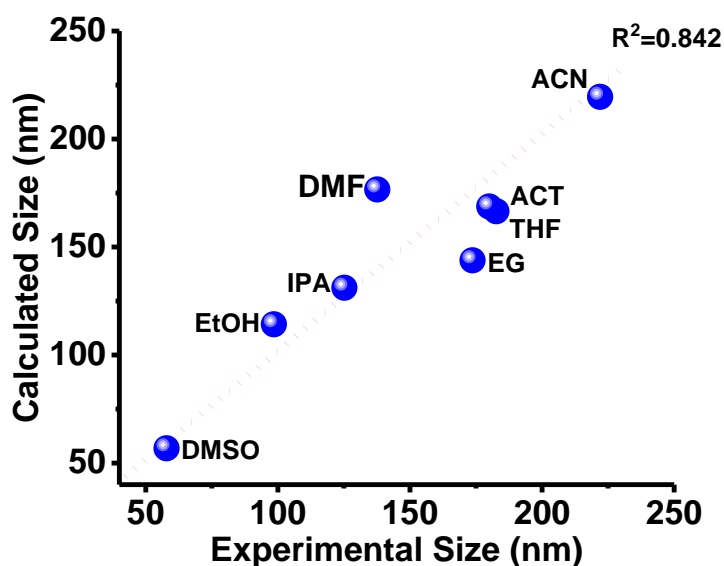
Figure 2.11. QSPR computational model showing correlation between experimental obtained Soysomes size and predicted size

When analyzed individually, each descriptor presents different behavior. For example, a strong nonlinear inverse relationship exists between the BLI of the solvent and the resulting Soysomes particle size. Therefore, a larger BLI for a solvent result in smaller size Soysomes particles. This is demonstrated clearly in the case of DMSO as the selected solvent; it exhibits the highest BLI and yields the smallest sized particles (Figure 2.12.).
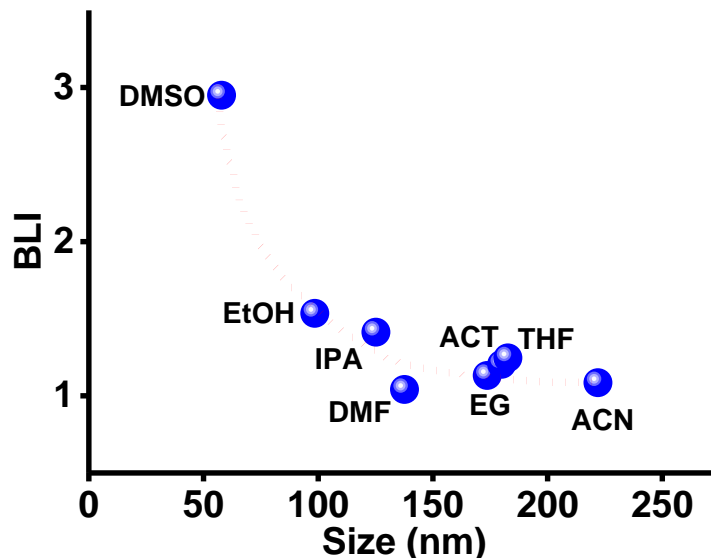
Figure 2.12. QSPR computational models showing correlation between Kier benzene-likeliness index (BLI) and experimentally determined Soysomes size

The distinct behavior of DMSO was attributed to the presence sulfur in its structure which made it unique in comparison to the other analyzed solvents. DMSO has a very strong affinity to water and creates a large hydration layer that stabilizes Soysomes particles preventing aggregation.

On the other hand, M_v has a linear relationship with particle size with exception of DMSO (Figure 2.13.). The larger M_v of the solvent leads formation of a larger size Soysomes particle during the nanoprecipitation stage. This was attributed to likely lack of uniform coverage of the surface of Soysomes particles by the large solvent molecules hence resulting in aggregation of MSSP into larger particles. In the case of smaller solvent molecules, surface coverage of the Soysomes is likely more uniform and increased thus minimizing the possibilities of aggregation.
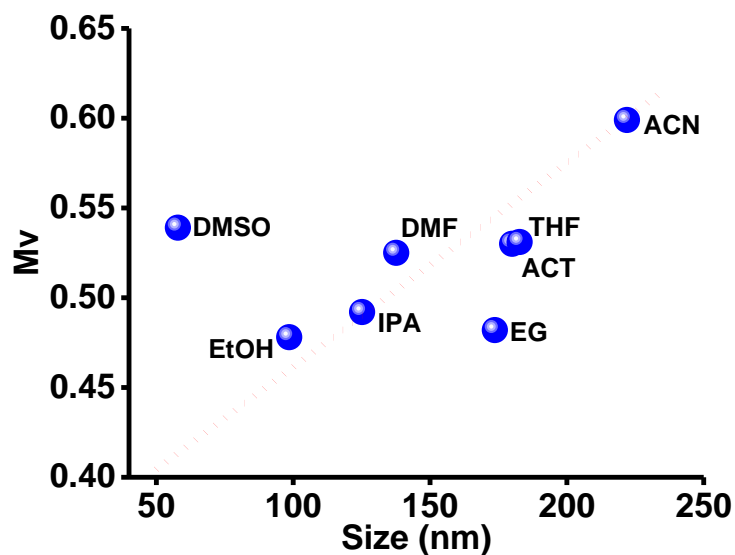
Figure 2.13. QSAR computational models showing correlation between mean atomic Van der Waals volume (M_v) and experimentally determined Soysomes size

Stable Ouzo Region

Mechanism of Soysomes formation could be explained in two possible ways. The first is the solvent displacement method, which attributes particle nucleation to variations in interfacial tensions between the two liquid phases not at equilibrium[24, 31, 49-51]. When the two phases come in contact, the solvent diffuses out of the organic phase into the aqueous phases. This introduces into water a small portion of still solubilized polymer. As the solvent continues to diffuse into water, polymer chains tend to aggregate, hence forming nanoparticles.

The second is known as Ouzo effect which describes liquid- liquid particle nucleation as spontaneous emulsification that takes place when oil or polymer dissolved in a solvent and water diffuses into the oil droplet and some solvent simultaneous diffuses into the water.[52-57] This continues until the oil becomes supersaturated leading to particle nucleation. The particles grow as the polymer diffuses into nearby particles resulting in decrease in super-saturation and nucleation stops. As the two phases mix, a region of metastable dispersion is achieved known as

the Ouzo region. This is found between the miscibility/solubility limit (binodal boundary) and the stability limit (spinodal boundary).[56, 58, 59]

We performed a systematic study to demonstrate the mechanism of Soysomes formation. Figure 2.14. shows our phase diagram mapping the composition of MSSP-acetone-water ternary system through the nanoprecipitation process. The phase diagram was constructed from determining the mass fractions of each individual component as the solution of MSSP dissolved in acetone was titrated into water until the MSSP precipitated out. At very low mass fractions of MSSP, there is some aqueous solubility which is slightly enhanced by increase the amount of acetone. However, a solubility limit was shortly reached and noted, as the point the mixture became instantaneous cloudy[52, 59]. This miscibility limit is identified as the binodal boundary.
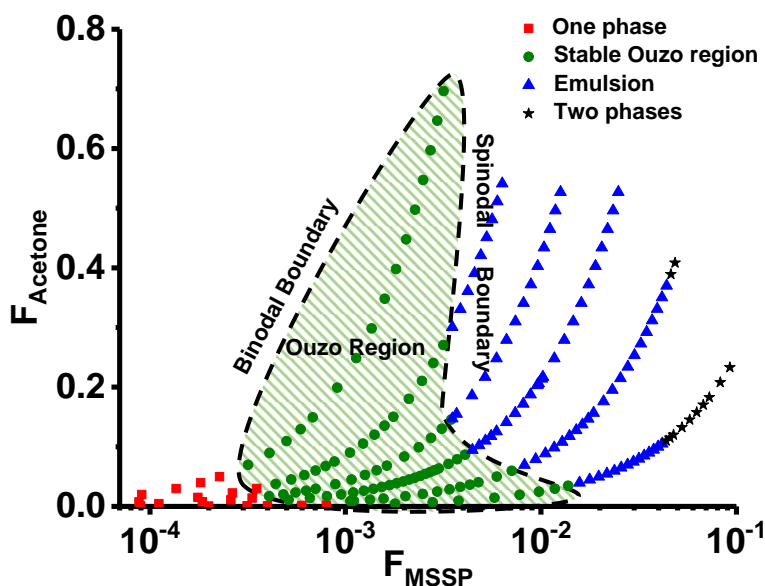
Figure 2.14. Phase diagram for the ternary system MSSP/acetone/water at 25°C represented by the mass fraction of MSSP as a function of mass fraction of acetone, depicting the one phase region (before the binodal boundary), stable "ouzo region" and unstable emulsion/two phase region (beyond the spinodal boundary)

As the amounts of MSSP and acetone, added increased, specific concentrations were reached that lay in the so-called ouzo region (shaded area) where stable nanoparticles are formed. The region is limited by the amount of MSSP and was determined as very narrow region

(about an order of magnitude) with respect to the mass fractions of MSSP. Addition of MSSP-
acetone solution leads to eventual phase separation between the MSSP and water due to
insolubility. The onset of the precipitation of MSSP noted as the spinodal boundary and observed
as increase in opacity of the mixture due to formation of large particles additionally some MSSP
formed oil droplets while other stuck to the vial and magnetic stirrer.

The binodal and spinodal boundaries were visually identified as the onset of turbidity
(and the mixture turns into opaque emulsion (phase separation), respectively (Figure 2.15.). At
low mass fractions of MSSP ($<10^{-4}$), the dissolved polymer is miscible with water as indicated
by the transparent single phase. Increasing mass of fraction of MSSP led to turbidity as nano-
suspension is formed reaching a metastable region. Further increase of the mass fraction of
MSSP ($>10\text{-}2$) resulted in formation of opaque emulsions or visible polymer aggregates.
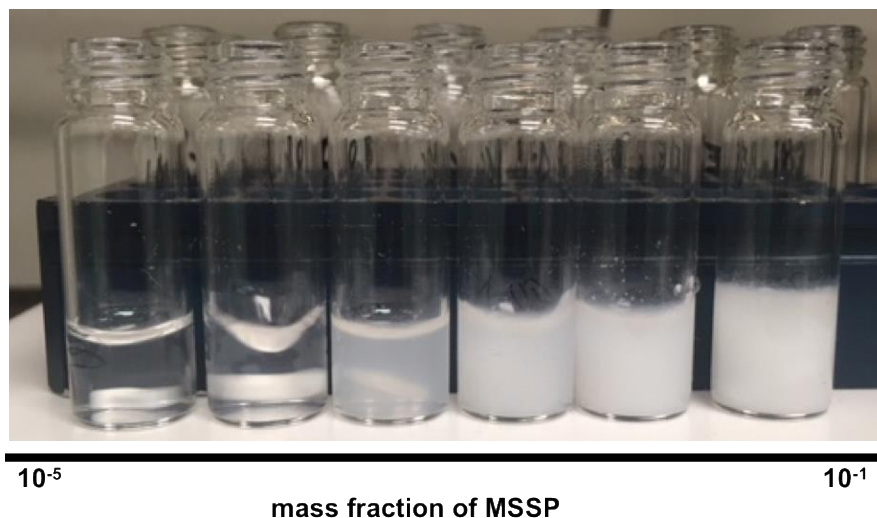
Figure 2.15. Photographic image of representative nano-suspensions with increasing MSSP mass
fractions

The organic solvent was evaporated off and resulting suspension analyzed to determine
particle size by means of DLS. Average particle size of the resulting nano-suspensions within the
ouzo region ranged from 70nm to 140nm (Figure 2.16.). These particles are within size range

(50-150nm) that ideal for applications in biological environment and encapsulation of guest molecules[36, 60-62]. On the other hand, higher mass fractions of MSSP produced larger particles with diameters reaching up to 490nm.
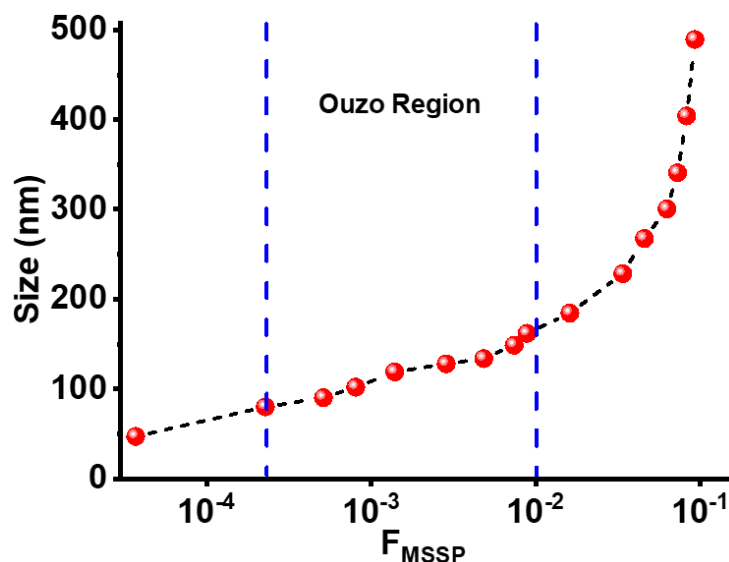
Figure 2.16. Soysomes particle size as a function of the mass fraction of MSSP

Factors Governing Soysomes Stability

The most interesting observation we had was that the Soysomes were stable and able to retain their particle size in aqueous conditions without the inclusion of surfactants. Stability of nanoparticles suspensions is crucial for application as encapsulants in drug formulations.[63] Stabilization of nanoparticulate systems is dependent on interfacial forces; and therefore, achieved by either steric or electrostatic effects.[64, 65] Many nanoparticle suspensions achieve steric stabilization via the addition of steric stabilizers[21, 67, 68]. On the other hand, electrostatic stabilization via charge on the surface of the particles. However, some particles nanoparticle or colloidal systems are stabilized from the combination of steric effect and electrostatic repulsion.[66] However, the structure of MSSP allows for steric stabilization without the addition of surfactants or other aids. The electrostatic contribution in the Soysomes, originates from the surface charge on the particles. This was supported by the negative zeta potential determined by

DLS (Table 2.3.). Zeta potential is a measure of the charge of the particle and is used as an index for particle stability. A larger the zeta potential value means there is more charge on the surface of the particle, which implies greater repulsive interactions, and hence more stable particles. In comparison to extensively studied and commercially relevant, PEG-PLGA nanoparticles, Soysomes have a negative zeta potential, indicative of some contribution of charge stabilization. However, Soysomes stabilization is thermodynamic, which is typical for lyophilic colloidal systems.

Table 2.3. Comparison of Surface Charge for Soysomes and PEG-PLGA NPs

Sample	Polymer	Zeta Potential, mV
Soysomes	MSSP	-20.55 ± 1.01
PEG-PLGA NPs	PEG: PLGA (50:50)	-13.04 ± 0.80

In order to assess the stability of the Soysomes further, we investigated the effect of temperature and pH on the nanoparticles post-fabrication. Figure 2.17 shows the effect of temperature on particle size of Soysomes. As such, the Soysomes were incubated at three different temperatures; 25°C to assess stability at standard room temperature, at 37°C to evaluate stability at average body temperature and at elevated temperature, 80°C in case of transportation conditions or heat sterilization. No significant changes in particle sizes were observed when a Soysomes suspension was maintained at 25 or 37 °C after short-term (3h) or long-term (24 h) temperature imposition; however, a slight increase in particle size was observed after 24 h when Soysomes were kept at 80 °C.
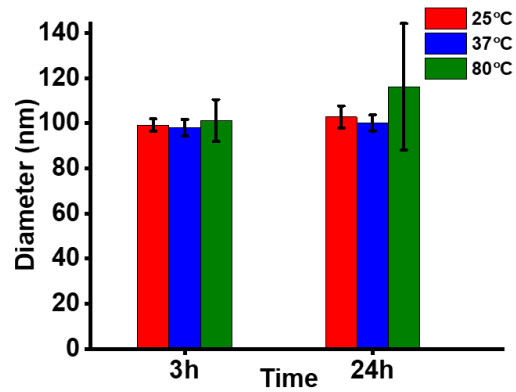
Figure 2.17. Effect of temperature on particle size of Soysomes after 3 h and 24 h period of exposure

For pH evaluation, three values were selected pH 5.5 representative of diseased tissue microenvironment, pH 7.4 representative of normal physiological pH and finally pH 12, as control conditions under which sucrose Soyate derivatives undergo alkaline hydrolysis. Soysomes particle sizes did not show significant changes when incubated at pH 5.5 and at pH 7.4, i.e., 126.17 ± 2.77 nm and 116.36 ± 4.61 nm (Figure 2.18), respectively, but decreased to 87.17 ± 1.84 nm at pH 12.0, most likely due to alkaline hydrolysis. Soysomes were also found to be stable for an extended period without coalescence, and we did not observe a substantial change in particle size or size distribution (Insert, Figure 2.18).
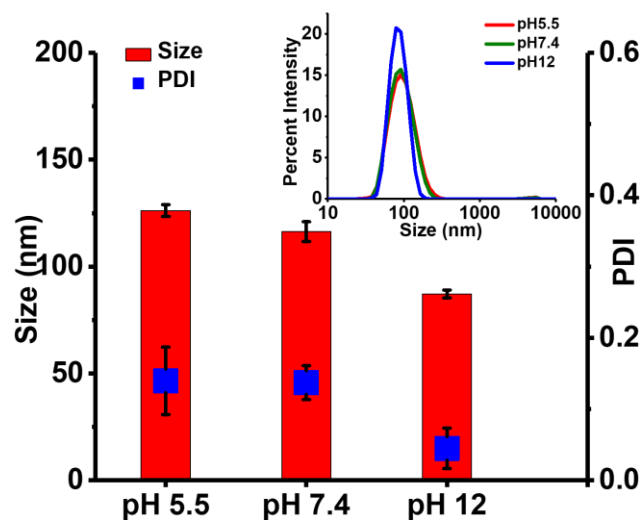
Figure 2.18. Effect of pH on the particle size of Soysomes. Insert: Effect of pH on particle size distribution profile of Soysomes

57

We evaluated the storage stability of Soysomes by incubating the nanoparticles at 4 °C in water and then analyzing particle size after 1 week and again after 5 months of storage. We observed that the Soysomes prepared from nanoprecipitation from DMF showed only a slight change in particle diameter from 137.63 ± 1.70 nm to 130.57 ± 1.45 nm after 5 months as displayed in Figure 2.19.
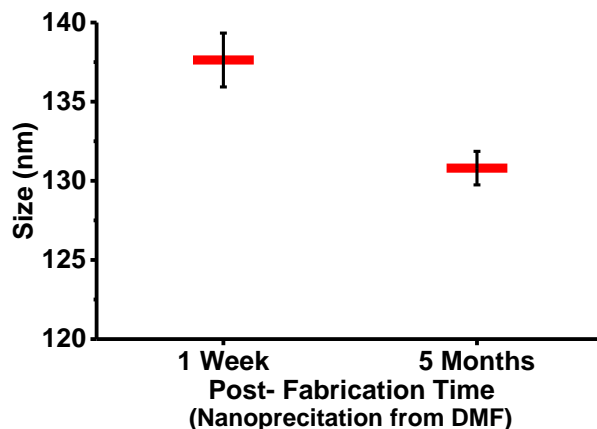
Figure 2.19. Effect of long-term (5 months) storage at 4°C on particle size of Soysomes prepared from DMF

This observation was attributed to an interplay of the solvent polarity, solvent-polymer interactions and rate of solvent diffusion. Solvents with a higher water miscibility have a diffusion rate fast enough to allow an efficient spontaneous emulsification of polymer in water. Hence, the diffusion rate of DMF out of nascent MSSP nanoparticles is much faster than that of acetonitrile and acetone, thereby giving smaller particles with a higher surface area of hydration around the particles, which most likely enhanced the stability of the nanoparticles in an aqueous environment.

In comparison, Soysomes prepared from acetone and acetonitrile, increased in particle size over long storage period by 20 nm for acetone (Figure 2.20. (a)) and by 40 nm for acetonitrile (Figure 2.20. (b)). Contrary to DMF, ACT and ACN, the diffusion rate is slower and likely competing closely with coalescence rate of MSSP; hence, larger particles were obtained

with these lower polarity solvents. Due to that large size, the particles become unstable in the aqueous environment and tend to flocculate over time. This was observed as an increase in particle size in Soysomes obtained from acetone and acetonitrile during the nanoprecipitation process. It, therefore, follows that DMF was selected as the solvent for preparing Soysomes due to the formation of nanoparticles within the optimal range for biological applications, i.e., between 50 and 120 nm.[23, 69]
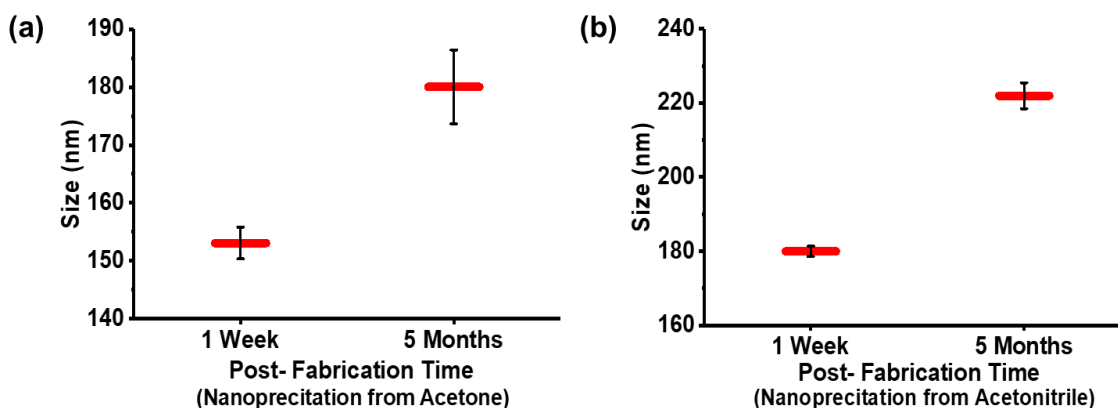
Figure 2.20. Effect of long-term (5 months) storage at 4°C on particle size of Soysomes prepared from (a) acetone and (b) acetonitrile

Determination of Critical Aggregation Concentration

To confirm the association behavior of MSSP and Soysomes stability in physiological environments, critical aggregation concentration, CAC, was determined using a well-known technique of measuring the solubilization of pyrene via fluorescence spectroscopy[70]. Pyrene is a hydrophobic molecule with a signature fluorescence signal that varies depending on the polarity of the environment[71-73]. We observed that the intensity of the vibrionic signals of pyrene in water increased with an increase in Soysomes and MSSP concentration in the suspension (Figure 2.21). This observation was due to the change in polarity of the microenvironment of pyrene from aqueous to hydrophobic, allowing pyrene to harbor itself within the nonpolar environment of the MSSP microstructure.
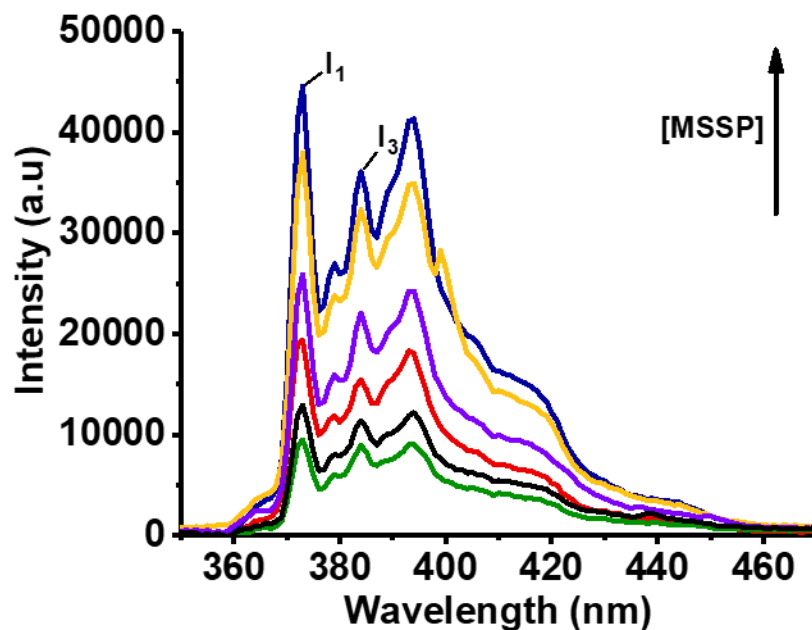
Figure 2.21. Fluorescence emission spectra showing the evolution of vibrionic signals (373 and 383 nm, I_1 and I_3 signals) of pyrene with increments of the Soysomes concentration in water, indicating the capacity of Soysomes to solubilize pyrene

The relationship between the ratio of intensity of pyrene signals at 373 and 383 nm, denoted as I_1 and I_3, respectively, and the polymer concentration enabled the determination of the critical aggregation concentration, CAC, of MSSP.[74-76] The ratio of intensities of pyrene vibrionic signals and 373nm and 383nm (i.e., I_1 and I_3 respectively), when plotted as a function of MSSP concentration (Figure 2.22.), showed an increase as the concentration of MSSP was increased, which abruptly plateaus around 10^{-4} M.

The CAC value was estimated from the intersection of the best-fit regression lines from this plot and found to be 0.364 mg/mL (1.06×10^{-4} M). The association behavior of nanoparticle-forming polymers and large molecules is critical as this parameter determines the solution and dilution stability of the aggregates in physiological conditions, particularly in blood circulation.
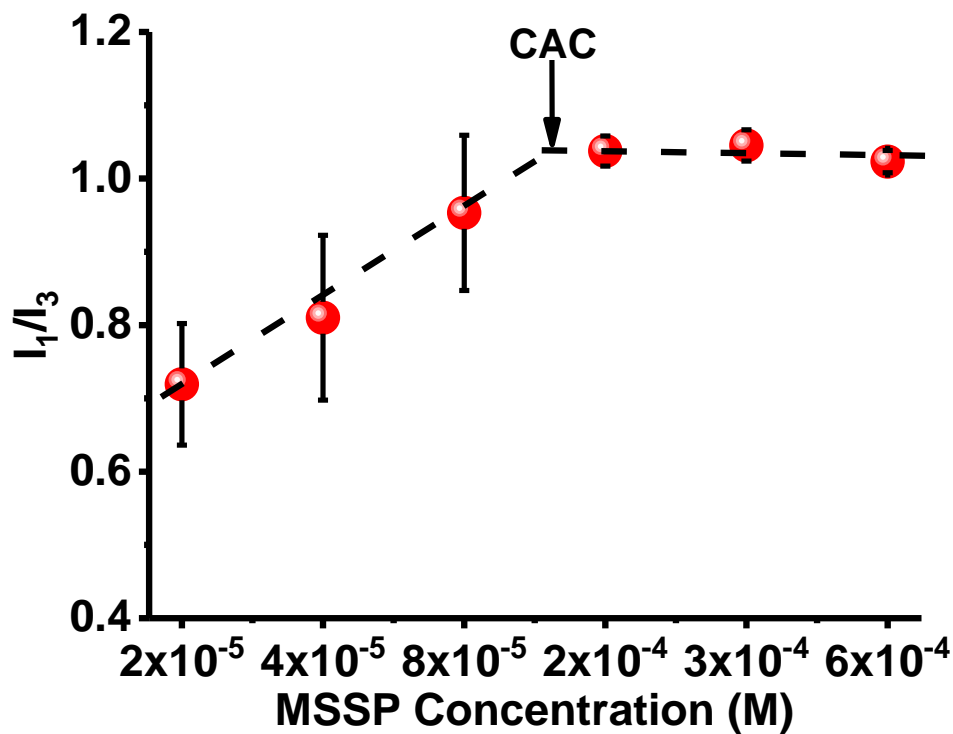
Figure 2.22. Plot of I_1/I_3 ratio as a function of MSSP concentration to determine the critical aggregation concentration (CAC)

The critical cloud point, i.e. concentration at which first colloidal structure is formed by the polymer, MSSP in water was identified using transmittance (Figure 2.23.). At low mass fractions of MSSP ($<10^{-3}$), the transmittance between 92-99% over 400-700nm range was observed. There was a sudden drop in transmittance after $f_{MSSP} \geq 10^{-3}$. The concentration of MSSP at the critical cloud point is within an order of magnitude of the critical aggregation concentration deduced using the pyrene-based fluorescence method.
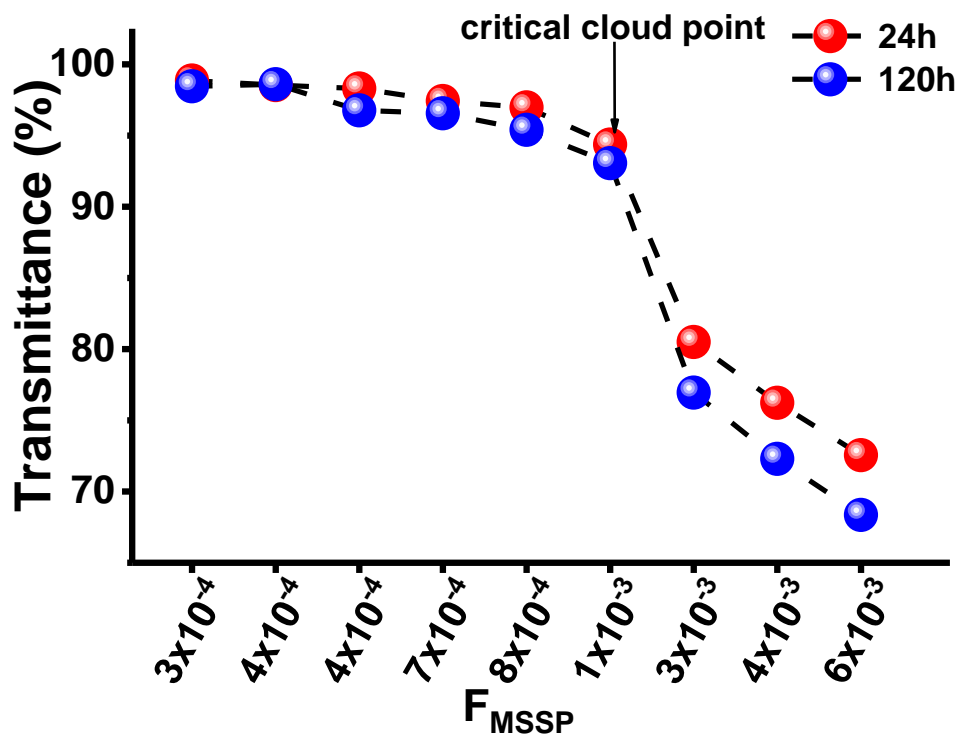
Figure 2.23. Critical cloud point identified as the inflection point on the of transmittance as a function of mass fraction of MSSP in the MSSP-acetone-water ternary system after removal of organic solvent

Generally, decrease in transmittance was observed after 120 h was observed in comparison to 24 h. This was attributed to evaporation of residual solvent, acetone. As the residual solvent diffuses out of the MSSP colloidal particles, this could result in some coalescence. As such, presence of larger particles increases the turbidity of the suspension resulting in more light scattering and reduces transmittance.

Conclusions

In this work, for the first time, the self-assembling behavior of methoxylated sucrose soyate polyol (MSSP), a sucrose octa-ester of soybean oil, was investigated. Using a facile nanoprecipitation technique, we established that MSSP possesses the unique property of forming stable colloidal particulate structures upon solvent-shifting, without the aid of surfactants. The MSSP nanoparticles, "Soysomes" exhibited narrow, monomodal distribution with particle sizes

suitable for use in a biological system. Computational studies confirmed the relationship between solvent type and formed Soysomes size. We observed that these nanoassemblies form stable nano-dispersions capable of encapsulating hydrophobic active pharmaceutical agents and exhibited long-term storage stability. Additionally, Soysomes were shown to be biodegradable in presence of enzyme lipase. Soysomes are a fascinating new platform for developing Biobased nanomaterials with the prospect of application as new biomaterials

References

1. Hammond, P. T., Nano tools pave the way to new solutions in infectious disease. ACS Infect. Dis. 2017, 3 (8), 554-558.

2. Dong, X.; Mattingly, C. A.; Tseng, M. T.; Cho, M. J.; Liu, Y.; Adams, V. R.; Mumper, R. J., Doxorubicin and paclitaxel-loaded lipid-based nanoparticles overcome multidrug resistance by inhibiting P-glycoprotein and depleting ATP. Cancer Res 2009, 69 (9), 3918-3926.

3. Forrest, M. L.; Yáñez, J. A.; Remsberg, C. M.; Ohgami, Y.; Kwon, G. S.; Davies, N. M. Paclitaxel prodrugs with sustained release and high solubility in poly (ethylene glycol)-b-poly (ε-caprolactone) micelle nanocarriers: pharmacokinetic disposition, tolerability, and cytotoxicity. Pharm. Res. 2008, 25 (1), 194-206.

4. Danhier, F.; Lecouturier, N.; Vroman, B.; Jérôme, C.; Marchand-Brynaert, J.; Feron, O.; Préat, V., Paclitaxel-loaded PEGylated PLGA-based nanoparticles: in vitro and in vivo evaluation. J. Controlled Release 2009, 133 (1), 11-17.

5. Yallapu, M. M.; Khan, S.; Maher, D. M.; Ebeling, M. C.; Sundram, V.; Chauhan, N.; Ganju, A.; Balakrishna, S.; Gupta, B. K.; Zafar, N., Anti-cancer activity of curcumin loaded nanoparticles in prostate cancer. Biomaterials 2014, 35 (30), 8635-8648.

6.   Duncan, R., Polymer conjugates as anticancer nanomedicines. Nat. Rev. Cancer 2006, 6 (9), 688.

7.   Farokhzad, O. C.; Cheng, J.; Teply, B. A.; Sherifi, I.; Jon, S.; Kantoff, P. W.; Richie, J. P.; Langer, R., Targeted nanoparticle-aptamer bioconjugates for cancer chemotherapy in vivo. Proc. Natl. Acad. Sci. U. S. A.2006, 103 (16), 6315-6320.

8.   Neibert, K.; Gopishetty, V.; Grigoryev, A.; Tokarev, I.; Al-Hajaj, N.; Vorstenbosch, J.; Philip, A.; Minko, S.; Maysinger, D., Wound-Healing with Mechanically Robust and Biodegradable Hydrogel Fibers Loaded with Silver Nanoparticles. Adv. Healthcare Mater. 2012, 1 (5), 621-630.

9.   Lligadas, G.; Ronda, J. C.; Galia, M.; Cádiz, V., Plant oils as platform chemicals for polyurethane synthesis: current state-of-the-art. Biomacromolecules 2010, 11 (11), 2825-2835.

10.   Lligadas, G.; Ronda, J. C.; Galià, M.; Cádiz, V., Poly (ether urethane) networks from renewable resources as candidate biomaterials: synthesis and characterization. Biomacromolecules 2007, 8 (2), 686-692.

11.   Lligadas, G.; Ronda, J. C.; Galia, M.; Cadiz, V., Renewable polymeric materials from vegetable oils: a perspective. Mater. Today 2013, 16 (9), 337-343.

12.   Miao, S.; Sun, L.; Wang, P.; Liu, R.; Su, Z.; Zhang, S., Soybean oil-based polyurethane networks as candidate biomaterials: Synthesis and biocompatibility. Eur. J. Lipid Sci. Technol. 2012, 114 (10), 1165-1174.

13.   Miao, S.; Wang, P.; Su, Z.; Zhang, S., Vegetable-oil-based polymers as future polymeric biomaterials. Acta Biomater. 2014, 10 (4), 1692-1704.

14. Pan, X.; Sengupta, P.; Webster, D. C., Novel biobased epoxy compounds: epoxidized sucrose esters of fatty acids. Green Chem. 2011, 13 (4), 965-975.

15. Howie, J. K.; Schaefer, J. J.; Trout, J. E., Synthesis of polyol medium fatty acid polyesters. Google Patents: 2006.

16. Nelson, T. J.; Bultema, L.; Eidenschink, N.; Webster, D. C., Bio-based high functionality polyols and their use in 1K polyurethane coatings. J. Renewable Mater. 2013, 1 (2), 141-153.

17. Ma, S.; Webster, D. C., Naturally occurring acids as cross-linkers to yield VOC-free, high-performance, fully bio-based, degradable thermosets. Macromolecules 2015, 48 (19), 7127-7137.

18. Tsujimoto, T.; Takayama, T.; Uyama, H., Biodegradable shape memory polymeric material from epoxidized soybean oil and polycaprolactone. Polymers 2015, 7 (10), 2165-2174.

19. Chitemere, R.; Stafslien, S.; Jiang, L.; Webster, D.; Quadir, M., Soy-Based Soft Matrices for Encapsulation and Delivery of Hydrophilic Compounds. Polymers 2018, 10 (6), 583.

20. Langer, R.; Peppas, N. A., Advances in biomaterials, drug delivery, and bionanotechnology. AIChE J. 2003, 49 (12), 2990-3006.

21. Leroueil-Le Verger, M.; Fluckiger, L.; Kim, Y.-I.; Hoffman, M.; Maincent, P., Preparation and characterization of nanoparticles containing an antihypertensive agent. Eur. J. Pharm. Biopharm. 1998, 46 (2), 137-143.

22. Cheng, J.; Teply, B. A.; Sherifi, I.; Sung, J.; Luther, G.; Gu, F. X.; Levy-Nissenbaum, E.; Radovic-Moreno, A. F.; Langer, R.; Farokhzad, O. C., Formulation of functionalized

PLGA–PEG nanoparticles for in vivo targeted drug delivery. Biomaterials 2007, 28 (5), 869-876.

23.   Hans, M.; Lowman, A., Biodegradable nanoparticles for drug delivery and targeting. Curr. Opin. Solid State Mater. Sci. 2002, 6 (4), 319-327.

24.   Yoo, H. S.; Lee, K. H.; Oh, J. E.; Park, T. G., In vitro and in vivo anti-tumor activities of nanoparticles based on doxorubicin–PLGA conjugates. J. Controlled Release 2000, 68 (3), 419-431.

25.   Rivas, C. J. M.; Tarhini, M.; Badri, W.; Miladi, K.; Greige-Gerges, H.; Nazari, Q. A.; Rodríguez, S. A. G.; Román, R. Á.; Fessi, H.; Elaissari, A., Nanoprecipitation process: From encapsulation to drug delivery. Int. J. Pharm. 2017, 532 (1), 66-81.

26.   Arias, J.; Gallardo, V.; Gomez-Lopera, S.; Plaza, R.; Delgado, A., Synthesis and characterization of poly (ethyl-2-cyanoacrylate) nanoparticles with a magnetic core. J. Controlled Release 2001, 77 (3), 309-321.

27.   Polk, A.; Amsden, B.; De Yao, K.; Peng, T.; Goosen, M., Controlled release of albumin from chitosan-alginate microcapsules. J. Pharm. Sci. 1994, 83 (2), 178-185.

28.   Fessi, H.; Puisieux, F.; Devissaguet, J. P.; Ammoury, N.; Benita, S., Nanocapsule formation by interfacial polymer deposition following solvent displacement. Int. J. Pharm. 1989, 55 (1), R1-R4.

29.   Rossi, L.; ten Hoorn, J. W. S.; Melnikov, S. M.; Velikov, K. P., Colloidal phytosterols: synthesis, characterization and bioaccessibility. Soft Matter 2010, 6 (5), 928-936.

30.   Thioune, O.; Fessi, H.; Devissaguet, J.; Puisieux, F., Preparation of pseudolatex by nanoprecipitation: influence of the solvent nature on intrinsic viscosity and interaction constant. Int. J. Pharm. 1997, 146 (2), 233-238.

31.   Quintanar-Guerrero, D.; Allémann, E.; Fessi, H.; Doelker, E., Preparation techniques and mechanisms of formation of biodegradable nanoparticles from preformed polymers. Drug Dev. Ind. Pharm. 1998, 24 (12), 1113-1128.

32.   Galindo-Rodriguez, S.; Allémann, E.; Fessi, H.; Doelker, E., Physicochemical parameters associated with nanoparticle formation in the salting-out, emulsification-diffusion, and nanoprecipitation methods. Pharm. Res. 2004, 21 (8), 1428-1439.

33.   Beck-Broichsitter, M.; Rytting, E.; Lebhardt, T.; Wang, X.; Kissel, T, Preparation of nanoparticles by solvent displacement for drug delivery: a shift in the "ouzo region" upon drug loading. European J. Pharm. Sci. 2010, 41 (2), 244-253.

34.   Govender, T.; Stolnik, S.; Garnett, M. C.; Illum, L.; Davis, S. S., PLGA nanoparticles prepared by nanoprecipitation: drug loading and release studies of a water soluble drug. J. Controlled Release 1999, 57 (2), 171-185.

35.   Barichello, J. M.; Morishita, M.; Takayama, K.; Nagai, T., Encapsulation of hydrophilic and lipophilic drugs in PLGA nanoparticles by the nanoprecipitation method. Drug Dev. Ind. Pharm. 1999, 25 (4), 471-476.

36.   Bilati, U.; Allémann, E.; Doelker, E., Development of a nanoprecipitation method intended for the entrapment of hydrophilic drugs into nanoparticles. European J. Pharm. Sci. 2005, 24 (1), 67-75.

37.   Farokhzad, O. C.; Jon, S.; Khademhosseini, A.; Tran, T.-N. T.; LaVan, D. A.; Langer, R., Nanoparticle-aptamer bioconjugates. Cancer Res 2004, 64 (21), 7668-7672.

38.   Sanson, C.; Schatz, C.; Le Meins, J.-F.; Soum, A.; Thévenot, J.; Garanger, E.; Lecommandoux, S., A simple method to achieve high doxorubicin loading in biodegradable polymersomes. J. Controlled Release 2010, 147 (3), 428-435.

39.   Stewart, J. J., Optimization of parameters for semiempirical methods V: modification of

        NDDO approximations and application to 70 elements. J. Mol. Model. 2007, 13 (12),

        1173-1213.

40.   Puzyn, T.; Suzuki, N.; Haranczyk, M.; Rak, J., Calculation of quantum-mechanical

        descriptors for QSPR at the DFT level: is it necessary? J. Chem. Inf. Model. 2008, 48 (6),

        1174-1180.

41.   Devillers, J., Neural networks in QSAR and drug design. Academic Press: 1996.

42.   Gramatica, P.; Chirico, N.; Papa, E.; Cassani, S.; Kovarich, S., QSARINS: a new

        software for the development, analysis, and validation of QSAR MLR models. J.

        Comput. Chem. 2013, 34 (24), 2121-2132.

43.   Salatin, S.; Barar, J.; Barzegar-Jalali, M.; Adibkia, K.; Kiafar, F.; Jelvehgari, M.,

        Development of a nanoprecipitation method for the entrapment of a very water soluble

        drug into Eudragit RL nanoparticles. Res. Pharm. Sci. 2017, 12 (1), 1.

44.   Miladi, K.; Sfar, S.; Fessi, H.; Elaissari, A., Polymer Nanoparticles for Nanomedicines.

        Springer International Publishing: Switzerland, 2016; 1, 641.

45.   Prat, D.; Wells, A.; Hayler, J.; Sneddon, H.; McElroy, C. R.; Abou-Shehada, S.; Dunn,

        P. J., CHEM21 selection guide of classical-and less classical-solvents. Green Chem.

        2015, 18 (1), 288-296.

46.   Schubert, S.; Delaney Jr, J. T.; Schubert, U. S., Nanoprecipitation and nanoformulation

        of polymers: from history to powerful possibilities beyond poly (lactic acid). Soft Matter

        2011, 7 (5), 1581-1588.

47.   Visaveliya, N.; Köhler, J. M., Control of shape and size of polymer nanoparticles aggregates in a single-step microcontinuous flow process: a case of flower and spherical shapes. Langmuir 2014, 30 (41), 12180-12189.

48.   Dan, K.; Bose, N.; Ghosh, S., Vesicular assembly and thermo-responsive vesicle-to-micelle transition from an amphiphilic random copolymer. Chem. Commun. 2011, 47 (46), 12491-12493.

49.   Miller, C. A., Spontaneous emulsification produced by diffusion—a review. Colloids Surf. 1988, 29 (1), 89-102.

50.   Reis, C. P.; Neufeld, R. J.; Ribeiro, A. J.; Veiga, F., Nanoencapsulation I. Methods for preparation of drug-loaded polymeric nanoparticles. Nanomedicine: Nanotechnology, Biology and Medicine 2006, 2 (1), 8-21.

51.   Davies, J. T., Interfacial phenomena. Elsevier: 2012.

52.   Yan, X.; Delgado, M.; Fu, A.; Alcouffe, P.; Gouin, S. G.; Fleury, E.; Katz, J. L.; Ganachaud, F.; Bernard, J., Simple but precise engineering of functional nanocapsules through nanoprecipitation. Angew. Chem., Int. Ed. 2014, 53 (27), 6910-6913.

53.   Sitnikova, N. L.; Sprik, R.; Wegdam, G.; Eiser, E., Spontaneously formed trans-anethol/water/alcohol emulsions: mechanism of formation and stability. Langmuir 2005, 21 (16), 7083-7089.

54.   Peng, S.; Xu, C.; Hughes, T. C.; Zhang, X., From nanodroplets by the ouzo effect to interfacial nanolenses. Langmuir 2014, 30 (41), 12270-12277.

55.   Hou, W.; Xu, J., Surfactant-free microemulsions. Curr. Opin. Colloid Interface Sci. 2016, 25, 67-74.

56. Vitale, S. A.; Katz, J. L. Liquid droplet dispersions formed by homogeneous liquid−liquid nucleation:"the Ouzo effect". Langmuir. 2003, 19 (10), 4105-4110.

57. Goller, M. I.; Obey, T. M.; Teare, D. O.; Vincent, B.; Wegener, M. R., Inorganic "silicone oil" microgels. Colloids Surf., A 1997, 123, 183-193.

58. Edmond, E.; Ogston, A., An approach to the study of phase separation in ternary aqueous systems. Biochem. J. 1968, 109 (4), 569-576.

59. Ganachaud, F.; Katz, J. L., Nanoparticles and nanocapsules created using the ouzo effect: spontaneous emulsification as an alternative to ultrasonic and high-shear devices. ChemPhysChem 2005, 6 (2), 209-216.

60. Legrand, P.; Lesieur, S.; Bochot, A.; Gref, R.; Raatjes, W.; Barratt, G.; Vauthier, C., Influence of polymer behaviour in organic solution on the production of polylactide nanoparticles by nanoprecipitation. Int. J. Pharm. 2007, 344 (1-2), 33-43.

61. Chorny, M.; Fishbein, I.; Danenberg, H. D.; Golomb, G., Lipophilic drug loaded nanospheres prepared by nanoprecipitation: effect of formulation variables on size, drug recovery and release kinetics. J. Controlled Release 2002, 83 (3), 389-400.

62. Lepeltier, E.; Bourgaux, C.; Couvreur, P., Nanoprecipitation and the "Ouzo effect": Application to drug delivery devices. Adv. Drug Delivery Rev. 2014, 71, 86-97.

63. Thorat, A. A.; Dalvi, S. V., Liquid antisolvent precipitation and stabilization of nanoparticles of poorly water soluble drugs in aqueous suspensions: Recent developments and future perspective. Chem. Eng. J. 2012, 181, 1-34.

64. Joye, I. J.; McClements, D. J., Production of nanoparticles by anti-solvent precipitation for use in food systems. Trends Food Sci. Technol. 2013, 34 (2), 109-123.

65. Chan, H.-K.; Kwok, P. C. L., Production methods for nanodrug particles using the bottom-up approach. Adv. Drug Delivery Rev. 2011, 63 (6), 406-416.

66. Lourenco, C.; Teixeira, M.; Simões, S.; Gaspar, R., Steric stabilization of nanoparticles: size and surface properties. Int. J. Pharm. 1996, 138 (1), 1-12.

67. Kwon, H.-Y.; Lee, J.-Y.; Choi, S.-W.; Jang, Y.; Kim, J.-H., Preparation of PLGA nanoparticles containing estrogen by emulsification–diffusion method. Colloids Surf., A 2001, 182 (1-3), 123-130.

68. Perez, C.; Sanchez, A.; Putnam, D.; Ting, D.; Langer, R.; Alonso, M., Poly (lactic acid)-poly (ethylene glycol) nanoparticles as new carriers for the delivery of plasmid DNA. J. Controlled Release 2001, 75 (1-2), 211-224.

69. Sonavane, G.; Tomoda, K.; Makino, K., Biodistribution of colloidal gold nanoparticles after intravenous administration: effect of particle size. Colloids Surf., B 2008, 66 (2), 274-280.

70. Aubry, J.; Ganachaud, F.; Cohen Addad, J.-P.; Cabane, B., Nanoprecipitation of polymethylmethacrylate by solvent shifting: 1. Boundaries. Langmuir 2009, 25 (4), 1970-1979.

71. Kalyanasundaram, K.; Thomas, J., Environmental effects on vibronic band intensities in pyrene monomer fluorescence and their application in studies of micellar systems. J. Am. Chem. Soc. 1977, 99 (7), 2039-2044.

72. Torchilin, V. P., Structure and design of polymeric surfactant-based drug delivery systems. J. Controlled Release 2001, 73 (2-3), 137-172.

73. Jones, M.-C.; Leroux, J.-C., Polymeric micelles–a new generation of colloidal drug carriers. Eur. J. Pharm. Biopharm. 1999, 48 (2), 101-111.

74.	Topel, Ö.; Çakır, B. A.; Budama, L.; Hoda, N., Determination of critical micelle concentration of polybutadiene-block-poly (ethyleneoxide) diblock copolymer by fluorescence spectroscopy and dynamic light scattering. J. Mol. Liq. 2013, 177, 40-43.

75.	Wilhelm, M.; Zhao, C. L.; Wang, Y.; Xu, R.; Winnik, M. A.; Mura, J. L.; Riess, G.; Croucher, M. D., Poly (styrene-ethylene oxide) block copolymer micelle formation in water: a fluorescence probe study. Macromolecules 1991, 24 (5), 1033-1040.

76.	Zhao, C. L.; Winnik, M. A.; Riess, G.; Croucher, M. D., Fluorescence probe techniques used to study micelle formation in water-soluble block copolymers. Langmuir 1990, 6 (2), 514-516.

CHAPTER 3. ENCAPSULATION AND TRANSPORT PROPERTIES OF SELF-ASSEMBLED SUCROSE SOYATES[12]

Abstract

A new class of biobased nanocarriers, Soysomes, has been discovered and investigated. These nanocarriers are derived from a synthetically accessible, scalable sucrose soyate, methoxylated sucrose soyate polyol (MSSP), derived from chemical building blocks obtained from soybean oil and sucrose. We observed for the first time that MSSP, when dissolved in an organic solvent of different polarity and slowly added to an aqueous phase at a predetermined rate under "nanoprecipitation" conditions, will form a stable, self-assembled structure with a size range from 100 to 200 nm depending on the polarity difference between the precipitating solvent pairs. We also found that the Soysomes were able to encapsulate and release a hydrophobic bioactive compound, such as curcumin. Both MSSP and their self-assembled structures were highly biocompatible and did not trigger cellular toxicity to mammalian cell lines. Our experiments showed that such 100% biobased, non-cytotoxic material as MSSP and a related class of products have the potential for use toward the sustainable manufacturing of drug nanocarriers for biomedical applications.

---

[1] This chapter contains some material adapted with permission from Chitemere, R. P.; Stafslien, S.; Rasulev, B.; Webster, D. C.; Quadir, M., Soysome: A surfactant-free, fully biobased, self-assembled platform for nanoscale drug delivery applications. ACS Appl. Bio Mater. 2018, 1 (6), 1830-1841. Copyright 2018 American Chemical Society.

[2] Some material in this chapter was co-authored by Ruvimbo Chitemere (Wright), Shane Stafslien; Dean Webster and Mohiuddin Quadir. Ruvimbo Chitemere (Wright) had primary responsibility for sample formulation, conducting experiments, materials characterization and data interpretation. Ruvimbo Chitemere (Wright) was the primary developer of the conclusions that are advanced here. Ruvimbo Chitemere (Wright) also drafted and revised all versions of this chapter. Shane Stafslien carried out the bright field microscopy study. Dean Webster and Mohiuddin Quadir conceived and designed the experiments. Mohiuddin Quadir served as proofreader and corresponding author.

Introduction

Efficient transport of therapeutic agents to pathological tissues constitutes a cornerstone of modern medicine. The popularly termed "drug delivery" is an area of research that has gained unprecedented traction in the pharmaceutical sector. Physiologically, drug delivery systems in most cases composed of synthetic polymers or self-assembling small molecular amphiphilic aggregates, encapsulate and protect the drug from systemic degradation and enhance their pharmacokinetic properties. An engineered drug delivery system can open up newer, sustainable avenues of so-termed "drug repurposing" and spare huge financial and environmental burdens required to synthesize a novel drug candidate. Pharmaceutical excipients, many of which are used to enhance drug delivery efficiency, have a projected market size in 2021 of 8.4 billion USD.[1]

The global surge of miniaturizing tools and technologies has also influenced a paradigm shift in this area, from conventional drug delivery toward the emergence of nanomedicine[2-11]. Polymer-based nanoparticles are the most commonly used platform for preparing nanodrug delivery systems affecting the pharmacokinetic and pharmacodynamics profile of the active agent[12-14]. However, achieving a "safe-by-design", self-assembling biocompatible polymer derived through a simplified and sustainable synthetic and purification pathway remains as one of the unmet challenges that are driving the research of polymer-derived drug delivery systems, and biomaterials in general, forward[15]. Hence, relatively newer polymers such as PEG-*b*-PLGA[16-18], PEG-*b*-poly (aspartate) [19] and PEG-*b*-poly (propargyl l-glutamate) [20] have gained traction as materials for forming nanodrug delivery systems.

Nanoparticles prepared from plant proteins such as zein, animal proteins such as albumin and gelatin, and complex carbohydrates such as chitosan, sodium alginate, and hyaluronic acids

have been successfully used for designing drug nanocarriers[21, 22]. However, biopolymers are often complex, heterogeneous and present batch-to-batch variability in comparison to the structural regularity of synthetic polymers. Agricultural resources, such as plant oils and sugars, are attractive monomeric platforms to generate customizable libraries of biobased large molecules with the added advantages of affordability, inherent biodegradability, low toxicity, high abundance, and accessibility[23-28]. For example, poly (glycerol sebacate) and poly (ester anhydride) derived from vegetable oil has found applications in soft tissue engineering and localized antitumor agent delivery[25, 29-34].

Owing to their high hydroxyl functionality and biobased content, structural diversity, ease of production, low price, and commercial abundance, vegetable oils such as soybean-derived polymers have been modified to prepare coating solutions, matrices for composites, and hybrid materials[27, 28, 37-39]. Additionally, soy-based products, i.e., hydrogenated soybean oil (NTIS accession no. PB266280) and soy protein isolate (NTIS accession no. PB300717), have long been classified as GRAS (generally regarded as safe by the FDA), rendering the material suitable for human use.[40]

Here we report the capacity and performance of nanoscale assembly of a fully biobased large molecule, MSSP as nanocarriers for hydrophobic guest molecules. Originally, MSSP was synthesized through a facile synthetic process involving the alcoholysis of the epoxidized sucrose ester of soybean oil fatty acids. Through this process, it was possible to synthesize MSSP of a molecular weight of 3.4 kDa with a moderately high viscosity of 2.5 kPa and a high hydroxyl functionality of 10.[37] MSSP like other sucrose Soyate derivatives were initially designed for coatings applications; however, MSSP has demonstrated self-assembling behavior, which opens fascinating new avenues for applications in biomedicine or pharmaceuticals. In this

report, we will discuss MSSP nanoparticles termed as "Soysomes" were prepared from MSSP using a nanoprecipitation method. These self-assembled nanoparticles were found to have the capacity to encapsulate and stabilize hydrophobic molecules in the aqueous phase and release them in a controlled pattern as well as increased bioavailability.

Experimental

Materials

Methoxylated Sucrose Soyate Polyol (MSSP) M_n 3442 g/mol obtained from Nelson et al. PEG–PLGA, curcumin, 5(6)-carboxyfluorescein, ACN, THF ACT, DMF, trifluoroacetic acid (TFA) and 1-octanol were purchased from Millipore Sigma. Triton CF-10 was used as a nonionic surfactant (Dow Chemical Co.). PTX purchased from LC Laboratories. All reagents were used as received unless otherwise stated. Pancreatic cancer cell line BxPC-3 was purchased from American Type Culture Collection (Manassas, VA). The BxPC-3 cells were cultured in RPMI media (Hyclone) supplemented with 10% fetal bovine serum (Hyclone) and 1% antibiotics, penicillin–streptomycin (Hyclone).

Preparation of Soysomes

Nanoprecipitation method[16, 17, 39, 40] was employed for the formation of soy-based nanoparticles. Briefly, MSSP (10mg/mL) was dissolved into organic solvent (DMF) which is miscible with water. The solution was allowed to stir for 30 min under ambient conditions. MSSP solution was added dropwise to water (1:3, organic solvent: water) using a syringe pump at a 0.2mL/min. The mixture was kept stirring under moderate speed through the addition procedure and maintained under same conditions for 15 h. To remove the organic solvent, the resulting colloidal suspension was dialyzed against water for 24 h using benzoylated dialysis

tubing MWCO 1200 (Sigma-Aldrich). The MSSP nanoparticles were purified by filtration using a 0.45 μm PES syringe filter (VWR).

A set of model compounds, i.e., curcumin and carboxyfluorescein, as well as paclitaxel have been encapsulated within Soysomes as representative hydrophobic molecules. In general, all guest compounds were co-dissolved with MSSP in respective organic solvents at a concentration of 1 mg/mL, giving a feed weight ratio (fwr) of 10%, as determined by equation 3.1:

$$fwr = \frac{Mass\ of\ Drug_{initial}}{Mass\ of\ Polymer_{initial}}\ x\ 100 \tag{3.1}$$

Solution was stirred for 30 min prior to nanoprecipitation to achieve encapsulation within Soysomes. All samples were prepared in triplicate. For curcumin, the amount of drug loaded within Soysomes was varied from 2–40 fwr % (i.e., 0.2, 1, 2, and 4 mg/mL) with respect to MSSP (10 mg/mL) to find out the critical encapsulation content.

To serve as a commercially relevant standard of comparison, PEG–PLGA nanoparticles (NPs) were prepared using a similar aforementioned nanoprecipitation method. In general, nanoparticles were formulated from a solution of PEG–PLGA (10 mg/mL) in DMF added dropwise to water at a 1:3 organic solvent–water ratio and a 0.2 mL/min infusion rate using a syringe pump. Curcumin-loaded PEG–PLGA NPs were prepared following same procedure after co-dissolving curcumin (1 mg/mL) and PEG–PLGA in DMF.

Characterization of Soysomes

Determination of Particle Size and Polydispersity by DLS

The hydrodynamic diameter and particle size distribution of Soysomes were measured by dynamic light scattering (Malvern Zetasizer Nano-ZS90) at 25 °C at a scattering angle of 90°

using disposable polystyrene cuvettes. After an equilibration period of 60 s, the intensity-weighted mean value was recorded as the average of three measurements.

Evaluation of Soysomes Morphology by TEM

A drop of the Soysomes suspension was placed on a 300 mesh Formvar-carbon-coated copper TEM grid (Electron Microscopy Sciences, Hatfield, Pennsylvania, USA) for 1 min and wicked off. Phosphotungstic acid (0.1%), pH adjusted to 7–8, was dropped onto the grid, allowed to stand for 2 min, and then wicked off. After the grids were dry, images were obtained using a JEOL JEM-2100 LaB6 transmission electron microscope (JEOL USA, Peabody, MA) running at 200 kV.

Determination of Partitioning of MSSP between Phases

Determination of MSSP Solubility in Octanol

The solubility of MSSP in octanol was evaluated using a dissolution test. Various amounts of MSSP (i.e., 1, 10, 50, 100 mg) were dissolved in 1 mL of 1-octanol and placed on a VWR vortex mixer at a fast speed.

Determination of the MSSP Concentration in Octanol

To determine whether MSSP crosses the interface between water and 1-octanol during a simulated release in a biphasic hydrophilic/lipophilic environment, 4 mL of a Soysomes suspension equivalent to 3.3 mg/mL of MSSP was mixed with an equal volume of 1-octanol and stirred at moderate speed for 8 h ($N = 3$). After 1, 3, 5, and 8 h intervals, the two phases were allowed to separate. The solvents were removed by evaporation, and the amount of MSSP in each phase was estimated gravimetrically[42]. The fraction of MSSP transferred to the organic phase was calculated using the following equation (3.2):

$$x = [\frac{MSSP_{org}}{MSSP_{aq}}]_0 = \frac{m(MSSP_{org})}{m(MSSP_{aq})} \tag{3.2}$$

where [MSSP$_{org}$] is the final MSSP concentration (mg/mL) in the organic phase, [MSSP$_{aq}$]$_0$ is the initial MSSP concentration in the aqueous phase, m (MSSP$_{org}$) is the weight of the MSSP (g) in the organic phase after the experiment, and m_0 (MSSP$_{aq}$) is the weight of the MSSP in the initial aqueous solution.

Evaluation of Content Stability

To identify the mechanistic and content encapsulation stability of Soysomes in fully aqueous conditions, we adopted a dye leakage experiment in pH 7.4. To this end, we used a freshly prepared, carboxyfluorescein-loaded Soysomes (500 µL) solution, taken in a dialysis cassette, Float-A-Lyzer G2 with MWCO 100–500 and placed in 5.5 mL of PBS (10 mM, pH 7.4). The dye leakage from Soysomes under such conditions was measured as a function of time, which was used as an indicator of structural instability of Soysomes at pH 7.4. In order to quantify the total carboxyfluorescein content in Soysomes, 20 µL of Triton CF-10, a nonionic surfactant, was added to a 500 µL Soysomes suspension at the end of the release experiment to degrade the particles and release all encapsulated dye[43]. For quantifying the amount of carboxyfluorescein released at an individual time point, the emission intensity of carboxyfluorescein at 515 nm was recorded in a Fluoromax-3 florescence spectrometer (Jobin Yvon Haribo) at an excitation wavelength of 480 nm. The percent release was determined using the following equation (3.3):

$$\% \ release \ of \ dye = \frac{F_i - F_0}{F - F_0} \ x \ 100 \tag{3.3}$$

where F_i is the emission intensity after release, F_0 is the emission intensity before release, and F is the emission intensity after Triton treatment.

Content Release Studies

The biphasic release pattern of curcumin from Soysomes was evaluated in water against octanol. This arrangement of drug release was used to mimic the environment prevailing at the interface between interstitial space (plasma rich) and cell membrane (phospholipid rich) [41]. A set of glass vials (4 mL) was charged with a certain volume of a curcumin-loaded MSSP nanoparticle suspension, and an equal volume of octanol was added to each vial; the release experiment was continued for 48 h with moderate stirring. The octanol phase was withdrawn and replaced with an equal volume of fresh octanol at an interval of 1 h for up to 8 h and then after 24 and 48 h. The withdrawn octanol samples were analyzed using UV–vis spectroscopy (Varian Cary 5000 UV–vis-NIR spectrophotometer) at $\lambda_{max} = 426$ nm. Percent release and cumulative percent release were calculated using the following equation (3.4):

$$\% \ release = \frac{M_t}{M_0} \ x \ 100 \tag{3.4}$$

where M_t is the amount of drug released at time t and M_0 is the total amount of drug loaded within Soysomes. Cumulative percentage release, on the other hand, was calculated using the following equation (3.5) and plotted as a function of time:

$$cumulative \ \% \ release = \frac{volume \ withdrawn}{volume \ of \ octanol \ phase} \ x \ \%release_t + \sum \%release_{t-1} \tag{3.5}$$

PTX loaded Soysomes were prepared at 0.5mg/mL PTX with 10mg/mL Soysomes. 0.5mL PTX-Soysomes were charged into a dialysis cassette, Float-A-Lyzer G2 MWCO 3.5-5kDa (Spectra-Por) and diluted to 1 mL with release media, PBS. The Float-A-Lyzer was placed in a holder receptacle with 3 mL of release media, equipped with a magnetic stir bar, and set at room temperature. At a regular interval, 100 µL aliquots were withdrawn from the bath volume and replenished with an equal volume of fresh media. The withdrawn samples were lyophilized and dissolved in ACN-water and concentrations determined by reverse-phase HPLC (LC 20AT,

Shimadzu). Reverse-phase HPLC was performed using isocratic flow 70:30 ACN: water with 0.01% (v/v) TFA at 40°C, with UV detection at 227nm.

Enzymatic Degradation Studies

The effect of enzymes esterase, lipase, and combination of the two on the Soysomes was evaluated by monitoring content stability of Soysomes. Curcumin loaded Soysomes were treated with the respective enzyme solution (3 mg/mL) at a 1:2 Soysomes to enzyme volumetric ratio. The enzyme treated Soysomes were incubated at 37 °C for 3 h. A sample of the media was withdrawn every 10 min for the first hour followed by 30 min sampling for the next 2 h, each time replacing the withdrawn volume with an equivalent of fresh media.

Cytotoxicity

Cell Culture

The pancreatic cancer cell line BxPC-3 was cultured in RPMI 1640 media (Hyclone) supplemented with 10% fetal bovine serum (Hyclone) and 1% penicillin–streptomycin (Hyclone). The cells were incubated in a chamber at 37 °C in 0.5 CO_2 and 74% relative humidity for 24 h. L929 mouse fibroblast cells were maintained in Eagle's minimum essential medium (EMEM) supplemented with 10% fetal bovine serum (FBS), penicillin (100 μg/mL), and streptomycin (100μg/mL).

Cell Viability Assessment

The cytotoxicity of curcumin-loaded and drug-free Soysomes and MSSP was assessed on BxPC-3 cells using the MTS assay. The cells were plated in 96-well plates at a seeding density of 5000 cells per well and allowed to grow in RPMI 1640 media supplemented with 10% fetal bovine serum and 1% penicillin–streptomycin. The plates were incubated for 24 h before treatment with curcumin-encapsulated Soysomes, Soysomes alone at an equivalent

concentration, curcumin, and 0.5% DMSO in water serving as a control. The curcumin

concentration was varied from 4.0 (10 µM) to 11.0 µg/mL (30 µM). The treated cells were

incubated for up to 48 h, and the cell toxicity was recorded after 24 and 72 h using the Cell Titer

96 cell proliferation assay kit (Promega) according to the supplier's protocol. The reagent was

added to all of the wells (20 µL) and incubated for 2 h. The absorbance at 490 nm was read using

a microplate reader (BioTek Synergy H1) and used for cell viability calculations. Cytotoxic

effects of pure MSSP (not assembled into nanoparticles) were also evaluated on noncancerous

cell lines, such as L929 mouse fibroblasts. For this experiment, cells were trypsinized and re-

suspended into fresh supplemented EMEM media and seeded into 96-well cell culture treated

plates at an inoculum density of 50 00 cells/mL. The plates were incubated for 24 h at 37 °C (5%

CO_2), and the EMEM was carefully removed using a multichannel pipet. Attached cells were

rinsed once with Hank's balanced salt solution (HBSS). Pure MSSP solutions prepared in HBSS

(0.01–100 µM) were transferred in triplicate to the rinsed, pre-cultured cells and incubated for 24

and 72 h at 37 °C (5% CO_2).

Bright field microscopy images were acquired on an inverted microscope prior to the

removal of MSSP-containing media for cell viability assessments. After the removal of spent

media, cells were rinsed 3 times with HBSS. A 0.5 g/L solution of MTT in HBSS (0.2 mL) was

added to each well and incubated for 4 h at 37 °C. After the stipulated period, the MTT solution

was removed from each well and 0.15 mL of DMSO was added. The plates were placed on an

orbital shaker (150 rpm; ambient temperature) for 15 min to solubilize the MTT dye. Absorbance

values were measured at 570 nm using a multi-well plate spectrophotometer (Tecan, Safire2).

Results and Discussion

Nanoparticle Synthesis

A facile solvent shifting technique, known as nanoprecipitation, was used for the preparation of Methoxylated Sucrose Soyate Polyol (MSSP) nanoparticles, "Soysomes". [16-18, 43-45] In this method, miscible solvent pair is utilized, in which the polymer is completely soluble in the one but insoluble in the other[46]. In this work, water was used as the nonsolvent (aqueous phase) and DMF was selected as the organic solvent based on water miscibility, good performance determined during investigation of factors that influence self-assembly behavior and properties of MSSP and capacity to solubilize a broad spectrum of compounds. We observed that MSSP dissolved in a water-miscible organic solvent formed an off-white suspension upon the addition of water. When the solution was subjected to dynamic light scattering, we observed the resulting suspension to have a tightly controlled particle size distribution with a low PDI (< 0.1).

Typical average particle size and polydispersity index (PDI) obtained from MSSP nanoparticles, termed Soysomes, are summarized in Table 3.1. The mean hydrodynamic diameter of Soysomes prepared from DMF ranged from 72.07 ± 2.86 nm to 147.00 ± 4.75 nm with marked increase in size as MSSP concentration was increased. All Soysomes had a very low PDI (<0.1) and narrow PDI width regardless of concentration of MSSP. The very low PDI observed indicated excellent homogeneity in preparation of Soysomes.

Table 3.1. Particle Size and Polydispersity Distribution of Soysomes Determined by DLS

MSSP concentration (mg/mL)	Average Size (nm)	PDI	PDI Width (nm)
1	72.07 ± 2.86	0.06 ± 0.04	13.84 ± 4.97
5	75.87 ± 1.40	0.05 ± 0.04	15.23 ± 5.74
10	100.06 ± 2.30	0.04 ± 0.03	18.07 ± 7.70
30	147.00 ± 4.75	0.07 ± 0.06	33.56 ± 16.86

TEM micrographs of the synthesized Soysomes are shown in Figure 3.1. The Soysomes were observed to be spherical in shape and exhibited a monomodal particle size distribution. The average particle size of the dehydrated particles measured from TEM ranged between 30-40nm.
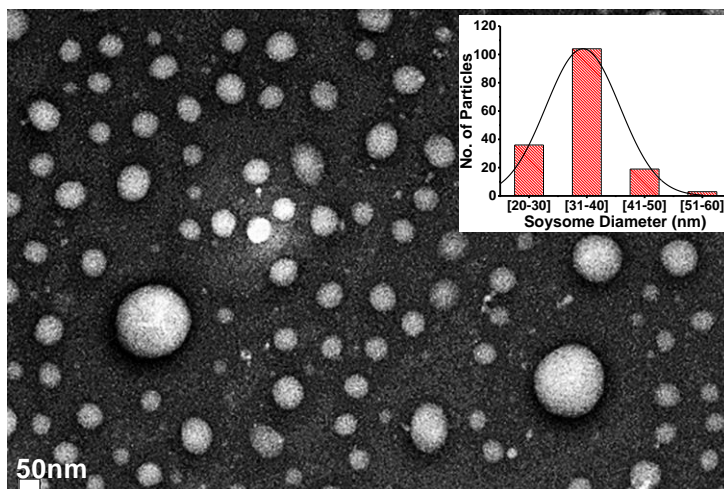
Figure 3.1. TEM micrograms of MSSP Soysomes with a scale bar of 50 nm. Insert: TEM histogram showing particle size distribution of Soysomes

Encapsulation and Release of Hydrophobic Guest Molecules

We observed that Soysomes were able to encapsulate a set of hydrophobic model compounds, as represented by curcumin. Encapsulation of the hydrophobic guest molecule was achieved by dissolving the compound and the MSSP in the respective organic phase, followed by slow precipitation of the mixed solution into the aqueous phase. Curcumin is a naturally occurring, hydrophobic compound with antioxidant, anti-coagulation, anti-inflammatory, and antitumor properties[22, 47-49]. Curcumin reportedly inhibits cell proliferation and induces apoptosis in several cancer cell lines including pancreatic, breast, lung, and prostate cancer[50-52]; however, its poor water solubility, stability, and low bioavailability restricts its antitumor efficacy and clinical use[53]. As with curcumin, the solubility and stability issue limit the therapeutic value of many potential hydrophobic drugs. Hence, we set out to investigate the property of Soysomes to encapsulate hydrophobic compounds.

Figure 3.2. shows the solubilization of curcumin (1mg/mL) by Soysomes compared to same concentration of free curcumin precipitating out in water. Using UV-Visible spectroscopy, we determined the critical point at which the Soysomes start encapsulating and transporting a substantial amount of hydrophobic drug, such as curcumin.
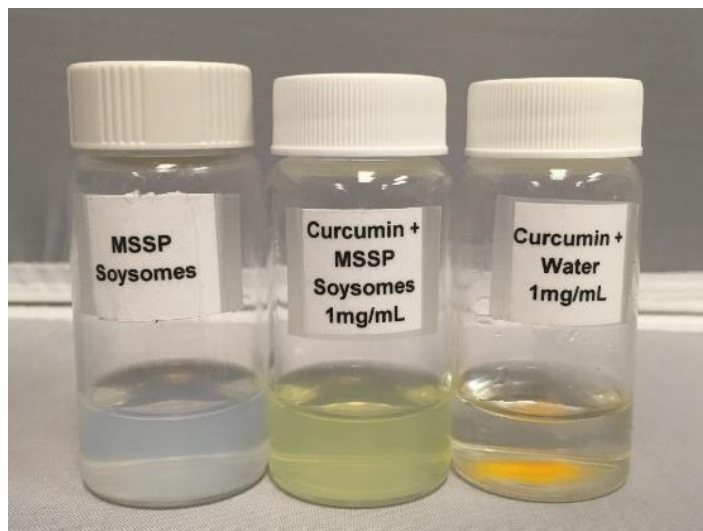
Figure 3.2. Photographic image representative of capacity of Soysomes to solubilize curcumin in comparison to water

A minimum loading 7.15 mol of curcumin/mol of MSSP in water was found as represented in Figure 3.3. For a nanocarrier system to be effective in a biological milieu, it has to release the encapsulated guest. Hence, we explored the pattern and rate of curcumin release from Soysomes microstructures. For these studies, Soysomes were first prepared with a fixed concentration of drug (1 mg/mL) and polymer (10 mg/mL) and loading efficiency determined as shown in Table 3.2. Loading efficiency was calculated according to equation 3.6:

$$Loading\ efficiency = \frac{mass\ of\ loaded\ drug}{initial\ mass\ of\ drug\ in\ solution - loss}\ x\ 100 \qquad (3.6)$$

In the case of curcumin as the encapsulated ingredient, Soysomes exhibited a 15.52% loading efficiency, which was 5% higher than the loading efficiency achieved with PEG–PLGA NPs.
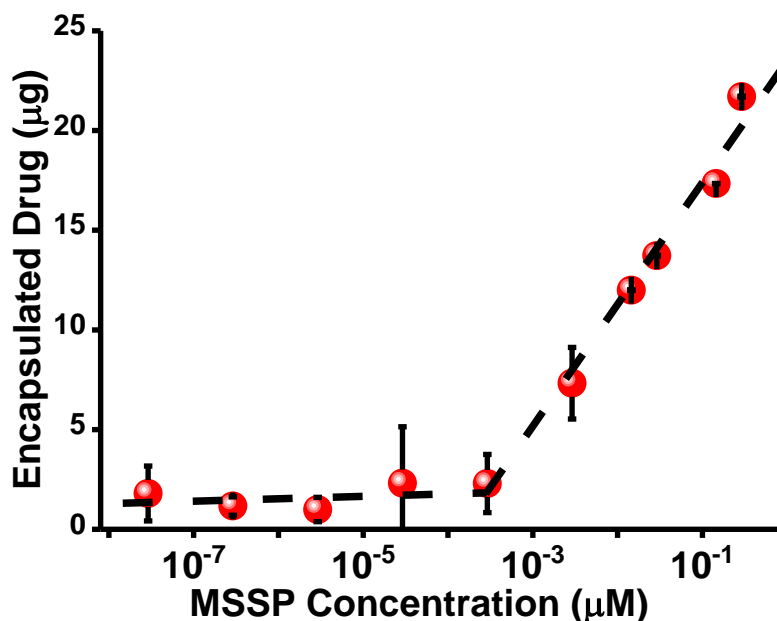
Figure 3.3. Determination of the minimum drug loading capacity of MSSP Soysomes

Table 3.2. Characterization of Loading Capacity of Soysomes in Comparison to PEG–PLGA NPs

Polymer in formulation	Payload	Fwr (wt. %)	Loading content (wt. %)	Loading efficiency (wt. %)	Size (nm)
MSSP	Curcumin	10	2.01	15.52	134.80 ± 3.02
	Carboxyfluorescein	10	2.68	35.19	111.90 ± 4.86
PEG–PLGA	curcumin	10	1.24	10.07	157.93 ± 3.74

To understand the mechanistic and content stability within the Soysomes structure, we conducted a dye-leaching experiment in aqueous conditions of pH 7.4 (to mimic systemic circulation). Soysomes were loaded with carboxyfluorescein in a similar manner as that for curcumin to yield carboxyfluorescein-loaded Soysomes. The loaded Soysomes were dialyzed against PBS pH 7.4 to ensure similar pH conditions prior to quantifying dye leaching that may result from water-mediated structural instability. Carboxyfluorescein encapsulation features are also presented in Table 3.2. We observed that Soysomes heavily suppressed nonspecific dye leaching in an aqueous environment for an extended period. We found that an almost insignificant amount (<1%) of the dye was liberated in PBS at pH 7.4 after 6 h (Figure 3.4.),

indicating an excellent aqueous stability of Soysomes and tight regulation over content leaching

from nanoparticles that can be induced as they circulate in the bloodstream.
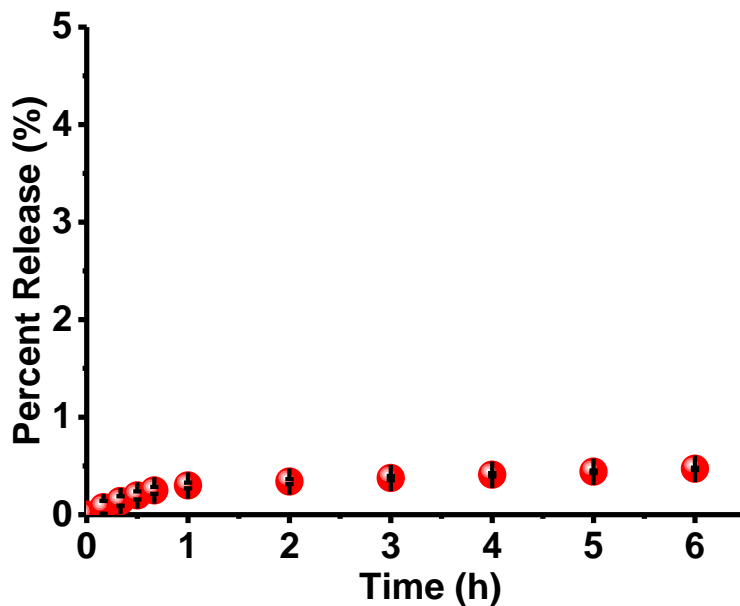
Figure 3.4. Release of encapsulated carboxyfluorescein from Soysomes under aqueous conditions.

Carboxyfluorescein was excited at 490nm and had maximum emission at 520nm. The

fluorescent spectra obtained from the released samples gave the characteristic signal of

carboxyfluorescein (Figure 3.5.). Encapsulation within Soysomes maintained the stability of the

dye.
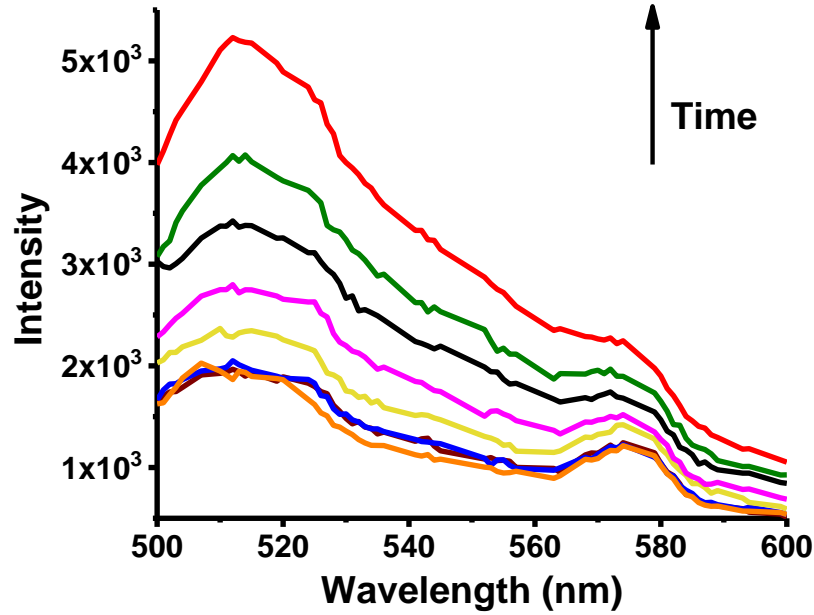
Figure 3.5. Evolution of fluorescence spectra of the released carboxyfluorescein over time

Contrary to the all aqueous environment set up for content stability studies, biphasic water–octanol system (Figure 3.6.) was used evaluate release at the interface of two phases which mimics drug release at the interfacial situation that exists between interstitial space (plasma-rich) and cell membrane (phospholipid-rich). The release of curcumin was studied as a function of temperature and pH using an octanol extraction method.
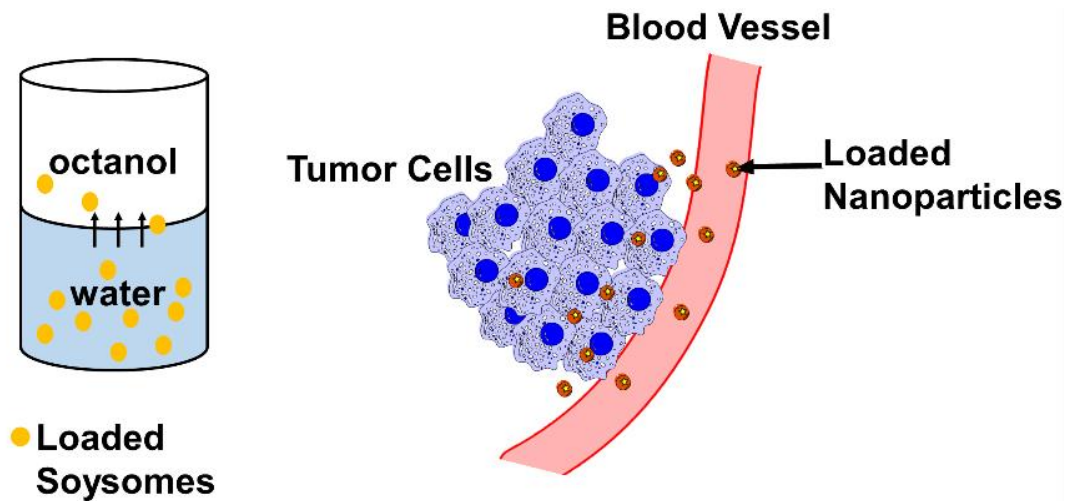
Figure 3.6. Schematic illustration of bi-phasic interfacial release between water and octanol in mimicking release from blood to cells

First, we observed that Soysomes mediated regulated release of the encapsulated drug in water for up to 8 h, after which 100% of the encapsulated content of curcumin was released at 25 °C. Elevating the temperature of the release media from 25 to 37 °C had no apparent effect on the rate of release of curcumin from Soysomes within a similar period (Figure 3.7.). The pH of the aqueous environment affected the release of curcumin from Soysomes significantly.
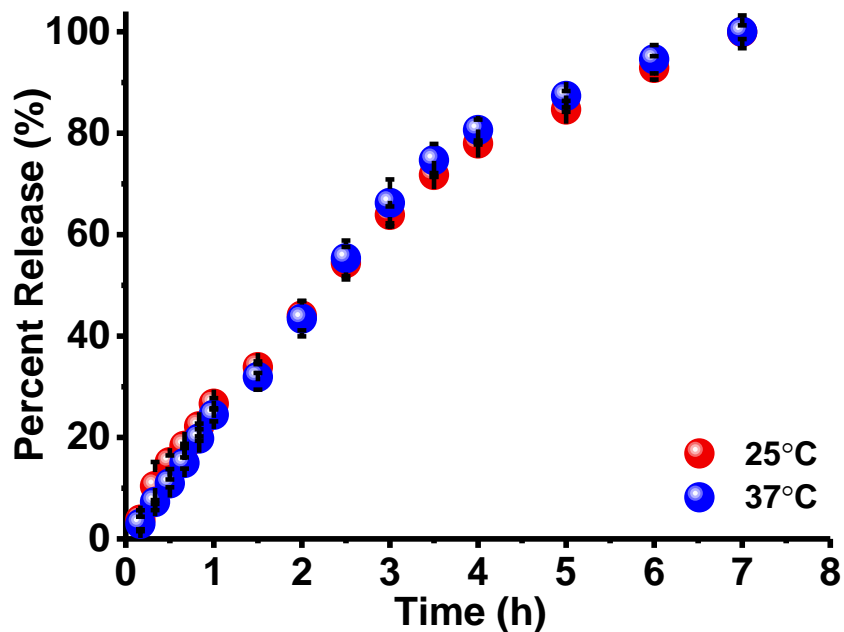
Figure 3.7. Curcumin release profile from Soysomes as a function of temperature

At pH 4.5, Soysomes released the encapsulated content almost quantitatively after 3 h (Figure 3.8.), compared to those at pH 7.4 where the release of the active drug was considerably sustained. Such release kinetics is valid in conditions where Soysomes are in close contact to lipid-rich media, i.e., a cell membrane or in a tissue microenvironment.
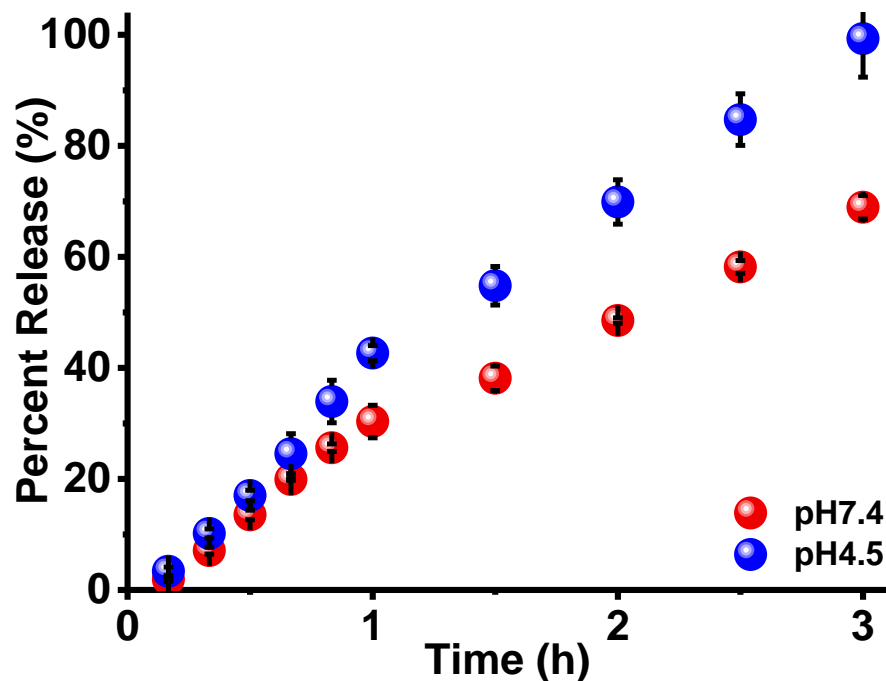
Figure 3.8. Curcumin release profile from Soysomes as a function of pH

We observed that during the release studies, some amount of Soysomes were also transferred to the octanol phase, accounting for $15.96 \pm 0.76\%$ of the mass of MSSP used for preparation of Soysomes. In comparison to amount of curcumin transported to octanol during biphasic release, a very small amount of MSSP is carried over into the octanol phase, up to five times less than the curcumin. Figure 3.9 shows the comparative percentage transfer of MSSP and Curcumin over 8 h; only $15.96 \pm 0.76\%$ of MSSP was transferred while an almost complete release of the encapsulated curcumin ($100 \pm 3.23\%$) occurred over that same time frame. This indicated that both diffusion of free curcumin out of Soysomes and Soysomes-mediated transfer of curcumin across the phases are occurring simultaneously during the release process.
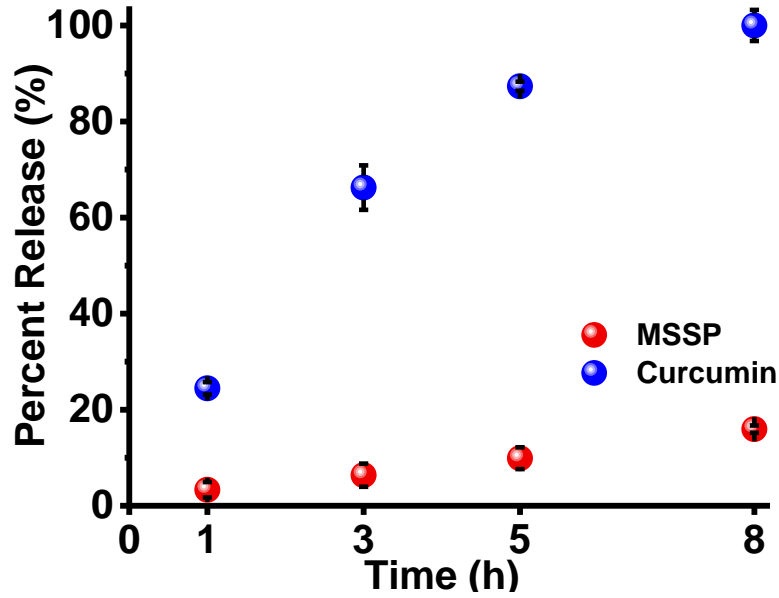
Figure 3.9. Comparison percent transfer of MSSP against release of curcumin into the octanol phase during drug release study

The release profile of curcumin from Soysomes was also compared to that from standard nanoparticle systems prepared with PEG–PLGA (Figure 3.10.).
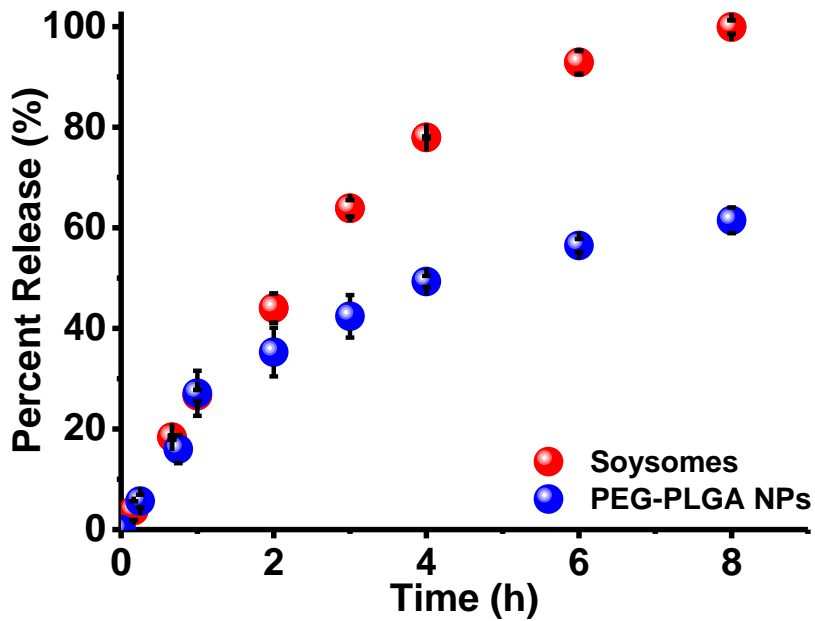
Figure 3.10. Comparative release profile of curcumin from Soysomes and PEG-PLGA NPs

PEG-PLGA based biomaterials have been previously studied for controlled release system because of the already established safety in clinical use[17, 54-57]. PEG-functionalization has been shown to increase pharmacokinetic properties of liposomes as well as improve systemic clearance of biomaterials[58-61]. We found out that under similar conditions, PEG–PLGA nanoparticles exhibited suppressed release in comparison to Soysomes; releasing only 60% of the encapsulated curcumin versus 100% from the Soysomes. Release profile of PTX was also evaluated.

To evaluate capacity to encapsulate a clinically relevant drug, PTX was loaded within Soysomes. PTX is highly toxic and hydrophobic anti-cancer drug that works as a microtubule inhibitor. It shows action against breast cancer, AIDS-related Kaposi sarcoma, non-small cell lung cancer and ovarian cancer. Due to its extremely poor water-solubility, efficient use of PTX is limited. Currently excipients used improve solubility for administration cause toxicity to cells upon repeated exposure. Encapsulation of PTX has the potential to increase solubility of the drug as well as reduce system toxicity. PTX was loaded into Soysomes, achieving stable nano-dispersion reaching up to 1mg/mL PTX. PTX was released under aqueous condition in PBS at room temperature. The released samples were quantified using reverse-phase HPLC. The amount of drug released in each aliquot was calculated from the calibration built from free drug (Figure 3.11.)
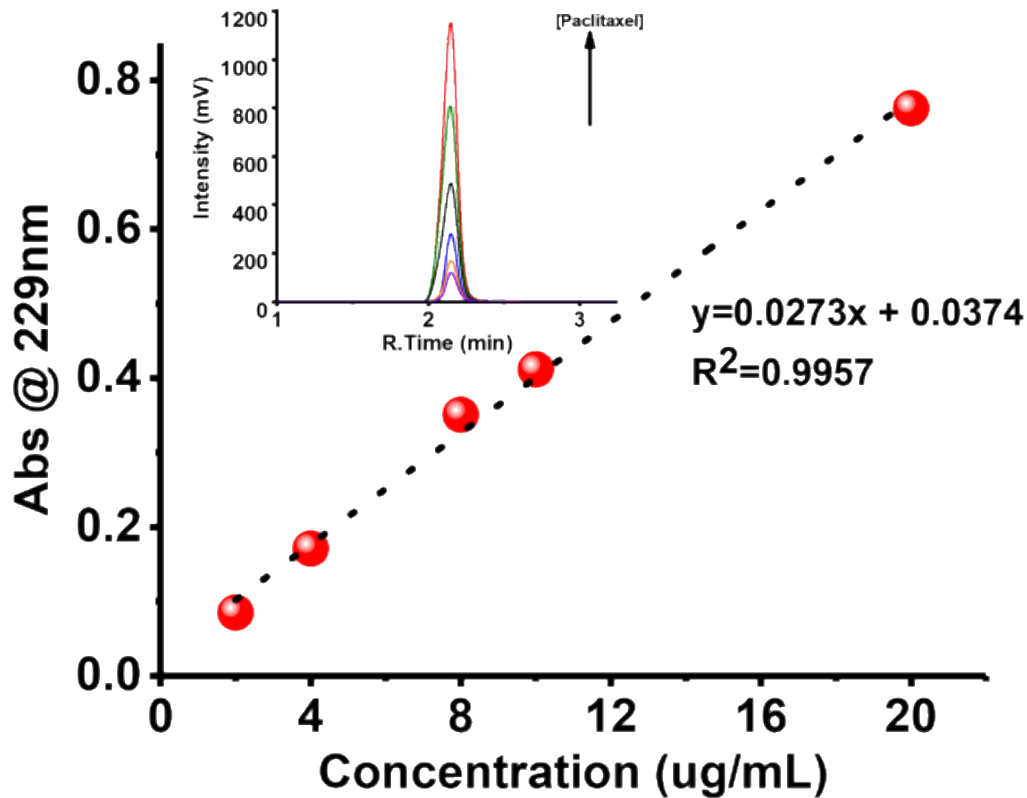
Figure 3.11. Paclitaxel reverse-phase HPLC calibration curve. Insert: HPLC chromatogram of Paclitaxel showing retention time at 2.19 min

The release profile of PTX from the Soysomes exhibited sustained release reaching only 20% after 96 h (Figure 3.12.). However, optimization of the formulation is required in order to give comparable results with the control, Cremophor EL, castor oil derivative excipient used as a surfactant.
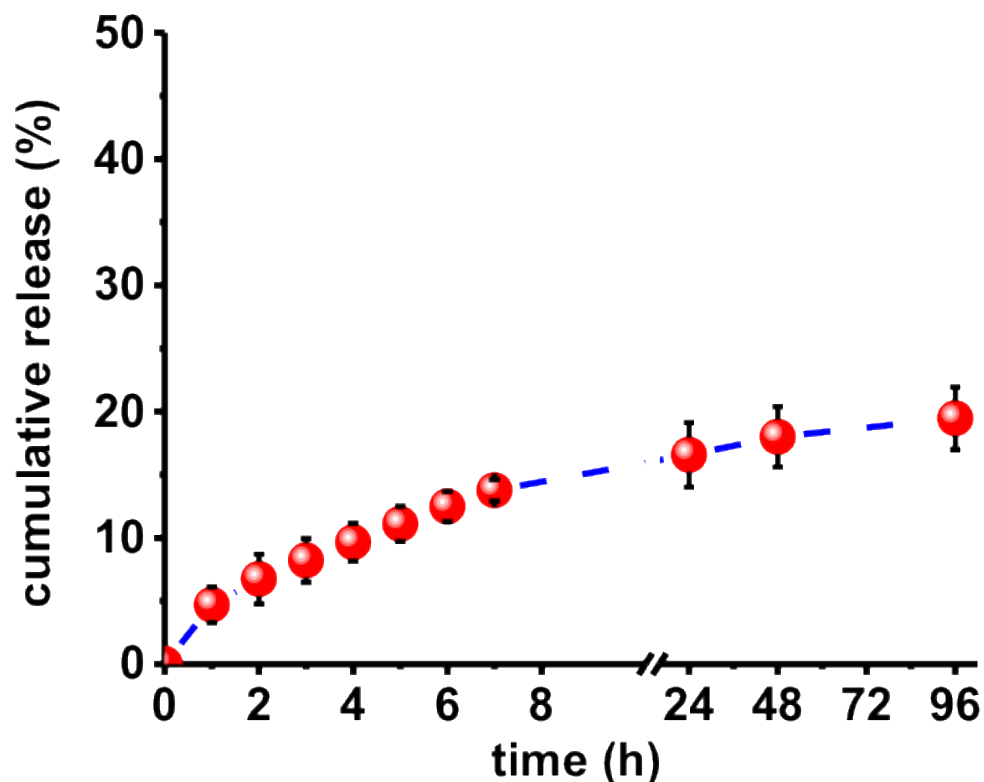
Figure 3.12. Paclitaxel release profile from Soysomes

Enzymatic Degradation

To evaluate the stability of Soysomes in physiologically relevant microenvironment, we treated curcumin-loaded Soysomes with three different enzyme solutions, i.e. lipase, esterase and a combination of the two enzymes. Lipase and esterase are two type of enzyme classified as hydrolase. The two enzymes effected different behavior with the Soysomes demonstrated by the resulting release profiles upon each treatment. Figure 3.13. shows that lipase facilitated the release of curcumin from Soysomes while esterase appears to slightly slowdown release in comparison to untreated curcumin-loaded Soysomes. Treatment with lipase lead to cumulative release of curcumin up to 85 % of encapsulated dosage within 3 h.

94
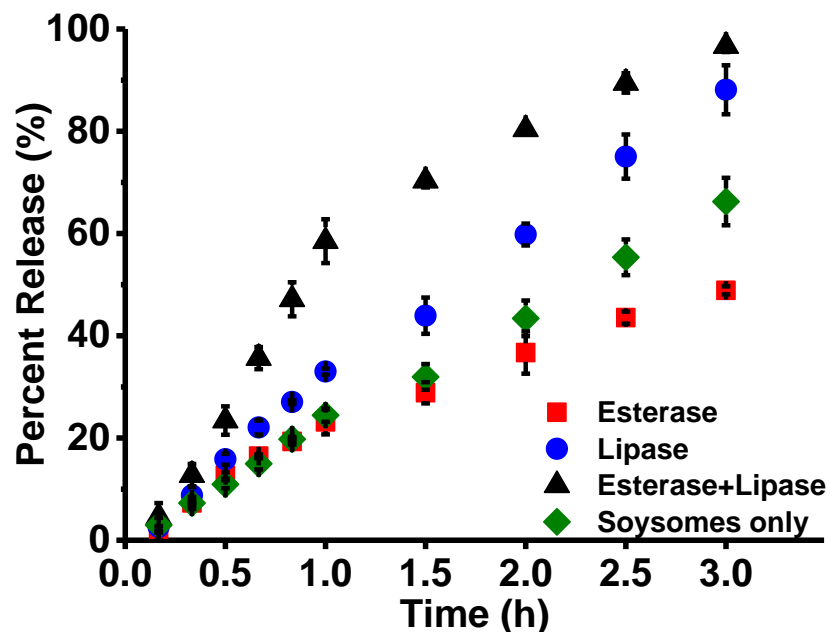
Figure 3.13. Effect of enzyme activity on the release of encapsulated guest molecules from Soysomes

On the other hand, curcumin-loaded Soysomes, when treated with esterase, released only 45% of the encapsulated content within the same period. In a release media spiked with a cocktail of the two enzymes, esterase and lipase at 1:1 ratio caused the highest amount of curcumin release with burst after first hour of treatment. The difference between the release profiles upon treatment with the enzymes was attributed to the distinct substrate specificity of the enzymes.

Esterase activity targets substrate of higher water-solubility and tend to hydrolyze ester linkages via the addition of a water molecule. On the other hand, lipase displays activity towards insoluble or poorly water-soluble substrate such as long-chain fatty acids and aggregated substrates[62]. Lipase-mediated faster release of curcumin from Soysomes likely due to hydrophobicity of the Soysomes core providing an optimal microenvironment for lipase activity. Furthermore, though, MSSP has several ester linkages within the core of the structure, they are sterically shielded and are relatively inaccessible to enzyme activity.

The enzyme treated Soysomes were analyzed post-treatment to evaluate changes in particle size and morphology. A general decrease in the Soysomes particle size in the presence of lipase or the combination of both lipase and esterase was observed (Figure 3.14.). This shrinkage in particle size over time supports that lipase-mediated digestion of the MSSP Soysomes. However, in the presence of esterase, an increase in Soysomes size was observed. Enzyme-induced nanoparticle aggregation results from destabilization of the nanoparticles leading flocculation of nanoparticles into large clusters, which tends to influence release profile of encapsulated cargo from the nanoparticles. [64-66]
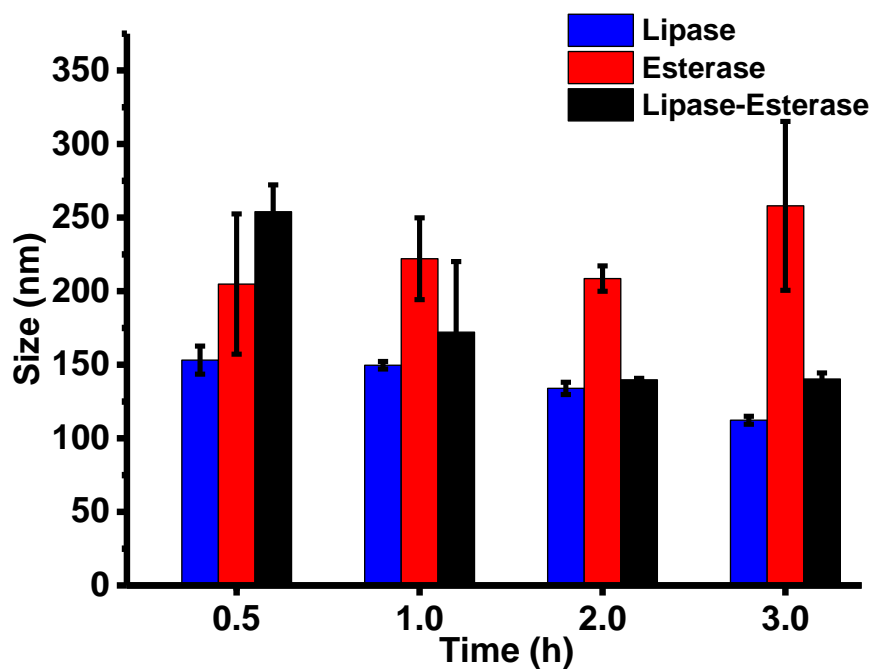
Figure 3.14. Effect of enzyme activity on the Soysomes particle size as a function of treatment time

Destabilization of nanoparticles is likely the reason for release mediated by combination of esterase and lipase shows a faster rate of diffusion of curcumin in the first hour of the experiment, which eventually slows down. This could be attributed to the synergistic effect of esterase-induced nanoparticle destabilization coupled with digestive action of lipase on the loaded Soysomes. TEM micrograms of the Soysomes after treatment with enzyme lipase (Figure

3.15. (a)) and enzyme esterase (Figure 3.15 (b)) reflect the difference in morphology induced by the enzyme treatment. Enzyme-induced aggregation is evident in the esterase treated Soysomes.
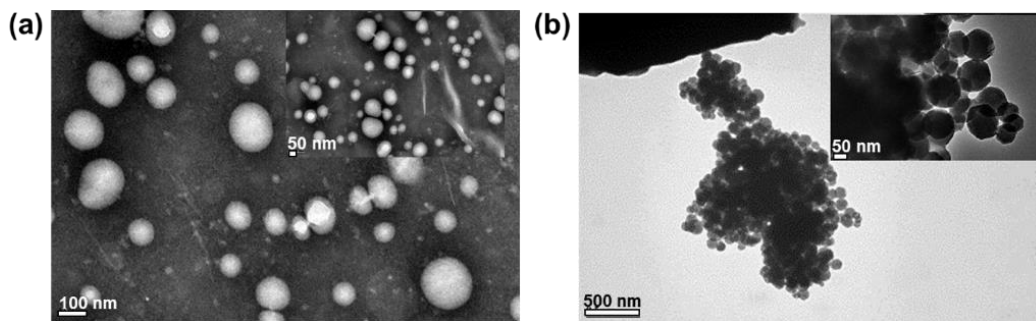
Figure 3.15. TEM micrograph of Soysomes after treatment with enzymes (a) lipase and (b) esterase

Cytotoxicity Assessment

We evaluated the cytotoxicity of MSSP (in resin form) with two different cell lines: L929 mouse fibroblasts and BxPC-3 pancreatic cancer cells. These cells were treated with increasing concentrations of MSSP for 24–72 h at 37 °C, and the cell viability was measured at the end of the treatment. MSSP was found to be nontoxic (>90% cell viability) to both cell lines; L929 mouse fibroblasts (Figure 3.16. (a)) and BxPC-3 pancreatic cancer cells (Figure 3.16. (b)) even at concentrations as high as 10 μM (34 μg/mL). We observed more than 80% survivability of cell which were treated with a very high concentration, i.e., 100 μM (344 μg/mL) MSSP for 72 h.
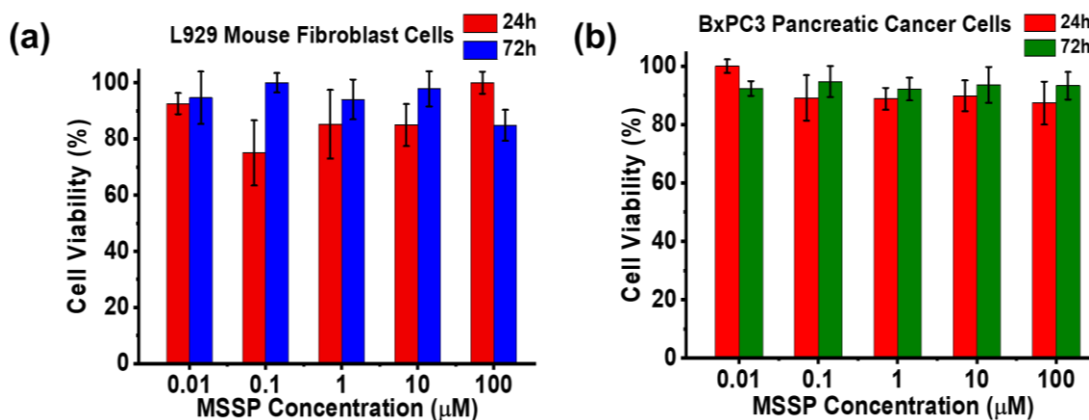
Figure 3.16. Cytotoxicity assessment of MSSP in (a). L929 mouse fibroblast cells and (b). BxPC-3 pancreatic cancer cells

The morphology of L929 fibroblast cells was monitored under bright field microscopy, showing no significant phenotypic changes (Figure 3.17.) were observed compared to the control, upon 24 or 72 h treatment of cell lines with MSSP at concentrations up to 34 µg/mL (10 µM). This result reflects an excellent biocompatibility of the structural component of Soysomes, i.e., MSSP, toward mammalian cells. Although, at high MSSP concentrations (i.e., 344 µg/mL (100 µM) image resolution was obscured), the cell morphology remained intact.
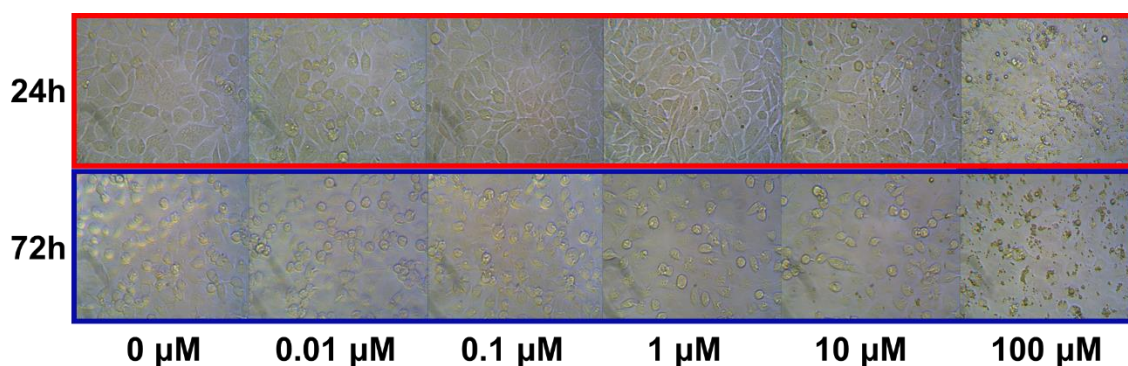
Figure 3.17. Bright field microscopy images depicting morphology of mouse L929 fibroblasts after 24 and 72 h treatment with increasing concentrations of MSSP

Upon demonstrating that MSSP was biologically safe, we treated pancreatic cancer cell lines, BxPC-3, with curcumin-loaded Soysomes at increasing curcumin concentrations (4–11 µg/mL (10–30 µM) for 24 and 72 h). The aim of this study was to demonstrate that Soysomes are capable of transporting their therapeutic payload to intracellular drug targets. For comparisons of drug efficiency, we treated the cells with similar concentrations of free curcumin. Curcumin is a hydrophobic molecule with a reduced aqueous solubility, hydrolytic instability, and low bioavailability[66, 67]. However, when curcumin was encapsulated in Soysomes, we observed an increment of solubility and cellular uptake of curcumin reminiscent of the functional trait of a lipid-based formulation[12, 68]. After short-term (24 h) treatment of BxPC-3 cells with Soysomes containing 4 µg/mL (10 µM) of curcumin, cell viability was reduced to 60%, while free

98

curcumin (at the same concentration) could not suppress cellular proliferation by more than 10% (Figure 3.18).
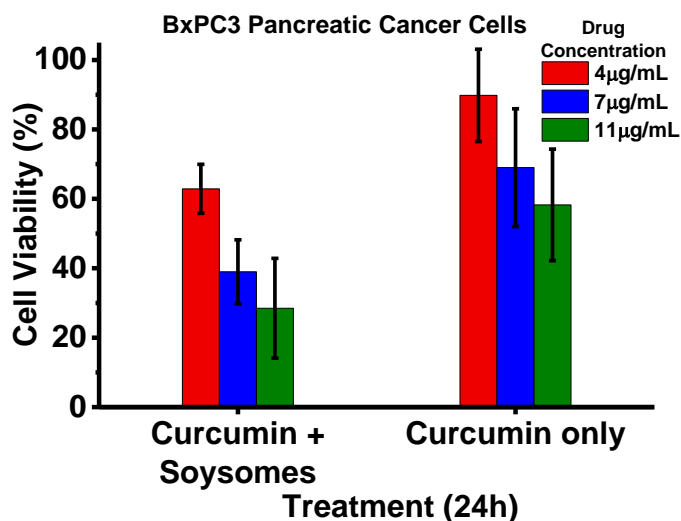
Figure 3.18. Cell viability of the BxPC-3 cells after treatment with curcumin-loaded Soysomes or with curcumin alone for 24 h (N= 3)

A similar trend of differential effectiveness of treatment was observed across all concentration ranges of curcumin either administered as a free drug or encapsulated within Soysomes. Curcumin loaded Soysomes exhibited more prominently enhanced capacity to suppress cellular proliferation after 72 h compared to free curcumin (Figure 3.19).
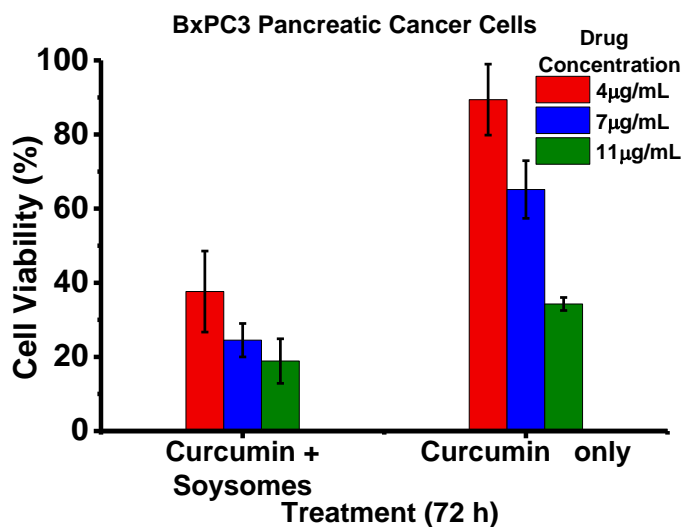
Figure 3.19. Cell viability of the BxPC-3 cells after treatment with curcumin-loaded Soysomes or with curcumin alone for 72 h (N = 3)

There is a 1.5- to 2-fold reduction of cellular viability on the cancer cell when treated with curcumin encapsulated within soysomes compared to the free drug, across different concentrations. Curcumin is reported to rapidly hydrolyze and degrade in an aqueous environment. Therefore, the increase in bioavailability of the drug to the cell can be attributed to reduction of hydrolytic conversion of curcumin when encapsulated within the Soysomes interior. The Soysomes confer stabilization of the drug molecule by shielding it and providing a local hydrophobic environment possibly delaying hydrolysis. As a result, enhanced cytotoxic efficacy of curcumin was observed from the Soysomes mediated treatment compared to the free drug. Such performance and properties put forward Soysomes nanocarriers of translational importance toward formulation development of hydrophobic and hydrolytically unstable drug molecules.

Conclusions

Nanoparticulate Soysomes have been prepared from methoxylated sucrose soyate polyol (MSSP), a soybean oil and sugar-derived polyester polyol. We showed that these sucrose soyates can be used as low-cost biomaterials for facile preparation of pharmaceutical nanocarriers. We also demonstrated that, by varying formulation parameters such as solvent type, solvent to water ratio, and polymer concentration, we could effectively control the size and polydispersity of the resulting nanoparticles. Interestingly, Soysomes were found to be stable at a range of pH and temperature conditions without the inclusion of any surfactants or stabilizers. Soy-derived nanoparticles were able to encapsulate and release hydrophobic molecules. Soysomes were nontoxic in vitro and, when encapsulated with a hydrophobic drug such as curcumin, showed a cytotoxic efficacy in pancreatic cancer cell lines. This work clearly showed that MSSP could be used as a sustainable biomaterial platform for synthesizing nanocarriers with an enhanced stability and potential controlled-release performance.

References

1.   Biomaterials Market by Type of Materials (Metallic, Ceramic, Polymers, Natural) & Application (Cardiovascular, Orthopedic, Dental, Plastic Surgery, Wound Healing, Neurology, Tissue Engineering, Ophthalmology) - Global Forecast to 2021. https://www.marketsandmarkets.com/Market-Reports/biomaterials-393.html.

2.   Hammond, P. T., Nano tools pave the way to new solutions in infectious disease. ACS Infect. Dis. 2017, 3 (8), 554-558.

3.   Chan, W. W.; Chhowalla, M.; Glotzer, S.; Gogotsi, Y.; Hafner, J. H.; Hammond, P. T.; Hersam, M. C.; Javey, A.; Kagan, C. R.; Khademhosseini, A., Nanoscience and nanotechnology impacting diverse fields of science, engineering, and medicine. ACS Publications: 2016.

4.   Ragelle, H.; Danhier, F.; Préat, V.; Langer, R.; Anderson, D. G., Nanoparticle-based drug delivery systems: a commercial and regulatory outlook as the field matures. Expert opinion on drug delivery 2017, 14 (7), 851-864.

5.   Kwon, E. J.; Skalak, M.; Lo Bu, R.; Bhatia, S. N., Neuron-targeted nanoparticle for siRNA delivery to traumatic brain injuries. ACS nano 2016, 10 (8), 7926-7933.

6.   Shi, J.; Votruba, A. R.; Farokhzad, O. C.; Langer, R., Nanotechnology in drug delivery and tissue engineering: from discovery to applications. Nano letters 2010, 10 (9), 3223-3230.

7.   Zhang, F.; Nance, E.; Zhang, Z.; Jasty, V.; Kambhampati, S. P.; Mishra, M. K.; Burd, I.; Romero, R.; Kannan, S.; Kannan, R. M., Surface functionality affects the biodistribution and microglia-targeting of intra-amniotically delivered dendrimers. J. Controlled Release 2016, 237, 61-70.

8.   Navath, R. S.; Kurtoglu, Y. E.; Wang, B.; Kannan, S.; Romero, R.; Kannan, R. M., Dendrimer− drug conjugates for tailored intracellular drug release based on glutathione levels. Bioconjugate chemistry 2008, 19 (12), 2446-2455.

9.   Liu, Q.; Das, M.; Liu, Y.; Huang, L., Targeted drug delivery to melanoma. Adv. Drug Delivery Rev. 2018, 127, 208-221.

10.   Neibert, K.; Gopishetty, V.; Grigoryev, A.; Tokarev, I.; Al-Hajaj, N.; Vorstenbosch, J.; Philip, A.; Minko, S.; Maysinger, D., Wound-Healing with Mechanically Robust and Biodegradable Hydrogel Fibers Loaded with Silver Nanoparticles. Adv. Healthcare Mater. 2012, 1 (5), 621-630.

11.   Master, A. M.; Williams, P. N.; Pothayee, N.; Pothayee, N.; Zhang, R.; Vishwasrao, H. M.; Golovin, Y. I.; Riffle, J. S.; Sokolsky, M.; Kabanov, A. V., Remote actuation of magnetic nanoparticles for cancer cell selective treatment through cytoskeletal disruption. Sci. Rep. 2016, 6, 33560.

12.   Annapragada, A.; Eriksen, J. L.; Tanifum, E. A.; Dasgupta, I.; Cook, S. C., Lipid-based nanoparticles. Google Patents: 2012.

13.   Barichello, J. M.; Morishita, M.; Takayama, K.; Nagai, T., Encapsulation of hydrophilic and lipophilic drugs in PLGA nanoparticles by the nanoprecipitation method. Drug Dev. Ind. Pharm. 1999, 25 (4), 471-476.

14.   Wang, J.; Byrne, J. D.; Napier, M. E.; DeSimone, J. M., More effective nanomedicines through particle design. Small 2011, 7 (14), 1919-1931.

15.   Dikmen, G.; Genç, L.; Güney, G., Advantage and disadvantage in drug delivery systems. Journal of Materials Science and Engineering 2011, 5 (4), 468.

16. Farokhzad, O. C.; Jon, S.; Khademhosseini, A.; Tran, T.-N. T.; LaVan, D. A.; Langer, R., Nanoparticle-aptamer bioconjugates. Cancer Res 2004, 64 (21), 7668-7672.

17. Farokhzad, O. C.; Cheng, J.; Teply, B. A.; Sherifi, I.; Jon, S.; Kantoff, P. W.; Richie, J. P.; Langer, R., Targeted nanoparticle-aptamer bioconjugates for cancer chemotherapy in vivo. Proc. Natl. Acad. Sci. U. S. A.2006, 103 (16), 6315-6320.

18. Cheng, J.; Teply, B. A.; Sherifi, I.; Sung, J.; Luther, G.; Gu, F. X.; Levy-Nissenbaum, E.; Radovic-Moreno, A. F.; Langer, R.; Farokhzad, O. C., Formulation of functionalized PLGA–PEG nanoparticles for in vivo targeted drug delivery. Biomaterials 2007, 28 (5), 869-876.

19. Nakanishi, T.; Fukushima, S.; Okamoto, K.; Suzuki, M.; Matsumura, Y.; Yokoyama, M.; Okano, T.; Sakurai, Y.; Kataoka, K., Development of the polymer micelle carrier system for doxorubicin. J. Controlled Release 2001, 74 (1-3), 295-302.

20. Zhao, X.; Poon, Z.; Engler, A. C.; Bonner, D. K.; Hammond, P. T., Enhanced stability of polymeric micelles based on postfunctionalized poly (ethylene glycol)-b-poly (γ-propargyl L-glutamate): the substituent effect. Biomacromolecules 2012, 13 (5), 1315-1322.

21. Weissmueller, N. T.; Lu, H. D.; Hurley, A.; Prud'homme, R. K., Nanocarriers from GRAS zein proteins to encapsulate hydrophobic actives. Biomacromolecules 2016, 17 (11), 3828-3837.

22. Anitha, A.; Deepagan, V.; Rani, V. D.; Menon, D.; Nair, S.; Jayakumar, R., Preparation, characterization, in vitro drug release and biological studies of curcumin loaded dextran sulphate–chitosan nanoparticles. Carbohydr. Polym. 2011, 84 (3), 1158-1164.

23.   Guo, A.; Demydov, D.; Zhang, W.; Petrovic, Z. S., Polyols and polyurethanes from hydroformylation of soybean oil. J. Polym. Environ. 2002, 10 (1), 49-52.

24.   Kumari, A.; Yadav, S. K.; Yadav, S. C., Biodegradable polymeric nanoparticles based drug delivery systems. Colloids Surf., B 2010, 75 (1), 1-18.

25.   Guo, B.; Chen, Y.; Lei, Y.; Zhang, L.; Zhou, W. Y.; Rabie, A. B. M.; Zhao, J., Biobased poly (propylene sebacate) as shape memory polymer with tunable switching temperature for potential biomedical applications. Biomacromolecules 2011, 12 (4), 1312-1321.

26.   Mohanty, A.; Misra, M.; Drzal, L., Sustainable bio-composites from renewable resources: opportunities and challenges in the green materials world. J. Polym. Environ. 2002, 10 (1), 19-26.

27.   Miao, S.; Wang, P.; Su, Z.; Zhang, S., Vegetable-oil-based polymers as future polymeric biomaterials. Acta Biomater. 2014, 10 (4), 1692-1704.

28.   Miao, S.; Sun, L.; Wang, P.; Liu, R.; Su, Z.; Zhang, S., Soybean oil-based polyurethane networks as candidate biomaterials: Synthesis and biocompatibility. Eur. J. Lipid Sci. Technol. 2012, 114 (10), 1165-1174.

29.   Motlagh, D.; Yang, J.; Lui, K. Y.; Webb, A. R.; Ameer, G. A., Hemocompatibility evaluation of poly (glycerol-sebacate) in vitro for vascular tissue engineering. Biomaterials 2006, 27 (24), 4315-4324.

30.   Redenti, S.; Neeley, W. L.; Rompani, S.; Saigal, S.; Yang, J.; Klassen, H.; Langer, R.; Young, M. J., Engineering retinal progenitor cell and scrollable poly (glycerol-sebacate) composites for expansion and subretinal transplantation. Biomaterials 2009, 30 (20), 3405-3414.

31.   Sundback, C. A.; Shyu, J. Y.; Wang, Y.; Faquin, W. C.; Langer, R. S.; Vacanti, J. P.; Hadlock, T. A., Biocompatibility analysis of poly (glycerol sebacate) as a nerve guide material. Biomaterials 2005, 26 (27), 5454-5464.

32.   Shikanov, A.; Shikanov, S.; Vaisman, B.; Golenser, J.; Domb, A. J., Paclitaxel tumor biodistribution and efficacy after intratumoral injection of a biodegradable extended release implant. Int. J. Pharm. 2008, 358 (1-2), 114-120.

33.   Shikanov, S.; Shikanov, A.; Gofrit, O.; Nyska, A.; Corn, B.; Domb, A. J., Intratumoral delivery of paclitaxel for treatment of orthotopic prostate cancer. J. Pharm. Sci. 2009, 98 (3), 1005-1014.

34.   Krasko, M. Y.; Golenser, J.; Nyska, A.; Nyska, M.; Brin, Y. S.; Domb, A. J., Gentamicin extended release from an injectable polymeric implant. J. Controlled Release 2007, 117 (1), 90-96.

35.   Nelson, T. J.; Bultema, L.; Eidenschink, N.; Webster, D. C., Bio-based high functionality polyols and their use in 1K polyurethane coatings. J. Renewable Mater. 2013, 1 (2), 141-153.

36.   Lligadas, G.; Ronda, J. C.; Galià, M.; Cádiz, V., Poly (ether urethane) networks from renewable resources as candidate biomaterials: synthesis and characterization. Biomacromolecules 2007, 8 (2), 686-692.

37.   Lligadas, G.; Ronda, J. C.; Galia, M.; Cadiz, V., Renewable polymeric materials from vegetable oils: a perspective. Mater. Today 2013, 16 (9), 337-343.

38.   FDA Generally Recognized as Safe (GRAS). https://www.fda.gov/food/food-ingredients-packaging/generally-recognized-safe-gras.

39.   Govender, T.; Stolnik, S.; Garnett, M. C.; Illum, L.; Davis, S. S., PLGA nanoparticles prepared by nanoprecipitation: drug loading and release studies of a water soluble drug. J. Controlled Release 1999, 57 (2), 171-185.

40.   Sanson, C.; Schatz, C.; Le Meins, J.-F.; Soum, A.; Thévenot, J.; Garanger, E.; Lecommandoux, S., A simple method to achieve high doxorubicin loading in biodegradable polymersomes. J. Controlled Release 2010, 147 (3), 428-435.

41.   Hevus, I.; Modgil, A.; Daniels, J.; Kohut, A.; Sun, C.; Stafslien, S.; Voronov, A., Invertible micellar polymer assemblies for delivery of poorly water-soluble drugs. Biomacromolecules 2012, 13 (8), 2537-2545.

42.   Marín-Menéndez, A.; Montis, C.; Díaz-Calvo, T.; Carta, D.; Hatzixanthis, K.; Morris, C. J.; McArthur, M.; Berti, D., Antimicrobial Nanoplexes meet Model Bacterial Membranes: the key role of Cardiolipin. Sci. Rep. 2017, 7, 41242.

43.   Thioune, O.; Fessi, H.; Devissaguet, J.; Puisieux, F., Preparation of pseudolatex by nanoprecipitation: influence of the solvent nature on intrinsic viscosity and interaction constant. Int. J. Pharm. 1997, 146 (2), 233-238.

44.   Quintanar-Guerrero, D.; Allémann, E.; Fessi, H.; Doelker, E., Preparation techniques and mechanisms of formation of biodegradable nanoparticles from preformed polymers. Drug Dev. Ind. Pharm. 1998, 24 (12), 1113-1128.

45.   Schubert, S.; Delaney Jr, J. T.; Schubert, U. S., Nanoprecipitation and nanoformulation of polymers: from history to powerful possibilities beyond poly (lactic acid). Soft Matter 2011, 7 (5), 1581-1588.

46.   Salatin, S.; Barar, J.; Barzegar-Jalali, M.; Adibkia, K.; Kiafar, F.; Jelvehgari, M., Development of a nanoprecipitation method for the entrapment of a very water soluble drug into Eudragit RL nanoparticles. Res. Pharm. Sci. 2017, 12 (1), 1.

47.   Sou, K.; Inenaga, S.; Takeoka, S.; Tsuchida, E., Loading of curcumin into macrophages using lipid-based nanoparticles. Int. J. Pharm. 2008, 352 (1), 287-293.

48.   Maheshwari, R. K.; Singh, A. K.; Gaddipati, J.; Srimal, R. C., Multiple biological activities of curcumin: a short review. Life Sci. 2006, 78 (18), 2081-2087.

49.   Pan, C. J.; Tang, J.; Weng, Y.; Wang, J.; Huang, N., Preparation, characterization and anticoagulation of curcumin-eluting controlled biodegradable coating stents. J. Controlled Release 2006, 116 (1), 42-49.

50.   Aggarwal, B. B.; Harikumar, K. B., Potential therapeutic effects of curcumin, the anti-inflammatory agent, against neurodegenerative, cardiovascular, pulmonary, metabolic, autoimmune and neoplastic diseases. Int. J. Biochem. Cell Biol. 2009, 41 (1), 40-59.

51.   Dhillon, N.; Aggarwal, B. B.; Newman, R. A.; Wolff, R. A.; Kunnumakkara, A. B.; Abbruzzese, J. L.; Ng, C. S.; Badmaev, V.; Kurzrock, R., Phase II trial of curcumin in patients with advanced pancreatic cancer. Clin. Cancer Res 2008, 14 (14), 4491-4499.

52.   Ali, S.; Ahmad, A.; Banerjee, S.; Padhye, S.; Dominiak, K.; Schaffert, J. M.; Wang, Z.; Philip, P. A.; Sarkar, F. H., Gemcitabine sensitivity can be induced in pancreatic cancer cells through modulation of miR-200 and miR-21 expression by curcumin or its analogue CDF. Cancer Res 2010, 70 (9), 3606-3617.

53.   Kunnumakkara, A. B.; Guha, S.; Krishnan, S.; Diagaradjane, P.; Gelovani, J.; Aggarwal, B. B., Curcumin potentiates antitumor activity of gemcitabine in an orthotopic model of pancreatic cancer through suppression of proliferation, angiogenesis, and

inhibition of nuclear factor-κB–regulated gene products. Cancer Res 2007, 67 (8), 3853-3861.

54.   Avgoustakis, K., Polylactic-co-glycolic acid (PLGA). Encycl. Biomater. Biomed. Eng. 2008, 2259-2269.

55.   Kitchell, J. P.; Wise, D. L., [32] Poly (lactic/glycolic acid) biodegradable drug—polymer matrix systems. Methods Enzymol. 1985; 112, 436-448.

56.   Ruiz, J.; Tissier, B.; Benoit, J., Microencapsulation of peptide: a study of the phase separation of poly (D, L-lactic acid-co-glycolic acid) copolymers 50/50 by silicone oil. Int. J. Pharm. 1989, 49 (1), 69-77.

57.   Sanders, L.; Kell, B.; McRae, G.; Whitehead, G., Prolonged controlled-release of nafarelin, a luteinizing hormone-releasing hormone analogue, from biodegradable polymeric implants: influence of composition and molecular weight of polymer. J. Pharm. Sci. 1986, 75 (4), 356-360.

58.   Gref, R.; Minamitake, Y.; Peracchia, M. T.; Domb, A.; Trubetskoy, V.; Torchilin, V.; Langer, R., Poly (ethyleneglycol)-coated nanospheres: potential carriers for intravenous drug administration. Protein Delivery, Springer: 2002, 167-198.

59.   Gref, R.; Minamitake, Y.; Peracchia, M. T.; Trubetskoy, V.; Torchilin, V.; Langer, R., Biodegradable long-circulating polymeric nanospheres. Science 1994, 263 (5153), 1600-1603.

60.   Owens III, D. E.; Peppas, N. A., Opsonization, biodistribution, and pharmacokinetics of polymeric nanoparticles. Int. J. Pharm. 2006, 307 (1), 93-102.

61. Moghimi, S. M.; Szebeni, J., Stealth liposomes and long circulating nanoparticles: critical issues in pharmacokinetics, opsonization and protein-binding properties. Prog. Lipid Res. 2003, 42 (6), 463-478.

62. Chahinian, H.; Nini, L.; Boitard, E.; Dubès, J.-P.; Comeau, L.-C.; Sarda, L., Distinction between esterases and lipases: a kinetic study with vinyl esters and TAG. Lipids 2002, 37 (7), 653-662.

63. Hu, J.; Zhang, G.; Liu, S., Enzyme-responsive polymeric assemblies, nanoparticles and hydrogels. Chem. Soc. Rev. 2012, 41 (18), 5933-5949.

64. de Graaf, A. J.; Mastrobattista, E.; Vermonden, T.; van Nostrum, C. F.; Rijkers, D. T.; Liskamp, R. M.; Hennink, W. E., Thermosensitive peptide-hybrid ABC block copolymers obtained by ATRP: synthesis, self-assembly, and enzymatic degradation. Macromolecules 2012, 45 (2), 842-851.

65. De La Rica, R.; Aili, D.; Stevens, M. M., Enzyme-responsive nanoparticles for drug release and diagnostics. Adv. Drug Delivery Rev. 2012, 64 (11), 967-978.

66. Yallapu, M. M.; Khan, S.; Maher, D. M.; Ebeling, M. C.; Sundram, V.; Chauhan, N.; Ganju, A.; Balakrishna, S.; Gupta, B. K.; Zafar, N., Anti-cancer activity of curcumin loaded nanoparticles in prostate cancer. Biomaterials 2014, 35 (30), 8635-8648.

67. Mukerjee, A.; Vishwanatha, J. K., Formulation, characterization and evaluation of curcumin-loaded PLGA nanospheres for cancer therapy. Anticancer Res. 2009, 29 (10), 3867-3875.

68. Dong, X.; Mattingly, C. A.; Tseng, M. T.; Cho, M. J.; Liu, Y.; Adams, V. R.; Mumper, R. J., Doxorubicin and paclitaxel-loaded lipid-based nanoparticles overcome

multidrug resistance by inhibiting P-glycoprotein and depleting ATP. Cancer Res 2009, 69 (9), 3918-3926.

CHAPTER 4. EXPLORATION OF FREE-STANDING FILMS PREPARED FROM BLENDS OF METHOXYLATED SUCROSE SOYATE POLYOL

Abstract

Biobased, flexible, drug-eluting composite free-standing films were prepared. Specifically, free-standing films were fabricated from blending methoxylated sucrose soyate polyol (MSSP) and polycaprolactone (PCL) at different composition ratios (w/w %) using a solvent displacement method. Blending PCL with sucrose soyate, reduces reliance on costly polymers such as PCL, introduces potential for post-fabrication functionalization while imparting biobased component. The resulting blended films exhibited porous microstructure with pore size varying with increasing amount of MSSP. Incorporation of up to 50% MSSP in the formulations rendered films more susceptible to biodegradation, using enzyme lipase, while maintaining the thermal properties and integrity of the film compared to those fabricated from PCL alone. The blended films were loaded with doxorubicin, a potent active anticancer drug, via layer-by-layer assembly with poly (lysine) and hyaluronic acid. Multi-layered drug-eluting films exhibited a controlled, sustained release, achieving only 20% cumulative release over a 24 h period.

Introduction

Biomaterials employed for highly specific application have to meet certain criteria such as biocompatibility, non-cytotoxic, drug eluting, i.e. have the ability to entrap and release loaded cargo, flexibility to accommodate interaction with soft tissues, which are often irregular, shaped after surgery. For example, drug-eluting films are used for slow release of therapeutic in surgically removed breast tissue to stop recurrence and propagation of cancer.[1-4] PCL has been extensively investigated as an ideal polymer for applications in tissue engineering wound

111

dressing and delivery technology due to its biocompatibility, biodegradability and versatile nature. However, PCL has limitation; degradation of PCL is slow and dependent on molecular weight, degree of crystallinity, and degradation conditions of the polymer.[5, 6] Furthermore, the hydrophobic surface properties and mechanical behavior of PCL result in poor interactions with cells. Success of biomaterials hinges on cell-biomaterials interaction.[6-8] Several strategies have been reported to modify surface properties of PCL; impart micro-topography which determines adsorption of biological molecules, or alter surface chemistry to enhance biocompatibility.[9-12] Often, surface modification is achieved by a simple technique –chemical etching; i.e. PCL materials undergo alkaline treatment which hydrolyzes esters in the polymer backbone rendering the substrate more hydrophilic and increases necessary micro-roughness.

Another way to alter properties of biomaterials is application of coating with the desired characteristics. An interesting technique gaining traction is layer-by-layer (LbL) or charge-by-charge layered deposition of charged polymer solutions.[13-18] This approach can be used to introduce micro-scale or nano-scale features on the surface with bioactive properties to serves as biological cues toward cells.[19-21] LbL has been reported to promote patterned growth or co-cultures of cells within the thin stacked layers created by the alternating polyanion and polycation.[22]

Finally, polymer blending is used to alter the surface as well as bulk properties of biomaterials. Mixing two or more polymers is common method used to develop new forms or functions via the combination of properties from the individual polymers. Combination of PCL with other polymer can be an important strategy to adjust the surface characteristics, mechanical behavior or even degradation kinetics to achieve the desired properties. Although, several FDA approved polymer candidates such as collagen, chitosan, poly (lactide-co-glycolide) and poly

(ethylene glycol) have found application in generating biomaterials for wound healing, surgical treatment and tissue-engineering applications, certain considerations need to be accounted for. Issues such as polymer compatibility, cost, poor degradation profile, toxicity, batch-to-batch variations render most of these polymers unsuitable candidates.

As a solution, biobased large molecules are emerging as new, promising platform to generate functional materials with tunable properties suitable for biomedical and pharmaceutical applications. These are synthesized from plant-derived building blocks; and easily functionalized, hence, can be customized to produce new target properties or serve as substitute to petrochemical derived alternate.[23-25] Particularly, plant-oil derived polymers offer the benefit of multivalence, biodegradability, and biocompatibility, versatile and unique physical, chemical, and mechanical properties. Sucrose Soyates, i.e. sucrose esters of soybean oil, have been reported to produce high performance coating with excellent characteristics.[26-28]

In this work, MSSP, a sucrose octa ester of soybean oil, was blended with PCL to generate soy-based drug-eluting blended free films using solvent displacement method. Blending MSSP with PCL resulting in highly flexible films that biodegrade in the presence of enzyme lipase. MSSP-PCL blended films were loaded with doxorubicin, an anthracycline chemotherapy drug, via surface modification by LbL technique. The mechanical properties and performance of the films was evaluated to determine their suitability as candidate for biomaterial applicable in wound healing, general surgery or tissue engineering.

Experimental

Materials

MSSP, M_n 3442 previously synthesized by Nelson et al.[26] ESS, with an epoxy equivalent weight of 243.4g/eq, synthesized earlier by Pan et al.[29] PCL, average M_n 80,000 by GPC, DMF,

113

and Poly-L-lysine hydrochloride (PLys), M_n 15,000-30,000 were purchased from Millipore Sigma. Doxorubicin hydrochloride (dox) purchased from Cayman Chemical. Sodium hyaluronate (HA), research grade was purchased from Lifecore Biomedical, LLC. All reagents were used as received unless otherwise stated.

Preparation of MSSP-PCL Blended Films

MSSP-PCL films was prepared by using diffusion-induced phase-separation process. A homogenous solution of MSSP-PCL was prepared by dissolving PCL (20 w/v%) in DMF at 60°C and incorporating MSSP 1, 10 and 50 wt.%. Solutions were allowed to cool to ambient temperature and degas. Using the draw-down method, the polymer solution was cast on a glass plate to yield a wet-film-thickness of 15mil (381μm). The glass plate was immersed in deionized water at room temperature for 24h after which films were thoroughly rinsed and dried at ambient conditions. MSSP-PCL films were treated with NaOH in order to modify film surfaces for cell adhesion. Films were incubated in 3N NaOH for periods of 0, 1.5 and 3 h, rinsed in PBS pH 7.4 and placed in DI water for 24h then air dried at ambient temperature.

Thin Film Deposition and Loading of Doxorubicin

Thin nano-coating was applied on the MSSP-PCL blended films as a substrate via LbL assembly polyelectrolytes, HA (5mg/mL) and PLys (2.5mg/mL). Fabricated films comprised N= 0, 10, 20 and 40 bilayers. These film samples will from hereon be referred to as MSSP 50% -0-LbL, MSSP 50% -10-LbL, MSSP 50% -20-LbL and MSSP 50% -40-LbL. Loading of MSSP-PCL blended films (d=12mm) was accomplished by alternating deposition of dox solution (2mg/mL) and solutions of PLys (5mg/mL) and HA(5mg/mL) resulting in a LbL assembly. Several layers were deposited on the films followed by washing with DI water to remove any unbound Dox.

Characterization of MSSP-PCL Blended Films

Attenuated Total Reflectance-Infrared (ATR-IR) Spectroscopy

ATR-IR of the MSSP-PCL films was performed using a Nicolet 8700 FT-IR with a Smart iTR diamond tip accessory (Thermo Scientific, Grand Island, NY, USA). Spectra representative of the film surface before and after NaOH treatment and before and after coating with HA and PLys were collected.

Thermal Analysis

Differential Scanning Calorimetry (DSC)

DSC Q2000 (TA Instruments, New Castle Delaware, USA) was used to thermal studies. Films of approximately 6mg sample size were placed in hematic pans and analyzed using conventional DSC under a temperature ramp method from -80 to 80°C at 10°C/min heating and cooling rate.

Thermogravimetric analysis (TGA)

All TGA was performed using a TA Instruments Q500 instrument to study the degradation of free films. Films were placed in a platinum pan and heated from 20 to 700°C under N_2 using a heating rate of 20°C/min. The instrument recorded the mass loss during the temperature ramp.

Surface Analysis

Scanning Electron Microscopy (SEM)

3D polymer films were attached to cylindrical aluminum mounts with carbon adhesive tabs (Electron Microscopy Sciences, Hatfield, Pennsylvania, USA), and then sputter coated (Cressington 108auto, Ted Pella, Redding, California USA) with a conductive layer of gold. Images were obtained with a JEOL JSM-6490LV scanning electron microscope (JEOL USA, Inc., Peabody, Massachusetts USA) at an accelerating voltage of 15 kV.

Atomic Force Microscopy (AFM) /Nano indentation

All surface analysis and indentation measurements were performed out at room temperature on Veeco DI-3100 AFM and Veeco Nanoscope IIIa MultiMode SPM USA). A RTESPA-300 silicone probe with a rotated (symmetric) tip (Bruker, USA), 8 nm nominal radius of curvature at the tip apex, 20° tip half angle and 40N/m spring constant was used for all analysis. The deflection sensitivity of the indenter was determined by calibration on a pre-mounted sapphire disc, Sapphire 12M (Bruker, USA).

Films were mounted on specimen discs, d=12mm (Ted Pella Inc., Redding CA USA). Images were acquired over 20μm scan area. Indentations were carried out in force mode with a minimum of nine indentations obtained per 3μm grid on each sample. The Z scan rate was set to 1.99 Hz; hence, each indentation took 0.50 s to execute. The relationship between force and distance was determined from measurement of cantilever deflection against the z-position during advancement and retraction of the probe. All AFM data including stiffness of films was analyzed using the NanoScope Analysis V1.50 software (Bruker).

Water Contact Angle

To assess the hydrophobicity of the MSSP-PCL blended films, the water contact angle was measured using FTA 200 dynamic contact angle/surface tension analyzer and FTA 32 video (First Ten Ångstroms, Portsmouth, VA, USA). Water contact angle measurements (n= 10) were taken on surfaces of the films of different formulations before and after NaOH treatment and before and after coating with HA and PLys.

Tensile Testing

The blended films of different formulations were cut using ASTM D683 Type **V** tensile specimen cutter (Qualitest) and thickness measured at least five different locations using digital

micrometer. Tensile testing was performed using Instron 5542 at strain rate 2.5mm/min under ambient conditions. The yield strength, the percent elongation at break, and modulus were extracted from the tensile data. Reported data are an average of at least five tensile experiments.

Water Absorption

PCL films were cut into discs (d=5mm), weighed (w_0) and incubated in PBS at 37 °C. At regular interval, the films were weighed (w_1) after removing surface water via wicking with filter paper. Three replicates were analyzed for each sample group. Water absorption was calculated using equation (4.1):

$$water\ absorption\ (\%) = \frac{w_1 - w_0}{w_0}\ x\ 100 \tag{4.1}$$

Biodegradation

To assess the in vitro enzymatic degradation profile of the films, samples were cut into discs (d=5mm), weighed (w_0) and incubated in 2 mL of PBS containing 2mg/mL lipase solution (Sigma Aldrich) at 37 °C. The enzyme solution was changed every 3 days and the samples rinsed three times with deionized water, dried, and then weighed (w_1). Three replicates were used for each film formulation at each time point. The mass remaining was calculated using equation 4.2:

$$remaining\ mass\ (\%) \frac{w_1}{w_0}\ x\ 100 \tag{4.2}$$

Release Studies

Standard release experiment was performed to evaluate the release profiles of the films. Dox loaded films (d=1.2cm) were immersed in 2 mL of release medium (PBS pH 7.4, 10 mM ionic strength). The release sample were subjected to low agitation by means of an oscillating shaker at low setting. At a specified time, interval 100μL aliquots of release medium were withdrawn from each sample and replaced with an equal volume of fresh media. Dox loaded

MSSP 50% films and PCL-0 films were analyzed over a 24 h period. PCL-0 served as a control

to determine effect of blending film formulation. All release studies were carried out under

ambient conditions. Three sample replicates were analyzed for each film formulation. The

absorbance spectra of the withdrawn sample were analyzed using Nanodrop One Microvolume

UV-Vis Spectrophotometer (Thermo Scientific, USA). Cumulative percent release was

determined using the following equation (4.3):

$$cumulative\ \%\ release = \frac{volume\ withdrawn}{volume\ of\ bath}\ x\ \%release\ at\ time\ t + \Sigma\ \%release\ at\ t - 1 \quad (4.3)$$

Results and Discussion

Fabrication and Characterization of MSSP-PCL Blended Films

MSSP-PCL blended films were prepared from co-dissolving PCL and varying amounts

of MSSP (1, 10 and 50 wt. %) and wet casting followed by solvent displacement (Figure 4.1.).

Film formed immediately upon contacting the aqueous phase. Repeated subsequent washing with

DI water facilitated diffusion of organic solvent from the films. The films were air-dried prior to

any further modification or testing. An increasing amount of MSSP was added to the formulation

reaching up to 50% reduction in amount PCL; however, beyond 50%, any additional MSSP in

the formulation resulted in tacky films (MSSP 60%) suck to the to the glass substrate or no

curing at all was achieved (>70%). These samples phase separated with MSSP forming oil

droplets on the surface of the water.
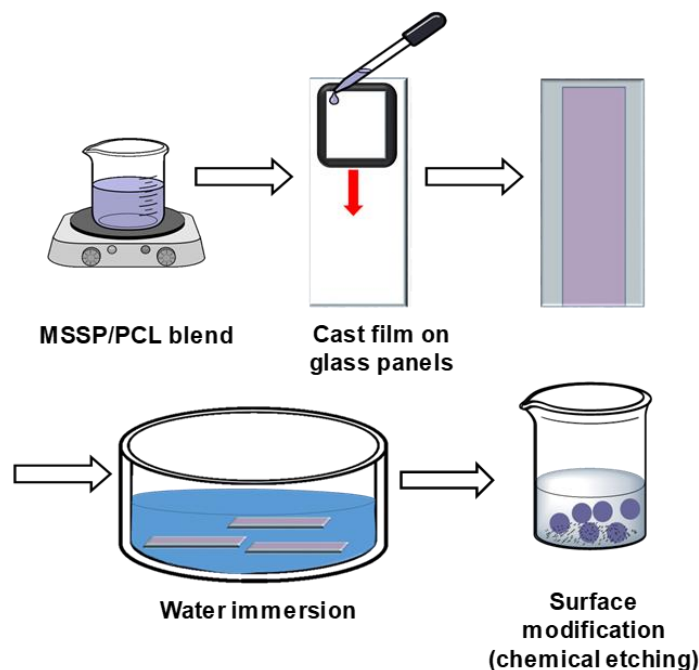
Figure 4.1. Illustrative diagram depicting the MSSP blended film formation process and subsequent chemical etching in NaOH to modify the surface properties of the films

The incorporation of MSSP into the film was verified by ATR spectroscopy. Generally, there were no major changes in the spectra, with an almost complete overlap in all regions for the different film formulations. However, as the MSSP concentration increased in the film formulation, the O-H stretch (3200-3500cm^{-1}) became more prominent (Figure 4.2.).
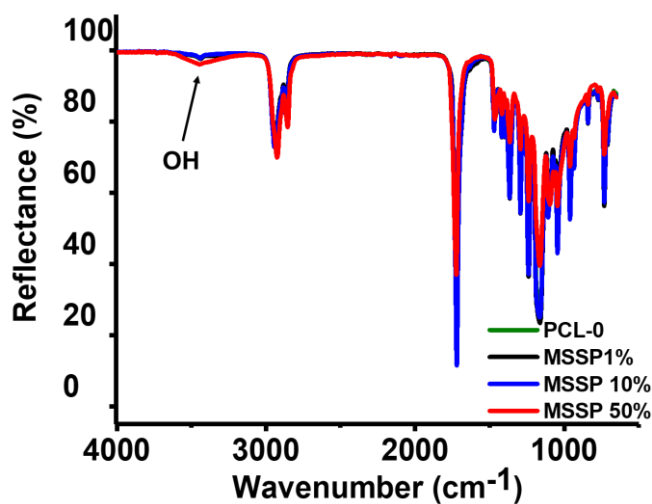
Figure 4.2. ATR spectra of MSSP blended films of various concentrations 1%, 10% and 50% in comparison to control film, PCL-0 (without any MSSP)

In order to demonstrate the compatibility between the sucrose soyate derivatives and PCL, a set of blended films was prepared from ESS following similar procedure. For up to 50% ESS added to the formulation blend with PCL, films were successfully formed upon water immersion. The incorporation of ESS into the blended film was confirmed by ATR spectroscopy. Figure 4.3. shows the presence of an epoxy band (820cm^{-1}) in an ESS 50% composite film which was absent in PCL alone (PCL-0) or any of the films formed from MSSP and PCL blend. Form all three film formulations, MSSP blends have more surface hydroxyls exposed than the other two (ESS and PCL).
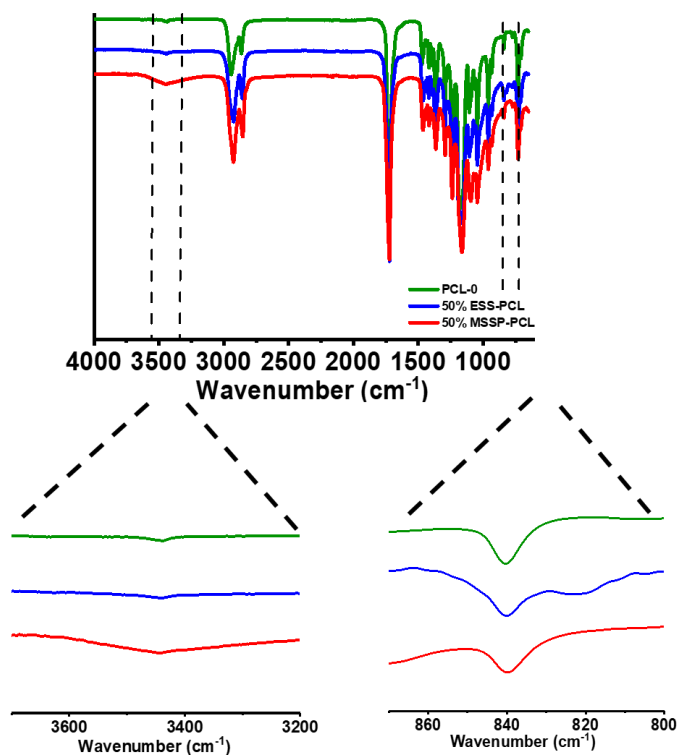
Figure 4.3. ATR spectra of MSSP and ESS composite films in comparison to control PCL film demonstrating compatibility of PCL with sucrose soyate derivatives

Both MSSP and PCL are rich in ester groups; therefore, treatment with NaOH aided in surface modification via ester hydrolysis. Hydrolyzing the esters exposes the hydroxyl and carboxylic acid groups rending the film surface more hydrophilic.[10, 30, 31] Effectiveness of the

chemical etching to reduce the hydrophobicity (impart some hydrophilicity) of the film surface

was time-dependent as demonstrated by the change in water contact angle (Figure 4.4.).

Generally, hydrophilicity increases as the treatment time increase regardless of film composition.

For instance, water contact angle reduces from $97.0°\pm3.3°$ to $70.5°\pm6.6°$ over a 3 h treatment

period of MSSP-1% films; or up $20°$ drop in water contact angle observed with the MSSP-50%

films. Films without no MSSP at all (PCL film) were hydrolyzed at a slower rate ($7°$ drop in

water contact angle over same 3 h treatment period). MSSP is highly susceptible to alkaline

hydrolysis[28]; therefore, NaOH treatment beyond 3 h resulted in the complete degradation of the

blended films.
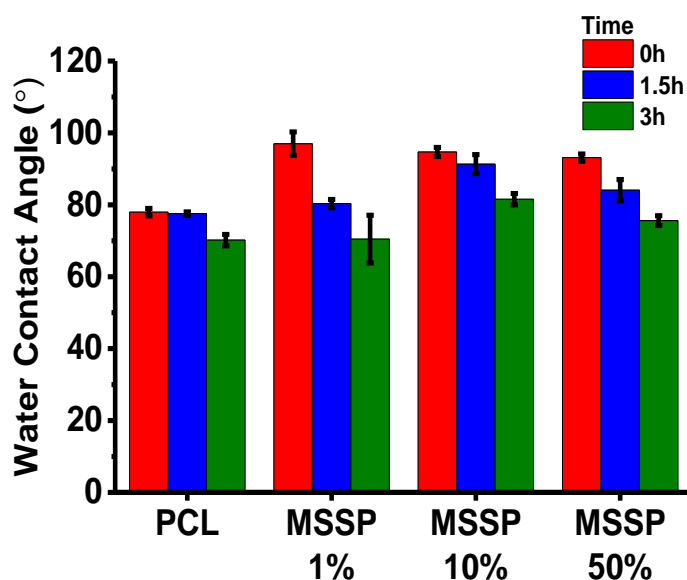
Figure 4.4. Measurement of water contact angle of MSSP blended film monitored for different
concentrations of MSSP over time

Thermal Analysis

The thermal properties and crystallinity of MSSP-PCL blended of the films were

evaluated using DSC and TGA. Melting temperatures (T_m) and enthalpy of fusion (ΔH_f) were

determined from the second heating cycle of the DSC endotherms (Figure 4.5.). The glass

121

transition temperature, T_g was not discernible; however, due to the semi-crystalline nature of PCL, the blended films exhibit a distinct melting temperature (T_m).
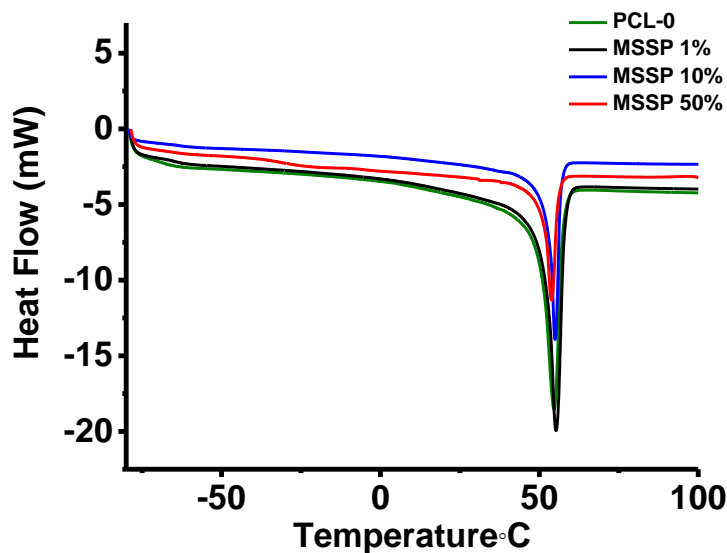
Figure 4.5. DSC endotherms of MSSP blended films at various concentrations of MSSP

The DSC endotherms of the MSSP-PCL films demonstrate that T_m was independent of concentration of MSSP in the blended films. However, incorporation of MSSP in the film composition influenced the thermal stability of the films.

Degradation temperature (T_D) determine by TGA indicated a decreasing trend, with up to 30°C decline in degradation temperature corresponding to 10% weight loss. Overall, the films have excellent thermal stability (Table 4.1.) at 90 wt. % remaining mass, T_D was above 340°C. Therefore, adding up to 50% Biobased content in the film formulation generates potentially viable biomaterials reducing reliance of petrochemical feedstock and reducing cost by substituting costly polymer with an affordable option.

Table 4.1. Thermal Properties of MSSP Blended Films

Sample Name	MSSP wt. % incorporated	T_m (°C)	T_D at 90%wt (°C)	ΔH_f (J/g)	Crystallinity, X_c %
PCL-0	0	54.6	373.8	93.0	68.9
MSSP 1%	1	55.3	370.3	107.9	79.9
MSSP 10%	10	55.0	362.9	101.1	74.9
MSSP 50%	50	53.9	343.9	48.4	35.9

The crystallinity (X_c, %) was calculated using Universal Analysis 2000 v4.5A (TA Instruments-Waters LLC) software according to the following equation 4.4:

$$X_c = \frac{\Delta H_f^{obs}}{\Delta H_f^{\circ}} \; x \; 100 \tag{4.4}$$

where ΔH_f^{obs} is the observed enthalpy of fusion and ΔH_f° is the enthalpy of fusion of a 100% crystalline PCL sample (139.0 J/g). As presented in Table 4.1., incorporating MSSP in the blend impacted crystallinity of the composite film. For instance, crystallinity in the MSSP-50% films reduced by over 50% in comparison to film composed of PCL only (35.87% and 61.84% crystallized, respectively). This can be attributed to increase in amorphous region in the blend from MSSP as well as reduced regularity in the PCL segments.

Tensile and Mechanical Properties

Elongation at break, tensile strain and modulus of the films were determined. MSSP blended films were found to be highly flexible. The films stretchability doubled when 50% of the formulation was MSSP in comparison to films formulated from PCL alone (Figure 4.6.), with films withstanding up to 180% tensile strain versus 90%, respectively.
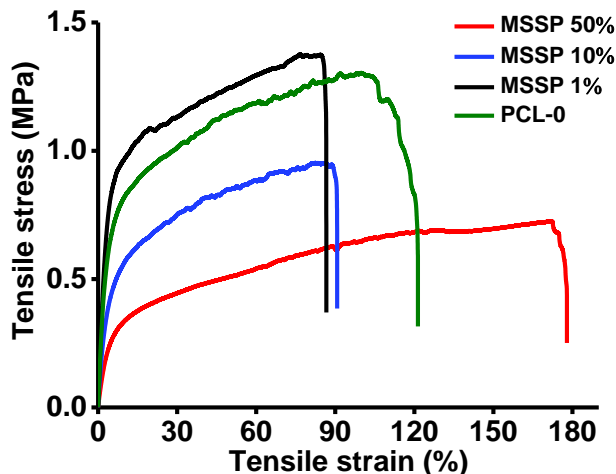
Figure 4.6. Stress-strain curves demonstrating the tensile behavior of MSSP blended films

A similar trend was observed with respect to elongation at break (Figure 4.7.); higher

concentration of MSSP in the films increased the flexibility of the films, MSSP-50 % stretch an

additional 59.7 ± 7.3mm. The modulus of the films showed a marked decrease with an increase

in MSSP content incorporated in the films; 9.63 ± 5.38MPa for MSSP-50% composition from

26.54 ± 5.94 MPa achieved by films without any MSSP (PCL alone). This is supported by the

decrease in crystallinity when a higher content of MSSP is blended in the films. The degree

of crystallinity in thermoplastics is reported to influence mechanical properties of the

materials.[32-34]
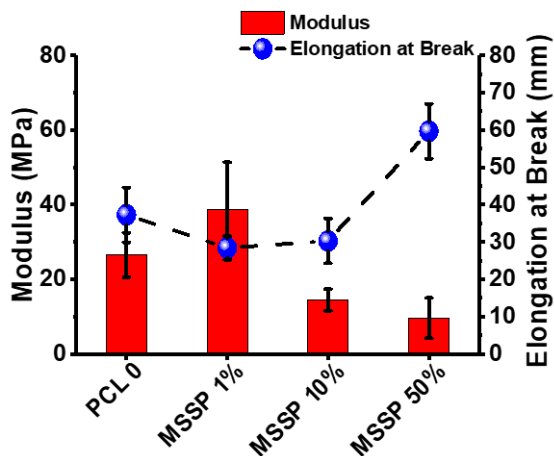
Figure 4.7. Modulus and elongation at break of MSSP blended films at various MSSP content as
determined from tensile testing

Materials properties of biomaterials such as the modulus and stiffness (rigidity) of the material are important in regulating the fate of cells including adhesion, differentiation and phenotype.[35, 36] Hence stiffness of the MSSP blended films was determined using AFM nanoindentation and calculated using NanoScope Analysis v1.5 software (Bruker, USA) from the relationship between the product of Young's modulus (E) and sample area as a function of sample area. Figure 4.8. shows that stiffness of the films can be modulated by the amount of MSSP incorporated into the films. Incorporation of low amounts of MSSP (< 10 wt. %) has minimal to negligible effect on the stiffness.
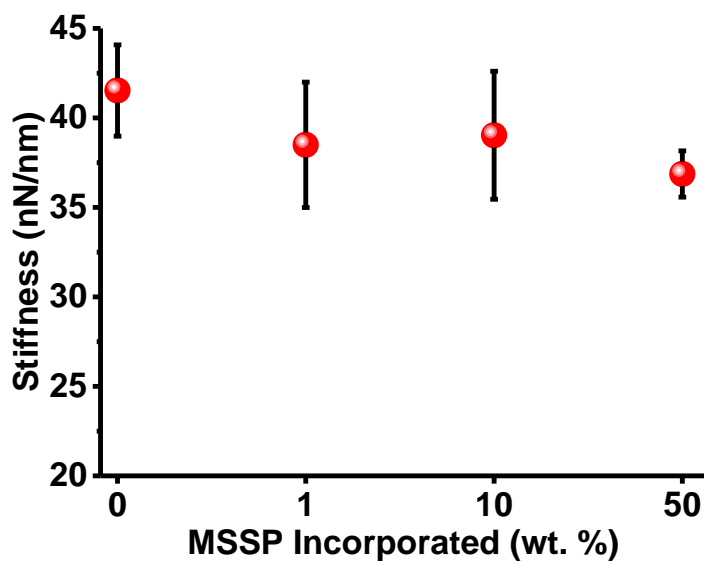
Figure 4.8. Stiffness of the MSSP blended films as a function of MSSP concentration

Similar observation was drawn with respect to Young's modulus of the films, which showed slight decrease when up to 10% MSSP was added to the film formulations (Figure 4.9.); from 1.10 ± 0.08 GPa given by PCL alone to 0.90 ± 0.11 GPa corresponding to MSSP 1%, 0.88 ± 0.09 GPa given by MSSP 10% and 0.90 ± 0.05 GPa from MSSP 50%. These values are within range of previously report data of PCL based films; hence it follows that, up to 50 wt.% MSSP can be successfully blended with PCL, increasing biobased content without compromising mechanical properties.
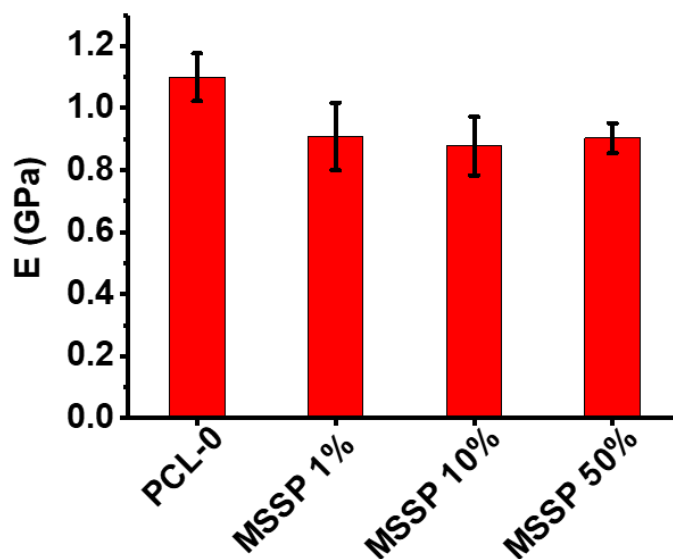
Figure 4.9. Young's modulus (E) determined for MSSP blended films from AFM
nanoindentation

Surface Analysis

MSSP blended films exhibited porous microstructure evidenced by the cross-sectional
SEM micrographs (Figure 4.10. (a)-(c)) obtained from the films. Pore size gradually increased
toward the surface with air-water interface as well as increased with amount of MSSP in film.
MSSP 50% had largest pore sizes ($10.4 \pm 6.0\mu m$) while MSSP 10% and PCL-0 had almost
similar pore sizes ($6.8 \pm 3.6\mu m$ and $5.4 \pm 1.0\mu m$, respectively).
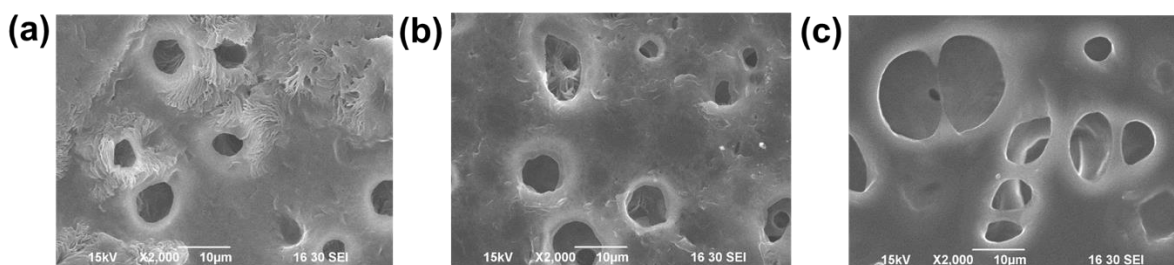
Figure 4.10. SEM micrograms showing porous microstructure of (a) PCL-0, (b). MSSP 10% and
(c). MSSP 50% films. Scalebar: 10μm

The surface morphology of the MSSP blended films was analyzed by AFM. Figure 4.11
shows three-dimensional AFM images of MSSP blended films, of varying MSSP concentrations,
over a scan area 20 μm x 20 μm. PCL-0 and MSSP 10% have similar topography and surface

roughness (Figure 4.11 (a) and (b), respectively) which implies MSSP and PCL blend homogenously without forming separate phases. While MSSP 50% films, on the other hand, exhibit a unique surface morphology, less surface roughness in comparison to the other formulations.
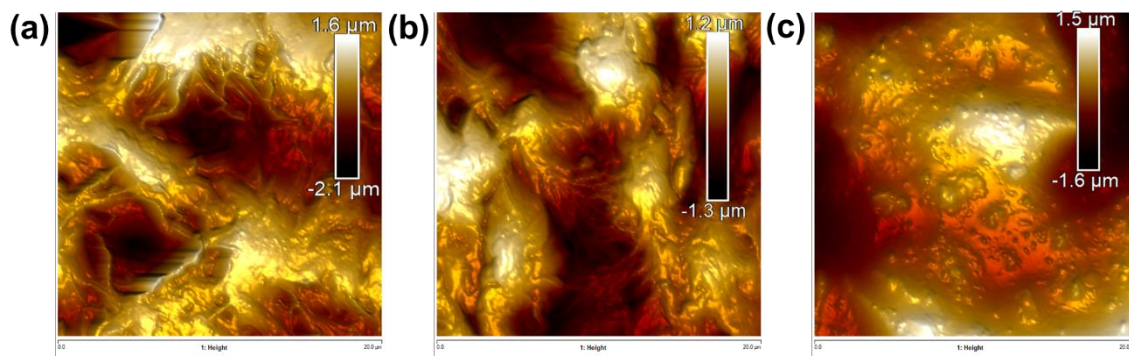
Figure 4.11. AFM height micrographs of MSSP blended films over a 20-µm scan; (a) PCL-0 film, (b) MSSP 10% film and (c) MSSP 50% film

Water Absorption

Low concentrations of MSSP in the composite films showed good water resistance similar to films prepared from PCL alone. Good water resistance is characteristic property of PCL films.[37] However, water absorption is observed to increase with the increasing amount of MSSP in the blended films as depicted in Figure 4.12. resulting in reduction in water resistance. Adding 10% MSSP into film formulations, reduced water resistance up to 54% in comparison the control formulation. MSSP 50% films had the highest water absorption, reaching 100% after 7 days, which continued to increase reaching 130% absorption after 21days. Higher water absorption in the MSSP-PCL 50% films was attributed to multiple hydroxyl groups in MSSP as well as the high porosity and large pore sizes. MSSP 10% films exhibited a swelling capacity (up to 65% water absorption) still higher than PCL-0 (25%), which performed similarly to MSSP 1% films. Swelling capacity of the composite films can influence the encapsulation or loading efficiency of desired payload.
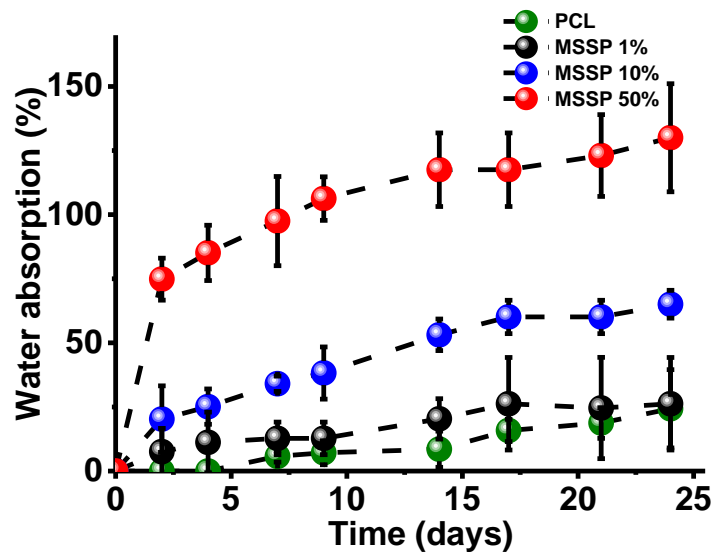
Figure 4.12. Water absorption profile of MSSP blended films over an extended period

Biodegradation

Biodegradation profile of the MSSP blended films was evaluated via enzymatic

degradation. Films were incubated in lipase solution (2mg/mL). Lipase is in a class of enzymes

known as hydrolases. These enzymes exhibit activity towards poorly water-soluble substrate

such as triglycerides or long-chain fatty acids[38]. MSSP is composed of derivatized soybean oil

fatty acid chains making it an ideal candidate for lipase activity. Although, PCL is biodegradable

by microorganisms such as fungi and bacteria due to hydrolysis of ester linkages, it is not a

suitable substrate for degradation by enzymes within human bodies[5, 39]. Figure 4.13. illustrates

that the higher content of MSSP in the film formulation facilitated enzymatic degradation of the

composites. Film containing 50% MSSP exhibited up four times more degradation (40%)

compared to pure PCL film (10%). Up to 40% of the film degraded in comparison to only 10%

over 24 days.

128
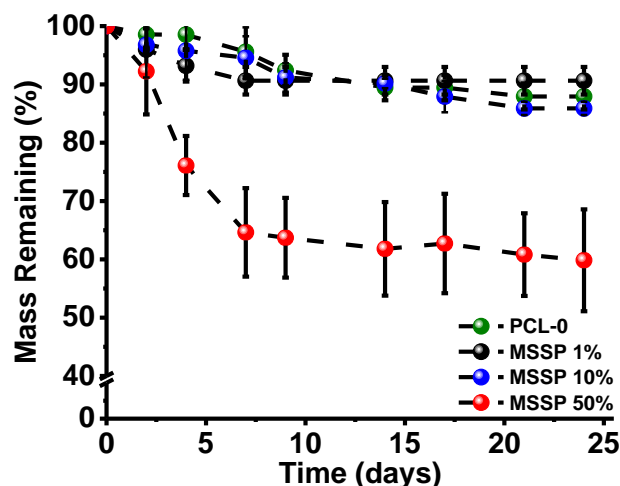
Figure 4.13. Biodegradation profile of MSSP blended films evaluated under treatment with enzyme Lipase over a prolonged period

Release of Doxorubicin

Dox loaded MSSP blended films were prepared using LbL deposition of dox dissolved in polyelectrolytes, and hyaluronic acid (Figure 4.14.).
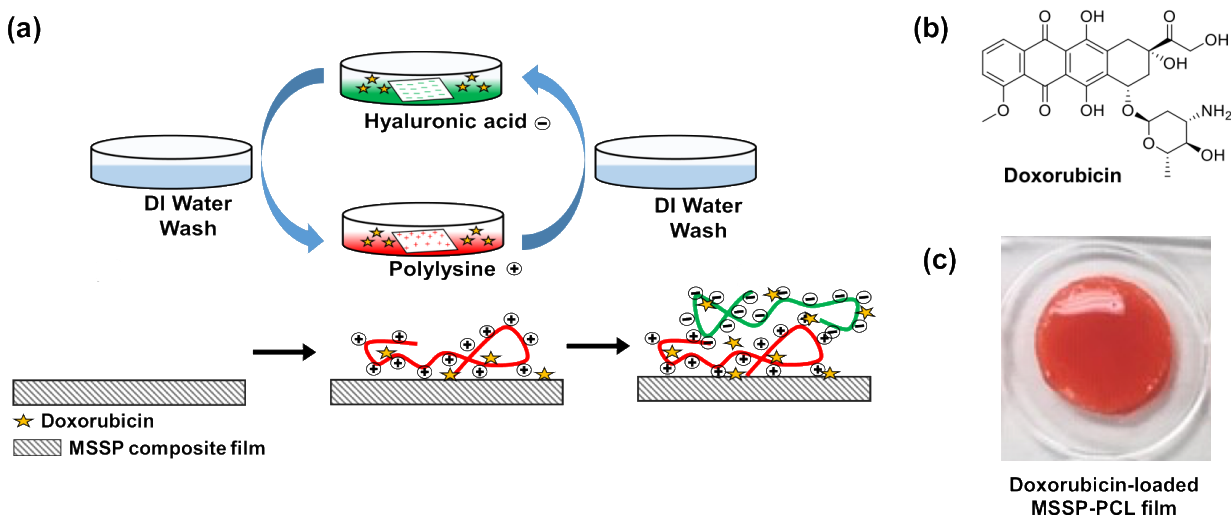
Figure 4.14. (a). Illustration of layer-by-layer coating of MSSP blended films with poly (Lysine) and hyaluronic acid including the doxorubicin loading, (b). Chemical structure of doxorubicin and (c). Photographic imaged of doxorubicin-loaded MSSP-PCL film.

Dox is a chemotherapeutic agent in the anthracycline family and has been reported to highly effective toward breast cancer treatment as well as several other cancers.[40-42] Despite this, dox has short residence time, is cumulative dose-dependent, and highly toxic which limits its

129

application. Therefore, we designed a depot-type drug-eluting film amenable for localized delivery of dox. Drug-loaded films were prepared using LbL technology. LbL complexation of hyaluronic acid and has been shown to form thin nano-scale multilayered films.[22] Resultant dox-loaded films took on the red color of dox.

Repeated alternation in the assembly of the polyanion and polycation onto the MSSP blended films facilitated higher drug loading. Additionally, film composition played a role in influencing loading, MSSP-50% films exhibited up to 13% higher loading capacity per square centimeter area than PCL-0 films (45.0 ± 10.6 μg/cm^2 and 39.8 ± 9.1 μg/cm^2, respectively). MSSP imparted surface properties with a higher affinity for the drug in polyelectrolyte solutions.

In vitro release profiles of dox from the MSSP blended films is shown in Figure 4.15. Both films exhibited slow releasing rate, achieving close to 20% dox release over a 24 h period. Although, MSSP 50% films had an overall slightly more sustained release than films PCL-0 films. Therefore, not only does incorporating up to 50% Biobased content into PCL films increase the loading capacity, it maintains the functional performance of the PCL films without any negative compromise.
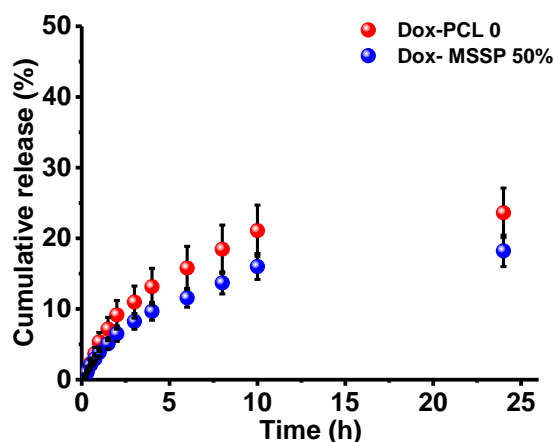
Figure 4.15. Comparative cumulative release of doxorubicin from MSSP 50% films and PCL-0 films

Figure 4.16 shows the effect of LbL coating on the surface properties of the composite films. The higher the number of complexed bilayers, the more hydrophobic the surface became; films with 40 bilayers had a water contact angle 10° higher than film without any surface coating. It was observed that 20 bilayers, or less, had no significant effect on the water contact angle.
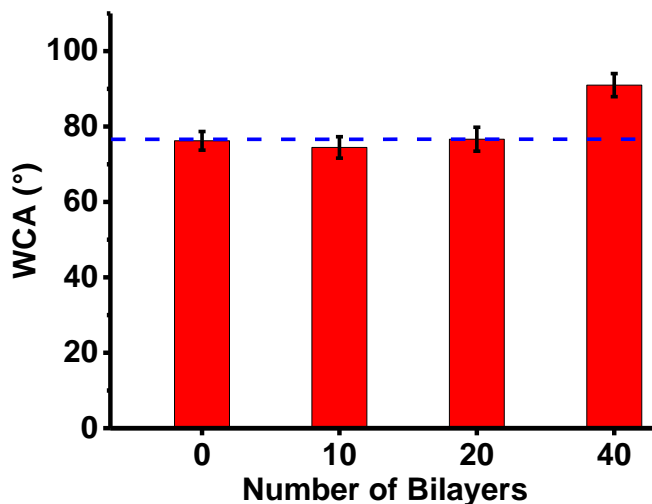
Figure 4.16. Water contact angle determine on the MSSP 50% composite films after LbL coating as a function of number of bilayers

AFM micrographs (Figure 4.16.) show the height and phase images of the representative MSSP -50% film before LbL and after layering with 40 bilayers. The films were scanned over a 20μm x 20μm area. Deposition of multiple layers resulted in fewer micro features and introduced more uniform submicron roughness. The AFM height micrographs, representative of the entire film, show larger distinction between the surface features of either films, MSSP 50%-0LbL (Figure 4.17 (a)) and MSSP-40LbL (Figure 4.17 (b)).
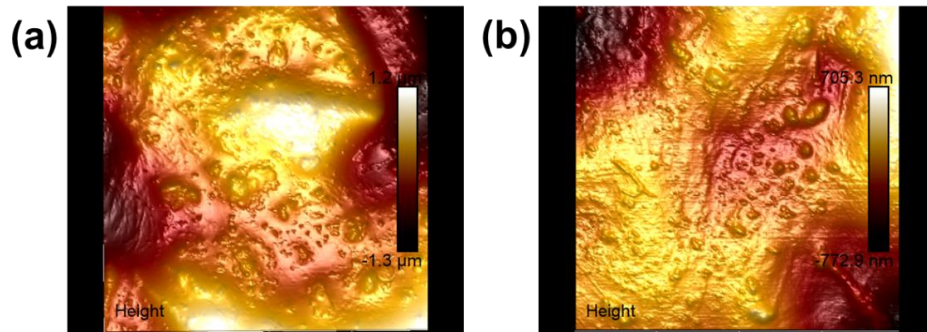
Figure 4.17. AFM micrograms showing height images of (a). MSSP 50 %-0LbL film without any alternating hyaluronic acid or poly (lysine) bilayers compared to (b). MSSP 50% after coating with 40 LbL bilayers over 20μm scan area

On the other hand, the color map of the phase images shows the dominance of mostly one phase which implies the components of composite films are compatible with each other. The neat MSSP 50%-0LbL has spotted areas, which appear out of phase with the majority of the film (Figure 4.18 (a)), while 40 bilayers result in more uniformity in the distribution of film composition (Figure 4.18 (b)).
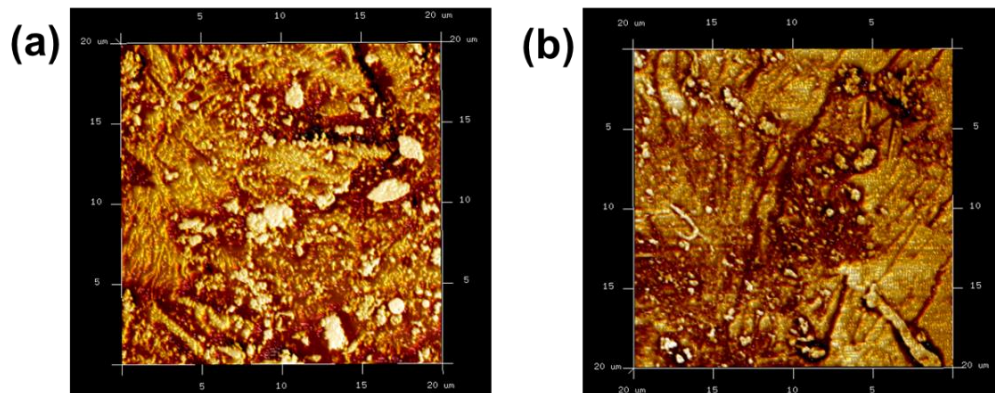
Figure 4.18. AFM micrograms showing the phase images of (a). MSSP 50 % film without any LbL bilayers, and (b). MSSP 50% after coating with 40 LbL bilayers

Conclusions

Biobased flexible drug-eluting films were successfully from a blend of MSSP and PCL. Blending MSSP and PCL reduced the modulus and increased film flexibility; as well as enhanced the biodegradation profile of the films. Multi-layer drug loaded on the films obtained

via layer-by-layer assembly of dox dissolved polyelectrolytes, and hyaluronic acid. MSSP imparted surface properties favorable for the adhesion of the polyelectrolyte, hence achieving higher drug loading. Incorporation of MSSP not only enhanced the performance of PCL films but introduce biobased content rendering the films more sustainable and affordable to manufacture. We envision that such soy-based flexible films present new potential biomaterials for applications in drug delivery, tissue engineering and general surgery.

References

1.   Wolinsky, J. B.; Colson, Y. L.; Grinstaff, M. W., Local drug delivery strategies for cancer treatment: gels, nanoparticles, polymeric films, rods, and wafers. J. Controlled Release 2012, 159 (1), 14-26.

2.   Liu, R.; Wolinsky, J. B.; Walpole, J.; Southard, E.; Chirieac, L. R.; Grinstaff, M. W.; Colson, Y. L., Prevention of local tumor recurrence following surgery using low-dose chemotherapeutic polymer films. Ann Surg Oncol. 2010, 17 (4), 1203-1213.

3.   Wolinsky, J. B.; Liu, R.; Walpole, J.; Chirieac, L. R.; Colson, Y. L.; Grinstaff, M. W., Prevention of in vivo lung tumor growth by prolonged local delivery of hydroxycamptothecin using poly (ester-carbonate)-collagen composites. J. Controlled Release 2010, 144 (3), 280-287.

4.   Luo, Y.; Kirker, K. R.; Prestwich, G. D., Cross-linked hyaluronic acid hydrogel films: new biomaterials for drug delivery. J. Controlled Release 2000, 69 (1), 169-184.

5.   Mondal, D.; Griffith, M.; Venkatraman, S. S., Polycaprolactone-based biomaterials for tissue engineering and drug delivery: Current scenario and challenges. Int. J. Polym. Mater. Polym. Biomater. 2016, 65 (5), 255-265.

6.   Choong, C. S.; Hutmacher, D. W.; Triffitt, J. T., Co-culture of bone marrow fibroblasts and endothelial cells on modified polycaprolactone substrates for enhanced potentials in bone tissue engineering. Tissue eng. 2006, 12 (9), 2521-2531.

7.   Ribeiro, C.; Panadero, J.; Sencadas, V.; Lanceros-Méndez, S.; Tamano, M.; Moratal, D.; Salmerón-Sánchez, M.; Ribelles, J. G., Fibronectin adsorption and cell response on electroactive poly (vinylidene fluoride) films. Biomed. Mater. 2012, 7 (3), 035004.

8.   Ranjan, A.; Webster, T. J., Increased endothelial cell adhesion and elongation on micron-patterned nano-rough poly (dimethylsiloxane) films. Nanotechnology 2009, 20 (30), 305102.

9.   Do, A. V.; Khorsand, B.; Geary, S. M.; Salem, A. K., 3D Printing of Scaffolds for Tissue Regeneration Applications. Adv. Healthcare Mater. 2015, 4 (12), 1742-1762.

10.   Serrano, M.-C.; Pagani, R.; Vallet-Regí, M.; Peña, J.; Comas, J.-V.; Portolés, M.-T., Nitric oxide production by endothelial cells derived from blood progenitors cultured on NaOH-treated polycaprolactone films: a biofunctionality study. Acta Biomater. 2009, 5 (6), 2045-2053.

11.   Yeo, A.; Wong, W.; Khoo, H.; Teoh, S., Surface modification of PCL-TCP scaffolds improve interfacial mechanical interlock and enhance early bone formation: An in vitro and in vivo characterization. J. Biomed. Mater. Res., Part A 2010, 92 (1), 311-321.

12.   Ng, K. W.; Achuth, H. N.; Moochhala, S.; Lim, T. C.; Hutmacher, D. W., In vivo evaluation of an ultra-thin polycaprolactone film as a wound dressing. J. Biomater. Sci., Polym. Ed. 2007, 18 (7), 925-938.

13.   Hammond, P. T., Building biomedical materials layer-by-layer. Mater. Today 2012, 15 (5), 196-206.

14. Gribova, V.; Auzely-Velty, R.; Picart, C., Polyelectrolyte multilayer assemblies on materials surfaces: from cell adhesion to tissue engineering. Chem. Mater. 2011, 24 (5), 854-869.

15. Li, Y.; Wang, X.; Sun, J., Layer-by-layer assembly for rapid fabrication of thick polymeric films. Chem. Soc. Rev. 2012, 41 (18), 5998-6009.

16. Andres, C. M.; Kotov, N. A., Inkjet deposition of layer-by-layer assembled films. J. Am. Chem. Soc. 2010, 132 (41), 14496-14502.

17. Castleberry, S. A.; Li, W.; Deng, D.; Mayner, S.; Hammond, P. T., Capillary flow layer-by-layer: a microfluidic platform for the high-throughput assembly and screening of nanolayered film libraries. ACS nano 2014, 8 (7), 6580-6589.

18. Richardson, J. J.; Björnmalm, M.; Caruso, F., Technology-driven layer-by-layer assembly of nanofilms. Science 2015, 348 (6233), aaa2491.

19. Zhang, J.; Senger, B.; Vautier, D.; Picart, C.; Schaaf, P.; Voegel, J.-C.; Lavalle, P., Natural polyelectrolyte films based on layer-by layer deposition of collagen and hyaluronic acid. Biomaterials 2005, 26 (16), 3353-3361.

20. Thierry, B.; Winnik, F. M.; Merhi, Y.; Tabrizian, M., Nanocoatings onto arteries via layer-by-layer deposition: toward the in vivo repair of damaged blood vessels. J. Am. Chem. Soc. 2003, 125 (25), 7494-7495.

21. Jaklenec, A.; Anselmo, A. C.; Hong, J.; Vegas, A. J.; Kozminsky, M.; Langer, R.; Hammond, P. T.; Anderson, D. G., High throughput layer-by-layer films for extracting film forming parameters and modulating film interactions with cells. ACS Appl. Mater. Interfaces 2016, 8 (3), 2255-2261.

22. Khademhosseini, A.; Suh, K. Y.; Yang, J. M.; Eng, G.; Yeh, J.; Levenberg, S.; Langer, R., Layer-by-layer deposition of hyaluronic acid and poly-L-lysine for patterned cell co-cultures. Biomaterials 2004, 25 (17), 3583-3592.

23. Miao, S.; Wang, P.; Su, Z.; Zhang, S., Vegetable-oil-based polymers as future polymeric biomaterials. Acta Biomater. 2014, 10 (4), 1692-1704.

24. Alam, M.; Akram, D.; Sharmin, E.; Zafar, F.; Ahmad, S., Vegetable oil based eco-friendly coating materials: A review article. Arabian J. Chem. 2014, 7 (4), 469-479.

25. Lligadas, G.; Ronda, J. C.; Galia, M.; Cadiz, V., Renewable polymeric materials from vegetable oils: a perspective. Mater. Today 2013, 16 (9), 337-343.

26. Nelson, T. J.; Bultema, L.; Eidenschink, N.; Webster, D. C., Bio-based high functionality polyols and their use in 1K polyurethane coatings. J. Renewable Mater. 2013, 1 (2), 141-153.

27. Pan, X.; Sengupta, P.; Webster, D. C., High biobased content epoxy–anhydride thermosets from epoxidized sucrose esters of fatty acids. Biomacromolecules 2011, 12 (6), 2416-2428.

28. Ma, S.; Webster, D. C., Naturally occurring acids as cross-linkers to yield VOC-free, high-performance, fully bio-based, degradable thermosets. Macromolecules 2015, 48 (19), 7127-7137.

29. Pan, X.; Sengupta, P.; Webster, D. C., Novel biobased epoxy compounds: epoxidized sucrose esters of fatty acids. Green Chem. 2011, 13 (4), 965-975.

30. Serrano, M. C.; Portolés, M. T.; Vallet-Regí, M.; Izquierdo, I.; Galletti, L.; Comas, J. V.; Pagani, R., Vascular endothelial and smooth muscle cell culture on NaOH-treated

poly (ε-caprolactone) films: a preliminary study for vascular graft development. Macromol. Biosci. 2005, 5 (5), 415-423.

31.   Woodruff, M. A.; Hutmacher, D. W., The return of a forgotten polymer— Polycaprolactone in the 21st century. Prog. Polym. Sci. 2010, 35 (10), 1217-1256.

32.   Ping, P.; Wang, W.; Chen, X.; Jing, X., The influence of hard-segments on two-phase structure and shape memory properties of PCL-based segmented polyurethanes. J. Polym. Sci., Part B: Polym. Phys. 2007, 45 (5), 557-570.

33.   Simoes, C.; Viana, J.; Cunha, A., Mechanical properties of poly (ε-caprolactone) and poly (lactic acid) blends. J. Appl. Polym. Sci. 2009, 112 (1), 345-352.

34.   Bai, H.; Xiu, H.; Gao, J.; Deng, H.; Zhang, Q.; Yang, M.; Fu, Q., Tailoring impact toughness of poly (L-lactide)/poly (ε-caprolactone)(PLLA/PCL) blends by controlling crystallization of PLLA matrix. ACS Appl. Mater. Interfaces 2012, 4 (2), 897-905.

35.   Lv, H.; Wang, H.; Zhang, Z.; Yang, W.; Liu, W.; Li, Y.; Li, L., Biomaterial stiffness determines stem cell fate. Life Sci. 2017, 178, 42-48.

36.   Shapira-Schweitzer, K.; Seliktar, D., Matrix stiffness affects spontaneous contraction of cardiomyocytes cultured within a PEGylated fibrinogen biomaterial. Acta Biomater. 2007, 3 (1), 33-41.

37.   Wu, C.-S., Physical properties and biodegradability of maleated-polycaprolactone/starch composite. Polym. Degrad. Stab. 2003, 80 (1), 127-134.

38.   Chahinian, H.; Nini, L.; Boitard, E.; Dubès, J.-P.; Comeau, L.-C.; Sarda, L., Distinction between esterases and lipases: a kinetic study with vinyl esters and TAG. Lipids 2002, 37 (7), 653-662.

39.   Sinha, V.; Bansal, K.; Kaushik, R.; Kumria, R.; Trehan, A., Poly-ϵ-caprolactone microspheres and nanospheres: an overview. Int. J. Pharm. 2004, 278 (1), 1-23.

40.   Cuong, N.-V.; Jiang, J.-L.; Li, Y.-L.; Chen, J.-R.; Jwo, S.-C.; Hsieh, M.-F., Doxorubicin-loaded PEG-PCL-PEG micelle using xenograft model of nude mice: Effect of multiple administration of micelle on the suppression of human breast cancer. Cancers 2011, 3 (1), 61-78.

41.   Kuerer, H. M.; Newman, L. A.; Smith, T. L.; Ames, F. C.; Hunt, K. K.; Dhingra, K.; Theriault, R. L.; Singh, G.; Binkley, S. M.; Sneige, N., Clinical course of breast cancer patients with complete pathologic primary tumor and axillary lymph node response to doxorubicin-based neoadjuvant chemotherapy. J. Clin. Oncol. 1999, 17 (2), 460-460.

42.   Chan, S.; Friedrichs, K.; Noel, D.; Pintér, T.; Van Belle, S.; Vorobiof, D.; Duarte, R.; Gil Gil, M.; Bodrogi, I.; Murray, E., Prospective randomized trial of docetaxel versus doxorubicin in patients with metastatic breast cancer. J. Clin. Oncol. 1999, 17 (8), 2341-2341.

CHAPTER 5. EVALUATION OF EPOXIDIZED SUCROSE SOYATE FOR THREE-DIMENSIONAL MATRIX FOR BIOMATERIAL APPLICATIONS[1][2]

Abstract

A new controlled-release platform for hydrophilic compounds has been developed, utilizing citric acid-cured ESS as the matrix forming material. By cross-linking epoxy groups of ESS with citric acid (CA) in the presence of a hydrophilic model molecule, sodium salt of fluorescein (Sod-FS), we were able to entrap the latter homogenously within the ESS matrix. No chemical change of the entrapped active agent was evident during the fabrication process. Hydrophobicity of the matrix was found to be the rate-limiting factor for sustaining the release of the hydrophilic model compound, while inclusion of release-modifiers such as PEG within the matrix system modulated the rate and extent of guest release. Using 5 kDa PEG at 5 % (w/w) of the total formulation made it possible to extend the release of the active ingredient for more than a month. In addition, the amount of modifiers in formulations also influenced the mechanical properties of the matrices, including loss and storage modulus. Mechanism of active release from ESS matrices was also evaluated using established kinetic models. Formulations composed

---

[1] This chapter contains material reprinted from Chitemere, R.; Stafslien, S.; Jiang, L.; Webster, D.; Quadir, M., Soy-Based Soft Matrices for Encapsulation and Delivery of Hydrophilic Compounds. Polymers 2018, 10 (6), 583.

[2] Material in this chapter was co-authored by Ruvimbo Chitemere (Wright), Shane Stafslien; Long Jiang; Dean Webster and Mohiuddin Quadir. Ruvimbo Chitemere (Wright) had primary responsibility for sample formulation, conducting experiments, materials characterization and data interpretation. Ruvimbo Chitemere (Wright) was the primary developer of the conclusions that are advanced here. Ruvimbo Chitemere (Wright) also drafted and revised all versions of this chapter. Dean Webster and Mohiuddin Quadir conceived and designed the experiments. Mohiuddin Quadir served as proofreader and corresponding author. Long Jiang designed and supervised the mechanical studies. Shane Stafslien conducted the cell studies.

entirely of ESS showed a non-Fickian (anomalous) release behavior while Fickian (Case I) transport was the predominant mechanism of active release from ESS systems containing varying amount of PEGs. The mean dissolution time (MDT) of the hydrophilic guest molecule from within the ESS matrix was found to be a function of the molecular weight and the amount of PEG included. At the molecular level, we observed no cellular toxicities associated with ESS up to a concentration level of 10 µM. We envision that such fully bio-based matrices can find applications in compounding point-of-care, extended-release formulations of highly water-soluble active agents.

Introduction

Extended-release formulations have been an attractive product platform for therapeutic and diagnostic applications.[1] Extending the release of water-soluble guest molecules is an unmet challenge in this area, since many therapeutically active drugs, diagnostic agents, biocides, and fungicides are formulated as the salt of the active molecule to impart maximum engagement with their substrate targets. A set of existing technologies for fabricating extended-release formulations for hydrophilic drugs and bioactive chemical moieties include direct-compression of the active compound into matrices using excipients, micro- and/or nano-encapsulation, or reversible chemical conjugation of the active species with a polymer. Among these fabrication processes, polymer-based matrix systems are commonly used for manufacturing extended- and controlled release delivery systems because it makes such manufacturing easy.[2] Using mechanically compressed or chemically cross-linked polymeric network to form a matrix, which is capable of suppressing the rate of diffusion of an entrapped molecule to the surrounding milieu, has been the basis of such controlled-release formulations.

Ideally, a matrix-forming polymer, intended for designing extended release formulations of hydrophilic active ingredients, needs to release the entrapped species at a controlled-rate to maintain a constant dosage range over an extended period. At the same time, the matrix forming candidates need to be bio- and environmentally compatible and should be commercially viable. Current limitations in controlled- and extended-release technology involves difficulties in attaining extended temporal control, premature (burst) release of the active agent, manufacturing and materials cost, and unwanted interactions of the matrix-forming materials with biotic components resulting in non-specific side-effects.

A large cohort of polymers and biomaterials has been employed as release retarding materials each of which presents a different approach to the matrix concept. For example, poly (hydroxyethyl methacrylate), poly(vinyl alcohol), poly(vinyl pyrrolidone), poly(ethylene oxide), sodium alginate[3], poly(ethylene glycol) (PEG)[4, 5], hydroxypropyl methylcellulose [6-8], and hydroxyethyl cellulose have been extensively used which impart control over active release through the formation of insoluble or hydrogel networks.[9, 10] Polymers forming insoluble or skeleton matrices, such as biodegradable polyanhydrides[11], polyhydroxyalkanoate[12], polyesters of poly(glycolic acid) (PGA), poly(lactic acid) (PLA), polylactide-co-glycolide (PLGA)[10], polyurethanes; or non-degradable poly(dimethyl siloxane) (PDMS), poly(ethylene vinyl acetate) (PVA), and polyvinyl chloride (PVC); poly(vinyl pyrrolidone) or poly(vinyl acetate) are extensively used to generate controlled-release delivery systems for drugs and biologically active macromolecules such as large peptides and proteins.

Natural materials, of a hydrophobic and water-insoluble nature, such as lipids, waxes, or fatty acids such as Carnauba wax, beeswax[13], micro crystalline wax[14], candelilla wax[15], ozokerite wax, and paraffin waxes, which are potentially erodible, have also been used as the more

141

economically-viable and environmentally-friendly material candidates to generate controlled-release platforms. Such lipid-based systems have drawn particular attraction due to the advantageous properties they offer in comparison to most synthetic polymers. These properties include an ability to load and release both hydrophilic and hydrophobic compounds, the superior biocompatibility profile of the matrix-forming agents, non-specific interactions with biological components, lower immunogenicity[16, 17] and degradation to biocompatible end products unlike many synthetic polymers[18]. Although lipid-based matrices show a lot of promise in designing extended release formulations, owing to high hydrophobicity, these systems also result in unreliable release kinetics, oftentimes resulting in incomplete or sub-optimal diffusion of the active agent from within the matrix interior. In addition, many of the FDA-approved hydrophobic matrix-formers, such as beeswax, carnauba wax, glyco- and phospholipids, possess complex chemical structures and exhibit significant variability in physical properties depending on the source and method of extraction.

Semi-synthetic and synthetic bio-based lipid-like materials are viable options to bypass these limitations of natural lipids and wax-based matrix-forming agents and can offer the benefit of batch-to-batch uniformity, affordability, biodegradability, low toxicity, accessibility, and straightforward synthesis of drug delivery systems[19-21]. For example, soybean oil derived fatty acids and synthetically modified products thereof have gained popularity due to facile preparative methods, tunable properties, versatility, low cost, biodegradability, and high bio-content[22, 23]. Epoxidation of triglycerides of soybean oils yields multi-functional lipid-like molecules amenable to application-guided post-synthetic modifications[24].

Oxirane ring opening reaction of epoxidized triglycerides derived from soy has been used for crosslinking modified triglycerides with a variety of acids and alcohols for facile preparation

of coatings and film formulations[22, 23, 25]. ESS, a sucrose ester derivative of soybean oil fatty acids, which has been studied for its capability to form cross-linked networks with excellent mechanical properties[25, 26]. Soybean oil and its derivatives have also been studied extensively for their applications in polyurethane production, polyesters, and potential application in biomaterials[21, 23, 27, 28].

In this study, we report a readily compoundable fabrication process of a hydrophobic matrix system composed of ESS that can be used to fabricate extended release delivery formulations of hydrophilic substances in the form of matrices. To realize this goal, ESS was cross-linked with CA in the presence of the model water-soluble compound, Sod-FS, to entrap the latter in a fully bio-based 3D matrix[26]. Sod-FS is a salt of a free basic dye, fluorescein, and has been used in this study as a representative molecule of compounds and drugs which are highly hydrophilic in nature. CA makes a suitable biocompatible cross-linker as it possesses multiple functional groups and capable of fast gelling with epoxides[29, 30].

We evaluated the capacity of ESS-derived matrices to sustain the release of hydrophilic Sod-FS, investigated the kinetics of active release as a function of matrix formulations and mechanical properties, and finally evaluated the biocompatibility of the ESS as a matrix-forming material. We evaluated the capacity of ESS-derived matrices to sustain the release of hydrophilic Sod-FS, investigated the kinetics of active release as a function of matrix formulations and mechanical properties, and finally evaluated the biocompatibility of the ESS as a matrix-forming material. We envision that such bio-based matrices can provide easy access towards the preparation of controlled-release delivery systems of water-soluble active ingredients, intended for pharmaceutical, diagnostic, and theragnostic applications.

Experimental

Materials

Epoxidized sucrose soyate (ESS), with an epoxy equivalent weight of 243.4g/eq synthesized according to previously reported procedure[26]. Citric acid (CA), PEG methyl ether (PEG, M_n =750, 2000 and 5000) and Sod-FS were purchased from Sigma-Aldrich (St Louis, MO, USA). THF and DMSO were acquired from Millipore Sigma (Billerica, MA, USA). PBS tablets (10 mM) were purchased from VWR (Solon, OH, USA), which was used to prepare PBS solution of pH 7.4. All reagents were used as received. L929 mouse fibroblast cell line was purchased from American Type Culture Collection (Manassas, VA, USA). Eagles minimum essential medium (EMEM), Hank's balanced salt solution (HBSS), fetal bovine serum (FBS), penicillin and streptomycin were acquired from HyClone Laboratories (GE Healthcare Life Sci., Logan, UT, USA). 3-(4, 5-dimethylthiazol-2-yl)-2, 5-diphenyltetrazolium bromide (MTT) reagent was purchased from Promega (Madison, WI, USA)

Preparation of ESS-CA Matrix

Soy-derived hydrophobic ESS-CA matrices were prepared by crosslinking ESS with CA following the composition and curing conditions listed in Table 5.1. First, CA was dissolved in deionized water to achieve a 1:6 or 1:8 acid to water molar ratio. In the following step, ESS was added to the CA solution in a glass vial and manually stirred for 2 min followed by high speed mixing in a VWR standard vortex system (VWR, Radnor, PA, USA) until a homogenous mixture was achieved. The mixture was then heated at 80°C with magnetic stirring for up to 3 h and allowed to cool to room temperature. For the preparation of Sod-FS loaded matrices, the active agent was dissolved in deionized water prior to adding CA. ESS was added to the CA-Sod-FS solution to form the matrix in a similar fashion as detailed above. The Sod-FS loading

was adjusted to achieve 0.026 wt. % (low [Sod-FS]) and 0.065 wt. % (high [Sod-FS]) by weight

of ESS. For inclusion of release modifiers within the formulation, different molecular weight of

PEGs was incorporated at 5 *w/v* % aqueous solution prior to adding CA and Sod-FS

Table 5.1. Compositions and Curing Conditions for ESS-Citric Acid Cross-linked Matrices.

Sample	Molar ratio					T °C/Time	Matrix type
	ESS	CA	Di-H$_2$O	PEG	Sod-FS		
EC-1	1	0.98	6			80/2 h	High [H$^+$]
EC-2	1	0.98	8			80/2 h	Low [H$^+$]
ECP-750	1	0.98	6	0.007		80/3 h	
ECP-2k	1	0.98	6	0.007		80/3 h	PEGylated
ECP-5k-5	1	0.98	6	0.007		80/3 h	Matrices
ECP-5k-1	1	0.98	6	0.003		80/2.5 h	
EC-Sod-FS-L	1	0.98	6		0.002	80/2.5 h	Low [Sod-FS]
EC-Sod-FS-H	1	0.98	6		0.005	80/2.5 h	High [Sod-FS]

Determination of Loading Content

ESS-CA matrices loaded with Sod-FS were cut into cubes (v = 3.41 mm3) for each

formulation. For estimation of active loading, the cubes were homogenized using a mortar and

pestle and incubated in 10 mM PBS (10 mL) for 24 h at 37°C with moderate stirring. The

samples were centrifuged at 5000 rpm for 1 h and then filtered through a 0.45 mm micro-filter.

The absorbance spectra of the filtered supernatant were analyzed using a Varian Cary 5000 UV–

Vis-NIR spectrophotometer (Agilent Technologies, Santa Clara, CA, USA) to quantify the Sod-

FS concentration.

Materials Characterization

ATR-IR Spectroscopy

ATR-IR of the components used to fabricate the ESS-CA matrices was performed using a

Nicolet 8700 FT-IR with a Smart iTR diamond tip accessory (Thermo Scientific, Grand Island,

NY, USA). Spectra representative of the top, bottom and internal surface of the matrices were collected. To analyze the internal surface, the matrices were sectioned along the transverse plane.

GPC

GPC was obtained using a TOSOH EcoSEC HLC-8320GPC system (TOSOH Bioscience, Japan) gel permeation chromatograph calibrated with polystyrene standards. ESS solution was prepared in THF at a concentration of 5 mg/mL.

SEM

To analyze the microstructures of ESS-CA matrices, SEM image analysis was performed. Samples were mounted on aluminum mounts using carbon adhesive tabs/ tape and then coated with a conductive layer of carbon in a high-vacuum evaporative coater (Cressington 208c, Ted Pella Inc., Redding, CA, USA). Images were obtained with a JEOL JSM-7600F scanning electron microscope (JEOL USA Inc., Peabody, MA, USA) operating at 2kV.

Viscoelasticity Testing

Viscoelasticity of the ESS-CA matrices was analyzed using an ARES-G2 Rheometer (TA Instruments, New Castle, DE, USA). Matrix samples were cut into 1–2 mm thick discs of 25 mm diameter using a 25 mm hollow steel punch. Samples were analyzed between two parallel plates at 37∘C using a frequency sweep method (0.02–628rad/s) under a constant 0.5% strain (within the linear viscoelastic region of the samples). The samples were equilibrated for 2 min prior to testing.

Water Contact Angle Measurement

Contact angle of the ESS-CA matrices of different formulations with and without PEGs was measured using FTA 200 dynamic contact angle/surface tension analyzer and FTA 32 video (First Ten Ångstroms, Portsmouth, VA, USA). Measurements were taken from both the top and

bottom surfaces of the matrices (n = 5). Three sample replicates were used for each formulation for each surface.

Content Release Studies

Different formulations of ESS-CA matrices containing Sod-FS (in the forms of cubes of 3.41 mm^3) were placed in 15 mL of PBS (10 mM, pH 7.4). The samples were incubated at 37 ◦C with moderate stirring. After every 24 h, 1.5 mL of sample solution was collected and replaced with an equal volume of fresh PBS (10 mM, pH 7.4). The absorbance spectra of the withdrawn sample were analyzed using a Varian Cary 5000 UV–VIS NIR spectrophotometer (Agilent Technologies, Santa Clara, CA, USA). Cumulative percent release was determined using the following equation 5.1.:

$$cumulative \text{ } \% \text{ } release = \frac{volume \text{ } withdrawn}{volume \text{ } of \text{ } bath} \text{ } x \text{ } \%release \text{ } at \text{ } time \text{ } t + \text{ } \Sigma \text{ } \%release \text{ } at \text{ } t-1 \quad (5.1)$$

Kinetic Analysis of the Release Data of SOD-FS from ESS-Matrices

The dissolution data for Sod-FS from within the ESS-CA matrices of different formulations were fitted to Higuchi model, equation 5.2.:

$$\frac{M}{M\alpha} = kt^{\frac{1}{2}} \quad (5.2)$$

where M/Mα indicates fractional release of the linear segment of the release profile, *t* is the time of release, and *k* is a Higuchi constant. As Higuchi equation does not include the swelling and erosion component of diffusion, release data have also been fitted with well-known bi-exponential model equation 5.3.:

$$\frac{M}{M\alpha} = kt^n \quad (5.3)$$

where M Mα is the fractional release of linear segment of the release profile, t is the release time, k is a constant incorporating the properties of the macromolecular polymeric systems and the

active ingredient, and n is the kinetic constant, which describes the mechanism of molecule transport. For matrices, an n value of 0.45 obtained from Equation (5.3) defines the profile to follow Fickian (Case I) release, $0.45 < n < 0.89$ describes non-Fickian (Anomalous) release, n=0.89 represents Case II (Zero order) release and n>0.89 refers to super case II release[31, 32].

Fickian (or Case I) diffusion refers to the kinetic mechanism where the polymer relaxation time during molecular release is significantly longer than the characteristic solvent diffusion time[33]. While, in a non-Fickian diffusion mechanism, polymer relaxation time during molecule release and the characteristic solvent diffusion time are equal. Typically, matrix-type devices exhibit Fickian behavior, as it accounts for concentration gradient, diffusion distance, and the degree of swelling [34, 35].

Case II diffusion, on the other hand, refers to the dissolution of the polymeric matrix due to the relaxation of the polymer chain, which is independent of the concentration. Mean dissolution time (MDT), which is a model independent parameter characterizing active release from a matrix system, was calculated from the Sod-FS dissolution data according to Mockel and Lippold[36] using the following equation 5.4.:

$$MDT = \left(\frac{n}{n+1}\right) \cdot k^{\frac{-1}{n}} \qquad (5.4)$$

Cytotoxicity Studies of ESS

The cytotoxic effect of the molecular form of ESS was tested on L929 mouse fibroblasts. L929 mouse fibroblast cells were maintained in EMEM supplemented with 10% fetal bovine serum (FBS), penicillin (100U/mL), and streptomycin (100 µg/mL). The cells were incubated for 24h at 37°C (5% CO_2), after which, cells were trypsinized, re-suspended into fresh supplemented EMEM, and seeded into 96-well cell culture treated plates at an inoculum density of 50,000 cells/mL. The plates were incubated for 24h at 37°C (5% CO_2) and EMEM was carefully

removed using a multichannel pipette and attached cells were rinsed once with HBSS. Pure ESS solutions prepared in HBSS (0.01–100 µM) were transferred in triplicate to the rinsed, pre-cultured cells and incubated for 24 and 72h at 37°C (5% CO_2). Bright field microscopy images were acquired on an inverted microscope prior to removal of ESS containing media for cell viability assessments. After removal of spent media, cells were rinsed 3 times with HBSS.A0.5g/L solution of MTT in HBSS (0.2mL) was added to each well and incubated for 4h at 37°C. The MTT solution was removed from each well and 0.15mL of DMSO was added. The plates were placed on an orbital shaker (150rpm; ambient temperature) for 15min to solubilize the MTT dye. Absorbance values were measured at 570nm using a multi-well plate spectrophotometer, Tecan Safire 2 microplate reader (Tecan, Switzerland).

Results and Discussion

Fabrication of the Matrices

Epoxidized sucrose esters of fatty acids have been reported as platform materials for bio-based epoxy resin technology due to the presence of a compact molecular structure, multivalent epoxy group functionality, high density[25, 37]. As represented in Figure 5.1. (a) ESS, which is composed of soybean oil fatty acid esters, has been shown to form excellent cross-linked materials where the rigid core of sucrose yields a desirable mechanical property, and the presence of multiple epoxy functionalities render the materials amenable to cross-linking induced by multi-functional carboxylic acid or anhydrides[26].
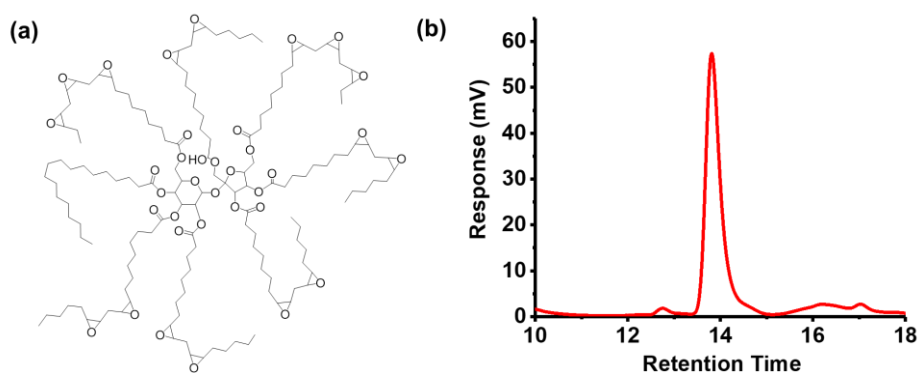
Figure 5.1. (a) Idealized structure of epoxidized sucrose soyate (ESS); (b) Gel permeation chromatograph (GPC) chromatogram of ESS

With a fairly monodispersed molecular weight of 3000 g/mol (Figure 5.1. (b)), ESS has a high content of ester linkages within its structure and curing with bio-based or natural carboxylic acids that cross-link the 3D matrix provides a mechanism for biodegradation of the scaffold and the controlled release of any incorporated active molecules.

We have utilized the CA mediated cross-linking methodology of ESS and developed a facile procedure to homogeneously disperse the hydrophilic active agent within the cross-linked matrix of ESS (Figure 5.2.). Ma et al.[26] reported the cross-linking efficiency of CA with ESS for the first time, and found out that, depending on the proton concentration, a cross-linking time of at least 20 min is required to cross-link all the epoxy groups of the sucrose ester by the acid at an equivalent molar ratio, as indicated by the measurement of gel time of the mixture. In this case, ESS-CA matrices were cured at 80°C for up to 3 h, after which the mixture formed solid, 3D, translucent thermoset matrices. The organoleptic properties of which are usually varied with the incorporation of the active ingredient and with different release modifiers (Figure 5.2.).
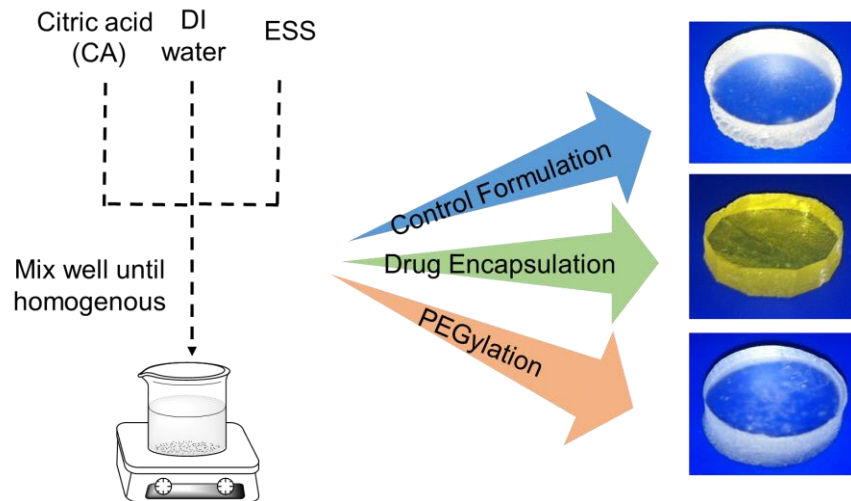
Figure 5.2. Schematic illustration of the preparation of cross-linked ESS matrix and images depicting typical ESS matrix sample with and without incorporation of guest molecules

One of the reasons for selecting citric acid to cross-link ESS epoxy group was the moderate pKa value of the acid, so that the pH of the local environment post-degradation is not altered significantly. Acidification of local pH upon degradation is one of the major problems with matrices prepared from PLGA or PLA, due to production of lactic acid on hydrolysis.[39, 40]

ATR-IR spectroscopy of a representative sample of the matrices (Figure 5.3.) demonstrates the presence of strong signals at 1750 cm^{-1}, indicating the presence of ester bonds of ESS, which is a critical structural component for ensuring biodegradation and the controlled release mechanism of the matrices.
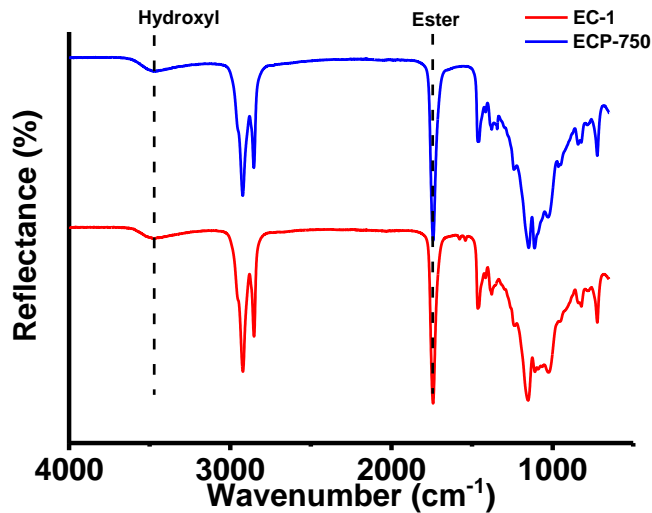
Figure 5.3. Attenuated Total Reflectance (ATR) spectra of EC-1 (control) matrix and ECP-750 (PEG modified) matrix

Surface, Micro-structural and Mechanical Property Analysis of ESS-CA Matrices

Contact angle measurement of water droplets on ESS-CA matrices indicated that the matrices have a highly hydrophobic surface. Irrespective of formulation, contact angle of matrix surfaces, which were in contact with, air were found to be within the range of 75°–80° shown in Figure 5.4 (a). The representative drop shapes of water on ESS-CA matrices is depicted in Figure 5.4. (b). Inclusion of PEG, at least in the tested weight ratio, did not change the surface hydrophobicity of matrices.
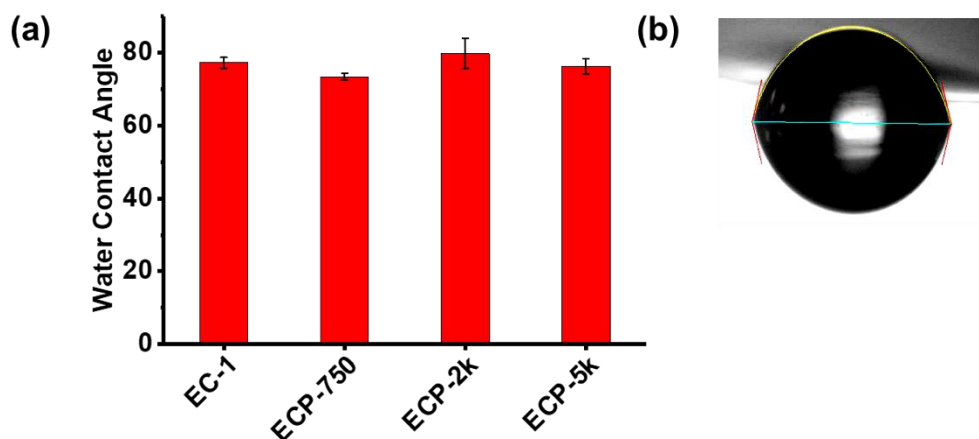
Figure 5.4. (a). Water contact angle on top surfaces of the cross-linked ESS matrices and (b). Image of typical water droplet on surface of the ESS matrix

152

Such surface hydrophobicity is significant for a matrix system, since an apolar surface will help to suppress the burst release of the active ingredient located on matrix surfaces when immersed in aqueous environment, thereby favoring more controlled release of the active substance. The internal microstructure of ESS-CA matrices was determined by capturing the SEM image of lateral cross section of matrices prepared with different formulations (Figure 5.5.).
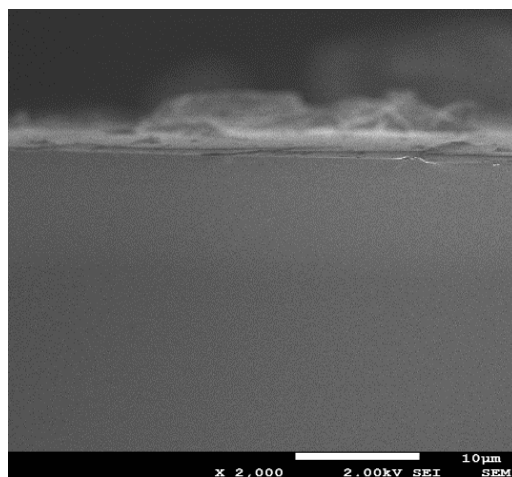
Figure 5.5. SEM Scanning electron microscopy (SEM) image of ESS-citric acid matrix loaded with Sod-FS

The SEM micrographs revealed that ESS-CA matrices alone possess a non-porous and uniform microstructure, indicating the formation of a monolithic matrix. No gross microstructural changes or defects were evident even after the addition of PEGs or Sod-FS within the matrix. SEM experiments indicated that ESS-CA matrices possess a homogenous microstructure, where the incorporated active agent is evenly distributed. Such monophasic distribution of the latter is critical for a highly controlled and monotonic release rate of the incorporated species from a macromolecular scaffold.

We have also analyzed the viscoelastic properties of different formulations of EC matrices and evaluated their loss and storage modulus as a function of the release-modifiers (i.e.,

PEGs of different molecular weights) being incorporated within the systems. We observed that

the inclusion of high molecular weight PEGs (at 5% w/w of total formulation) increases both the

loss and storage moduli of the matrices (Figure 5.6. (a)), compared to those prepared without

PEG (EC-1). Inclusion of low molecular weight PEG (i.e. 750 g/mol), decreased both the loss

and storage moduli. More crystalline structures and higher strength/modulus of the high

molecular weight PEGs are most likely to be the contributing factors for such observations,

indicating that the matrices were more visco-elastic in consistency than rubbery (Figure 5.6 (b)).
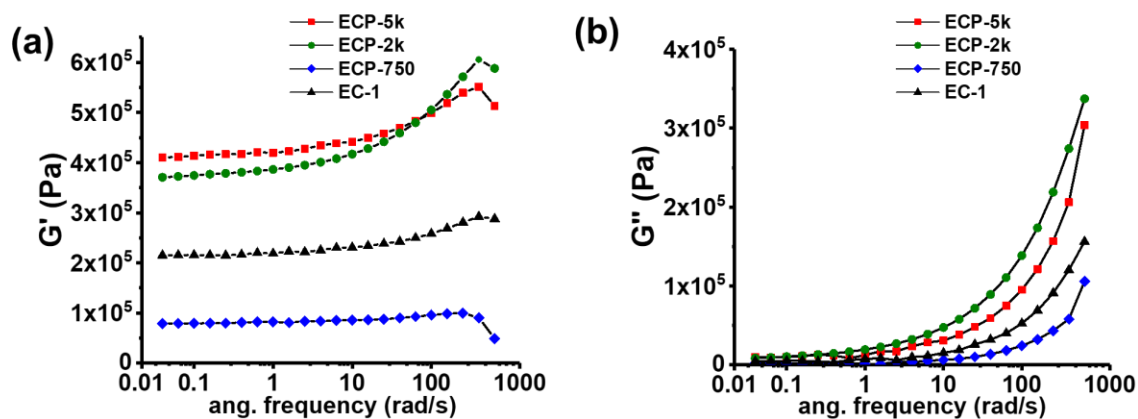
Figure 5.6. (a) G' storage modulus curves of control and PEG modified ESS citric acid matrices; (b) G" loss modulus curves of control and PEG modified ESS citric matrices

Analysis of Content Release

Active release from non-porous lipid matrices occurs through diffusion of molecules

from the polymer matrix and in some cases through erosion of the polymer matrix. The ESS-CA

based matrices designed in this study were intended for use as a molecular delivery platform,

particularly for controlling the release of small, hydrophilic active molecules for an extended

period. In clinical settings, such matrices are important for designing delivery systems for

contraceptive agents, growth factors, enzymes, analgesics, and orthopedic medications, and

antibacterial compounds. We have used Sod-FS as such a model small molecular agent for our

154

study. A tightly controlled diffusion of Sod-FS, spanning over a period of more than 20 days, was observed from all the ESS-CA derived lipid matrices.

We tested if the curing process alters the chemical functionality of the model compound. Figure 5.7. shows the UV–Vis spectral profiles of Sod-FS indicating the compatibility of the agent with matrix forming materials and processes. The signature absorption signal of Sod-FS is observed without distortions or shifting even after the 14-day release.
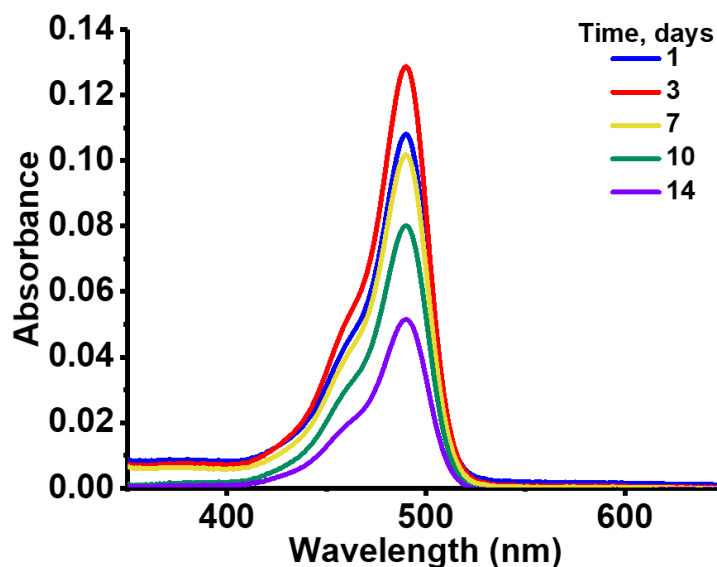
Figure 5.7. Example of absorption spectra of Sod-FS released from a typical ESS-CA matrix

The effect of acid concentration on the release profile of Sod-FS from EC matrix (EC-1 vs EC-2) is displayed in Figure 5.8. Formulations cross-linked with higher acid concentration (EC-1), released up to 70% of the FSS within 21 days, while formulations cross-linked with lower acid concentration (EC-2) released 10% less Sod-FS cumulatively within the same period. The steep increase of Sod-FS release for the first 5 days could be attributed to the Sod-FS molecules accumulated at or near the surfaces of ESS-CA matrices. However, these PEG free cross-linked ESS matrices did not show any signs of scaffold disintegration within this period. This finding is in accordance with the work carried out by Dakkuri et al.[41] with wax type

matrices. Cross-linked ESS matrices with no PEGs are extremely hydrophobic in nature with lower wettability.
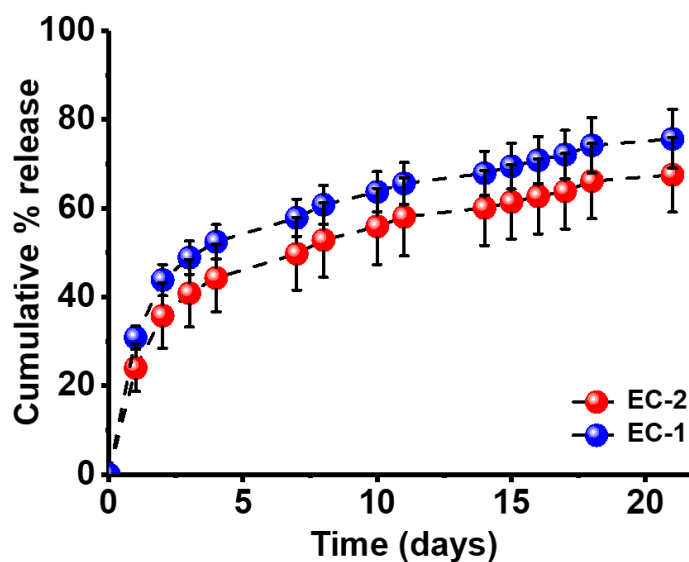
Figure 5.8. Effect of acid concentration in formulation on the release profile of Sod-FS from the ESS-CA matrices

Complete release of Sod-FS from an EC-1 or EC-2 matrix system was not possible since a certain fraction of the active molecule is always coated with impermeable hydrophobic film. In addition, it has been reported earlier that in the absence of additives, active release is oftentimes prolonged and non-linear from hydrophobic matrix systems[42]. Since our formulations contain no channeling agents, formation of pores and cracks did not occur to facilitate Sod-FS release. As a result, the water-impervious hydrophobic EC matrices showed sustained Sod-FS release for almost over a month.

A set of factors such as loading content of the active ingredient, amount, and molecular weight of PEGs that have been included as release modifiers were found to influence the release of Sod-FS from the ESS matrix. Figure 5.9. shows the amount of active loading on release rate. High drug loading led to a burst release of Sod-FS from matrices and close to 30% of the entrapped compound was released within the first 48 h from this formulation (EC-Sod-FS-H).

156

On the other hand, reducing drug loading helped formulation EC-Sod-FS-L to achieve almost a zero-order release profile liberating approximately 40% of the incorporated amount of Sod-FS over 20 days.
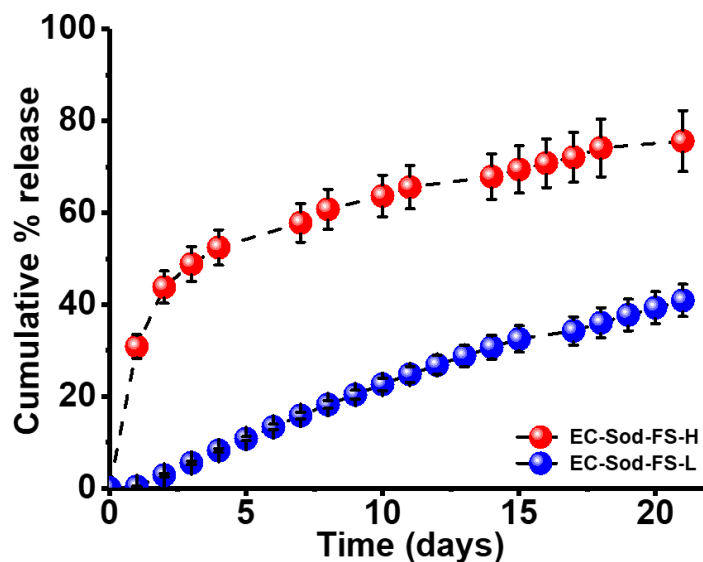
Figure 5.9. Release profile of Sod-FS indicating the effect of loading concentration

Inclusion of PEG resulted in a more uniform release of Sod-FS over extended period (>60 days) and suppressed burst release (Figure 5.10.). Extent of Sod-FS release was also found to depend on the amount of PEG included in the formulations. Inclusion of 5% w/w of PEG (5 kDa) per matrix formulation resulted in a higher amount of Sod-FS release compared to that containing 1% w/w of PEG of the similar molecular weight. The rate of Sod-FS release, if not extent, was found to depend on the molecular weight of PEGs and amount (wt. %) of PEG incorporated most likely due to the differences of aqueous solubility of PEGs of different molecular weight.
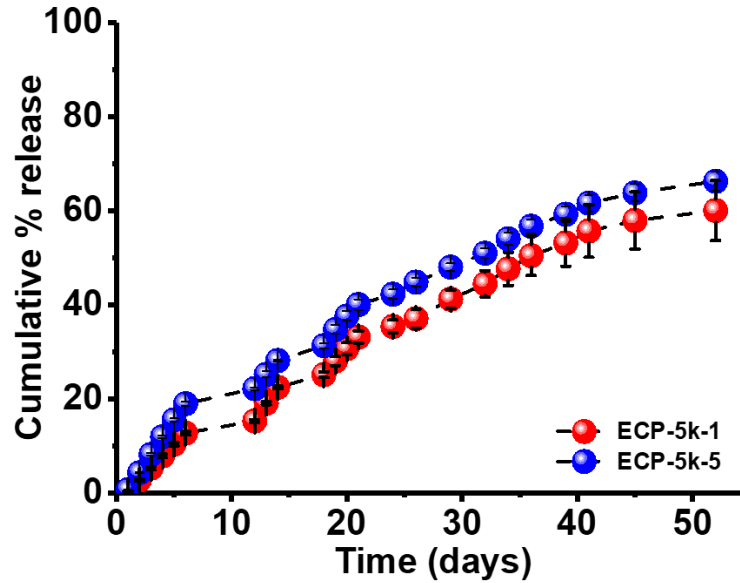
Figure 5.10. Effect of amount of PEG in a modified matrix on the release profile of Sod-FS

Release Kinetics

Mathematical models were used to determine the mechanism of solute transport from the matrices, such as Higuchi and biexponential equations (Equation (5.2) and (5.3), respectively). Linearity of Higuchi-type release kinetics (fractional release vs. square root of time) is an indicator of diffusion of the active compound occurring from a typical matrix-based system, where the active ingredient is homogenously dispersed within a consolidated polymeric phase. As evident from Figure 5.11. incorporation of high molecular weight PEGs, i.e. 2 kDa or 5 kDa, caused the release profile to follow Higuchi kinetics compared to those containing low molecular weight PEGs, or without PEGs.
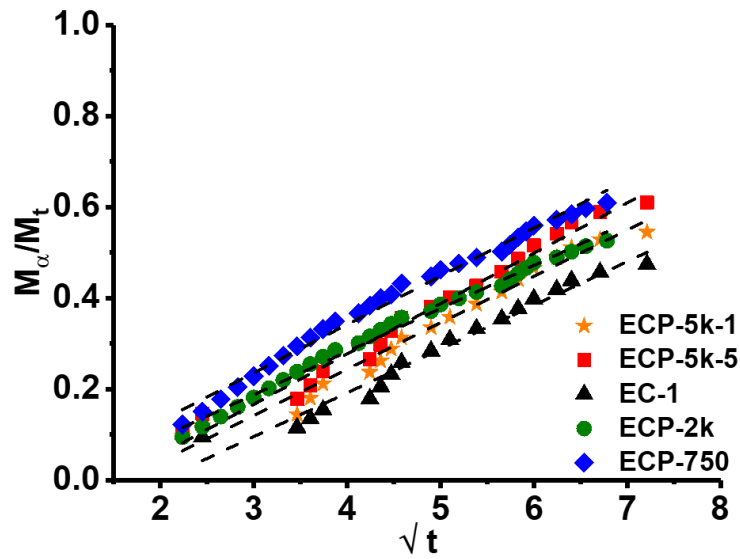
Figure 5.11. Kinetic analysis of active release from ESS matrices using Higuchi model

The fitting of the linear fraction of Sod-FS release in determined using the bi-exponential model (Equation (5.3)) are described in Figure 5.12.
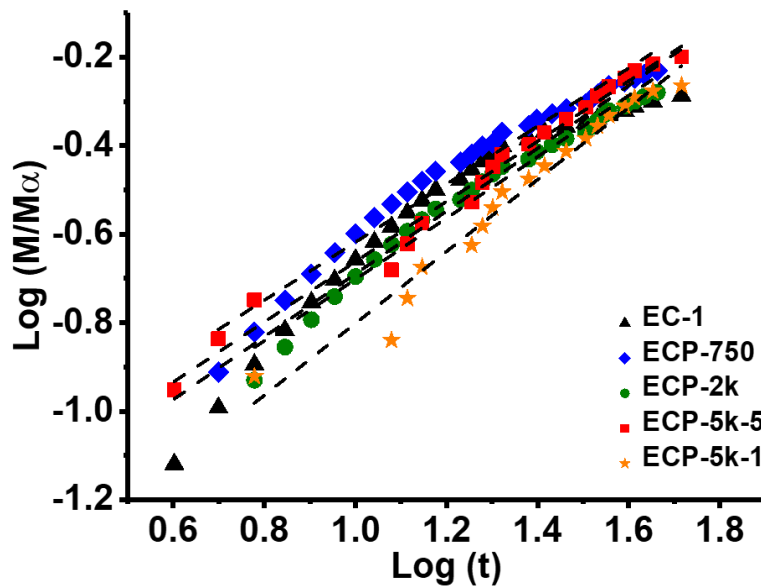
Figure 5.12. Kinetic analysis of active release from ESS matrices using bi-exponential model

Values for release exponent (n), kinetic rate constant (k) obtained using Equation (5.3) ($r^2 > 0.96$) is reported in Table 5.2. The n values obtained using the bi-exponential model also

showed that matrices composed of only ESS and CA (i.e., EC-1) exhibited non-Fickian

(anomalous) diffusion mechanism.

Table 5.2. Release Kinetics Values of The Release Exponent (n), Kinetic Constant (k) and Correlation Coefficient (r^2)

Sample	n	k	r^2
EC-1	0.87±0.05	0.02±0.003	0.97±0.004
ECP-750	0.71±0.01	0.05±0.003	0.96±0.004
ECP-2K	0.72±0.02	0.04±0.004	0.97±0.004
ECP-5K-5	0.68±0.01	0.05±0.002	0.98±0.003
ECP-5K-1	0.80±0.05	0.03±0.004	0.97±0.002

Earlier work with wax matrix systems also revealed that pure hydrophobic matrix-

forming agents oftentimes followed non-Fickian type of release behavior irrespective of physico-

chemical nature of the drug, making it difficult to draw any clear inference regarding the kinetics

of active release from such matrices[6, 42]. In our cases, the mechanism of Sod-FS release could be

attributed to the rate of fluid entry through the cracks and pores of the matrices, which initiates

the diffusion of Sod-FS out of the matrix. However, due to high hydrophobicity of the matrix

surface, such fluid entry through the matrices, was insignificant[43, 44], resulting in significant

deviation of n value from Fickian or diffusion controlled mechanisms for EC-1 formulations.

The effect of PEGs on release kinetics of Sod-FS from the hydrophobic matrices is also

evident when the release rate of the later is compared among different formulations.

Incorporation of PEG within the matrix decreases the n value towards Fickian (Case I diffusion-

controlled) behavior. The presence of PEG in the formulations increases the wettability of the

matrix surfaces, thereby contributing to diffusional component of release kinetics for a highly

water soluble active compound such as Sod-FS.

Using the intercept value (k) obtained from the bi-exponential model, mean dissolution

time (MDT) was calculated from Equation (4). MDT value is used to characterize the release rate

of the active ingredient from a delivery system and the retarding efficacy of the polymer. A

higher value of MDT indicates an efficient active retaining ability of the polymer and vice-versa.

As represented in Figure 5.13., the highest MDT value was associated with EC-1 matrices, which

does not contain any PEG (51 days), and the lowest MDT value of 30 days was found with ECP-

750 matrices containing PEG of an M_n value of 750 g/mol. Rapid diffusion of small molecular

weight PEG out of the matrix skeleton might be an attributable factor for such an observation.

Inclusion of PEGs of higher molecular weight, i.e. 2 or 5 kDa, increases the MDT value by

approximately 10 days, most likely due to molecular entanglement and swelling associated with

high molecular weight PEGs.
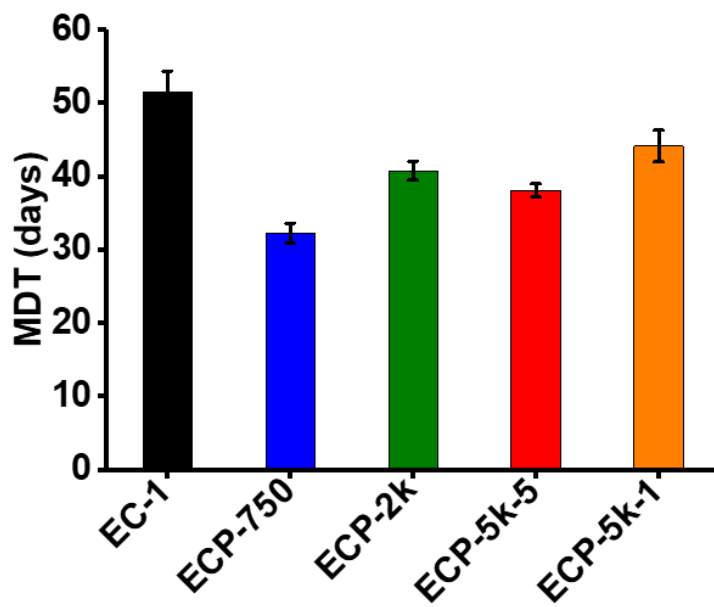
Figure 5.13. Mean dissolution time (MDT) of entrapped Sod-FS from different formulations of ESS matrixes

Cytotoxicity Assessment

Upon evaluation of the materials and kinetic properties of the ESS matrices, we

determined the biocompatibility profile of the major matrix forming agent, ESS, using L929

mouse fibroblast cells. Cells were treated with an increasing concentration of ESS for 24–72 h at

37 °C, and the cell viability was quantified at the end of the treatments using an MTT

colorimetric assay. Although epoxy functional groups were present in the ESS molecule, to our

surprise, we did not observe any severe cytotoxic effects when compared to non-treated cells

after 24 or 72 h of exposure. ESS was found to be non-toxic (>85% cell viability) at

concentrations as high as 100 μM (Figure 5.14.).
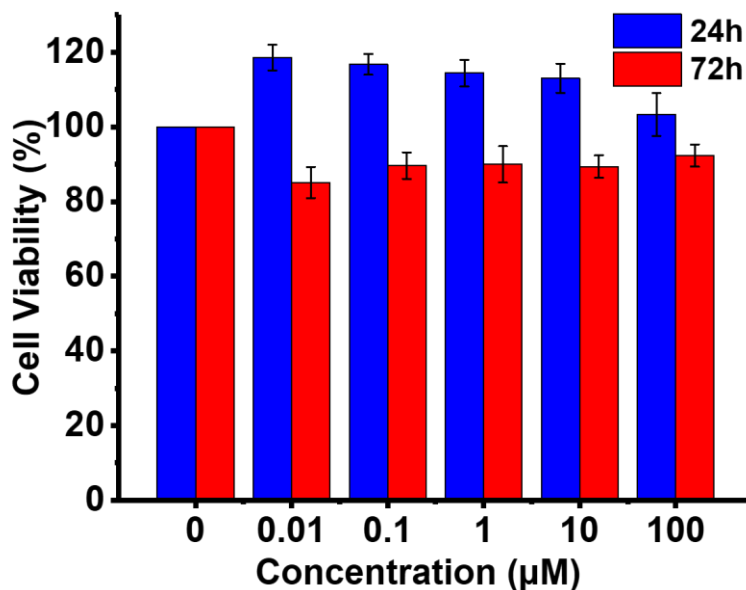
Figure 5.14. Cytotoxicity assessment of ESS in Mouse L929 fibroblast cells; after 24 and 72 h
treatment with increasing concentration of ESS

We have also evaluated the morphology of L929 fibroblast cells with bright field

microscopy (Figure 5.15.). When compared to control, no severe phenotypic or morphological

changes were evident in mouse L929 cells, indicating excellent biocompatibility of the matrix

forming materials towards mammalian cell lines. Biocompatibility of ESS is most likely due to

the very low cytotoxic potential of the molecular components of ESS, that is, soybean oil fatty

acid and sugar, which are connected through ester bonds. Hence, cellular and metabolic

degradation of ESS most likely generate non-toxic end products.
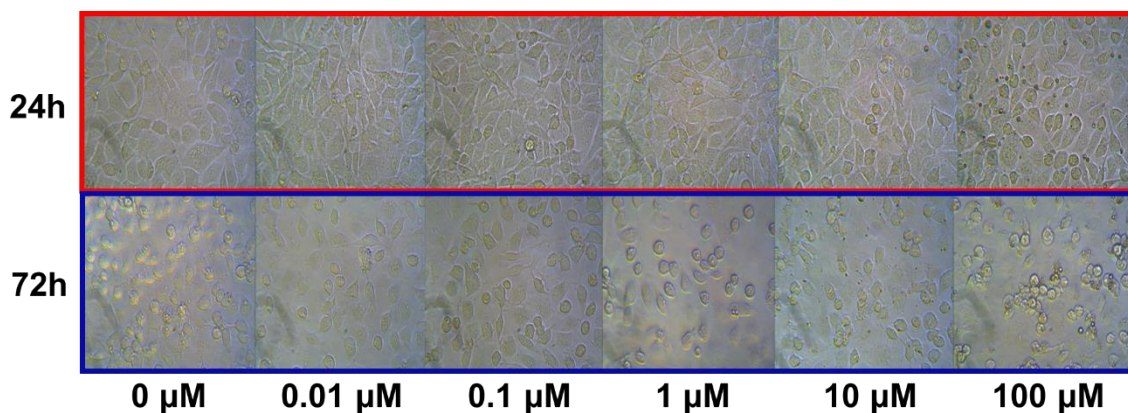
Figure 5.15. Cell morphology of mouse L929 fibroblasts as captured by Bright Field Microscopy after 24 and 72 h treatment with increasing concentration of ESS

Soy-based products, that is, hydrogenated soybean oil (NTIS accession number, PB266280) and soy protein isolate (NTIS accession number, PB300717) have long been classified as GRAS (Generally Regarded as Safe by FDA) rendering the material suitable for human use (accessdata.fda.gov).

Conclusions

We have evaluated a new bio-based material, ESS, for fabrication of controlled- and extended release matrices for water-soluble small molecules. We observed that ESS provided dual benefits of having cross-linkable epoxy groups for imparting structural rigidity and hydrolysable ester bonds suitable for biodegradation within the same molecule. Hence, it was possible to readily generate a freestanding, biocompatible, and biodegradable 3D matrix that can entrap and extend the release of a hydrophilic model substance for over a month. The mechanical and physico-chemical properties of these new matrix-forming materials have been investigated and are correlated with their molecular loading and release capacity. ESS behaves like a wax-type matrix forming material as evident from release kinetic analysis. By incorporation of release modifiers such as PEGs, it was possible to attain the diffusion-controlled release profile of the model active compound from these matrices without burst release. We envision that such

163

platform technology will find a multitude of applications, such as to design point-of-care

extended release drug and cosmetic delivery systems, and to prepare biological scaffolds.

<div align="center">

References

</div>

1.   Ulery, B. D.; Nair, L. S.; Laurencin, C. T., Biomedical applications of biodegradable

polymers. J. Polym. Sci., Part B: Polym. Phys. 2011, 49 (12), 832-864.

2.   Dash, A.; Cudworth, G., Therapeutic applications of implantable drug delivery systems.

J. Pharmacol. Toxicol. Methods 1998, 40 (1), 1-12.

3.   Rowley, J. A.; Madlambayan, G.; Mooney, D. J., Alginate hydrogels as synthetic

extracellular matrix materials. Biomaterials 1999, 20 (1), 45-53.

4.   Li, C., Poly (L-glutamic acid)–anticancer drug conjugates. Adv. Drug Delivery Rev.

2002, 54 (5), 695-713.

5.   Tibbitt, M. W.; Rodell, C. B.; Burdick, J. A.; Anseth, K. S., Progress in material design

for biomedical applications. Proc. Natl. Acad. Sci. U. S. A. 2015, 112 (47), 14444-14451.

6.   Siepmann, J.; Peppas, N., Modeling of drug release from delivery systems based on

hydroxypropyl methylcellulose (HPMC). Adv. Drug Delivery Rev. 2012, 64, 163-174.

7.   Tahara, K.; Yamamoto, K.; Nishihata, T., Overall mechanism behind matrix sustained

release (SR) tablets prepared with hydroxypropyl methylcellulose 2910. J. Controlled

Release 1995, 35 (1), 59-66.

8.   Tiwari, S. B.; Murthy, T. K.; Pai, M. R.; Mehta, P. R.; Chowdary, P. B., Controlled

release formulation of tramadol hydrochloride using hydrophilic and hydrophobic matrix

system. AAPS PharmSciTech 2003, 4 (3), 18-23.

9.   El-Sherbiny, I. M.; Yacoub, M. H., Hydrogel scaffolds for tissue engineering: Progress

and challenges. Global Cardiology Science and Practice 2013, 38.

10.   Jeong, B.; Bae, Y. H.; Kim, S. W., Drug release from biodegradable injectable thermosensitive hydrogel of PEG–PLGA–PEG triblock copolymers. J. Controlled Release 2000, 63 (1), 155-163.

11.   Natarajan, J.; Rattan, S.; Singh, U.; Madras, G.; Chatterjee, K., Polyanhydrides of castor oil–sebacic acid for controlled release applications. Ind. Eng. Chem. Res. 2014, 53 (19), 7891-7901.

12.   Chen, G.-Q.; Wu, Q., The application of polyhydroxyalkanoates as tissue engineering materials. Biomaterials 2005, 26 (33), 6565-6578.

13.   Attama, A.; Schicke, B.; Müller-Goymann, C., Further characterization of theobroma oil–beeswax admixtures as lipid matrices for improved drug delivery systems. Eur. J. Pharm. Biopharm. 2006, 64 (3), 294-306.

14.   De, C.; Vervaet, C.; Görtz, J.; Remon, J. P.; Berlo, J., Bioavailability of ibuprofen from matrix mini-tablets based on a mixture of starch and microcrystalline wax. Int. J. Pharm. 2000, 208 (1-2), 81-86.

15.   Toro-Vazquez, J.; Morales-Rueda, J.; Dibildox-Alvarado, E.; Charó-Alonso, M.; Alonzo-Macias, M.; González-Chávez, M., Thermal and textural properties of organogels developed by candelilla wax in safflower oil. J. Am. Oil Chem. Soc. 2007, 84 (11), 989-1000.

16.   Humberstone, A. J.; Charman, W. N., Lipid-based vehicles for the oral delivery of poorly water soluble drugs. Adv. Drug Delivery Rev. 1997, 25 (1), 103-128.

17.   Shogren, R. L.; Petrovic, Z.; Liu, Z.; Erhan, S. Z., Biodegradation behavior of some vegetable oil-based polymers. J. Polym. Environ. 2004, 12 (3), 173-178.

18.   Chandran, S.; Asghar, L. F.; Mantha, N., Design and evaluation of ethyl cellulose based matrix tablets of ibuprofen with pH modulated release kinetics. Indian J. Pharm. Sci. 2008, 70 (5), 596.

19.   Miao, S.; Sun, L.; Wang, P.; Liu, R.; Su, Z.; Zhang, S., Soybean oil-based polyurethane networks as candidate biomaterials: Synthesis and biocompatibility. Eur. J. Lipid Sci. Technol. 2012, 114 (10), 1165-1174.

20.   Zhang, C.; Garrison, T. F.; Madbouly, S. A.; Kessler, M. R., Recent Advances in Vegetable Oil-Based Polymers and Their Composites. Prog. Polym. Sci. 2017.

21.   Miao, S.; Wang, P.; Su, Z.; Zhang, S., Vegetable-oil-based polymers as future polymeric biomaterials. Acta Biomater. 2014, 10 (4), 1692-1704.

22.   Nelson, T. J.; Bultema, L.; Eidenschink, N.; Webster, D. C., Bio-based high functionality polyols and their use in 1K polyurethane coatings. J. Renewable Mater. 2013, 1 (2), 141-153.

23.   Guo, A.; Demydov, D.; Zhang, W.; Petrovic, Z. S., Polyols and polyurethanes from hydroformylation of soybean oil. J. Polym. Environ. 2002, 10 (1), 49-52.

24.   List, G.; Neff, W.; Holliday, R.; King, J.; Holser, R., Hydrogenation of soybean oil triglycerides: Effect of pressure on selectivity. J. Am. Oil Chem. Soc. 2000, 77 (3), 311-314.

25.   Pan, X.; Sengupta, P.; Webster, D. C., High biobased content epoxy–anhydride thermosets from epoxidized sucrose esters of fatty acids. Biomacromolecules 2011, 12 (6), 2416-2428.

26.   Ma, S.; Webster, D. C., Naturally occurring acids as cross-linkers to yield VOC-free, high-performance, fully bio-based, degradable thermosets. Macromolecules 2015, 48 (19), 7127-7137.

27.   Lligadas, G.; Ronda, J. C.; Galià, M.; Cádiz, V., Poly (ether urethane) networks from renewable resources as candidate biomaterials: synthesis and characterization. Biomacromolecules 2007, 8 (2), 686-692.

28.   Kolanthai, E.; Sarkar, K.; Meka, S. R. K.; Madras, G.; Chatterjee, K., Copolyesters from soybean oil for use as resorbable biomaterials. ACS Sustainable Chem. Eng. 2015, 3 (5), 880-891.

29.   Yang, J.; Webb, A. R.; Pickerill, S. J.; Hageman, G.; Ameer, G. A., Synthesis and evaluation of poly (diol citrate) biodegradable elastomers. Biomaterials 2006, 27 (9), 1889-1898.

30.   Yang, J.; Webb, A. R.; Ameer, G. A., Novel citric acid-based biodegradable elastomers for tissue engineering. Adv. Mater. 2004, 16 (6), 511-516.

31.   Reza, M. S.; Quadir, M. A.; Haider, S. S., Comparative evaluation of plastic, hydrophobic and hydrophilic polymers as matrices for controlled-release drug delivery. J Pharm Pharm Sci 2003, 6 (2), 282-91.

32.   Hakim, M.; Jalil, R., Evaluation of a New Rate Retarding Polymer Kollidon SR as Matrix Tablets. M. Pharm thesis, DU, Bangladesh 2001.

33.   Fu, Y.; Kao, W. J., Drug release kinetics and transport mechanisms of non-degradable and degradable polymeric delivery systems. Expert opinion on drug delivery 2010, 7 (4), 429-444.

34.   Siepmann, J.; Siepmann, F., Mathematical modeling of drug delivery. Int. J. Pharm. 2008, 364 (2), 328-343.

35.   Siepmann, J.; Göpferich, A., Mathematical modeling of bioerodible, polymeric drug delivery systems. Adv. Drug Delivery Rev. 2001, 48 (2-3), 229-247.

36.   Möckel, J. E.; Lippold, B. C., Zero-order drug release from hydrocolloid matrices. Pharm. Res. 1993, 10 (7), 1066-1070.

37.   Pan, X.; Sengupta, P.; Webster, D. C., Novel biobased epoxy compounds: epoxidized sucrose esters of fatty acids. Green Chem. 2011, 13 (4), 965-975.

38.   Kitchell, J. P.; Wise, D. L., [32] Poly (lactic/glycolic acid) biodegradable drug—polymer matrix systems. Methods Enzymol., Elsevier: 1985; 112, 436-448.

39.   Lasprilla, A. J.; Martinez, G. A.; Lunelli, B. H.; Jardini, A. L.; Maciel Filho, R., Poly-lactic acid synthesis for application in biomedical devices—A review. Biotechnol. Adv. 2012, 30 (1), 321-328.

40.   Dakkuri, A.; Schroeder, H. G.; Deluca, P. P., Sustained release from inert wax matrixes II: Effect of surfactants on tripelennamine hydrochloride release. J. Pharm. Sci. 1978, 67 (3), 354-357.

41.   Lordi, N. G., Sustained release dosage forms. The theory and practice of industrial pharmacy 1986, 3, 430-456.

42.   Siepmann, J.; Siepmann, F., Modeling of diffusion controlled drug delivery. J. Controlled Release 2012, 161 (2), 351-362.

43.   Schwartz, J. B.; Simonelli, A. P.; Higuchi, W. I., Drug release from wax matrices I. Analysis of data with first-order kinetics and with the diffusion-controlled model. J. Pharm. Sci. 1968, 57 (2), 274-277.

44.   Schwartz, J. B.; Simonelli, A. P.; Higuchi, W. I., Drug Release from Wax Matrices II: Application of a Mixture Theory to the Sulfanilamide–Wax System. J. Pharm. Sci. 1968, 57 (2), 278-282.

CHAPTER 6. OVERALL CONCLUSIONS

The goal of this work was to develop and characterize a new set of biomaterials from sucrose soyates. Biomaterials serves as interventional tools in medicine to treat, improved or replace diseased tissues, organs or bodily functions. Biobased feedstock are an exciting new avenue to design and generate new value-added materials from renewable resources amenable for biomedical or pharmaceutical applications. Plant-oil derivatives such as sucrose soyates are very promising candidates to obtain biomaterials with a new form and enhanced function. In this work, three groups of biomaterials were fabricated from sucrose soyate derivatives: i). Soysomes, stable nanoparticles of MSSP, ii). Flexible, free-standing, MSSP blended films and iii). Three-dimensional cross-linked ESS matrix. All these soy-based materials were evaluated for application as platforms for molecule transport (delivery systems).

The first group, soy-based nano-constructs obtained from the self-assembly of MSSP. MSSP nanoparticles, termed Soysomes, were prepared using a facile nanoprecipitation (solvent-shifting) method without the aid of surfactants. Soysomes were characterized and classified as stable, surfactant-free, lipid-based nanostructures with particle sizes suitable for use in a biological system. We demonstrated, both experimentally and computationally, that parameters such as solvent type, solvent to water ratio, polymer concentration and polymer-solvent interactions control the size and polydispersity of the resulting nanoparticles. Soysomes were found to be stable under different pH, temperature or simulated biological conditions as well exhibited long-term storage stability. These soy-based nano-dispersions were capable of encapsulating and releasing hydrophobic active pharmaceutical agents such as Paclitaxel and Curcumin. In vitro cell studies showed that Soysomes were nontoxic yet increased the bioavailability of encapsulated drugs demonstrated by the increased cytotoxic efficacy of

curcumin in pancreatic cancer cell lines. This work puts forward MSSP as a suitable candidate for a sustainable biomaterial platform for synthesizing nanocarriers with an enhanced stability and potential controlled-release performance.

To demonstrate the versatility of sucrose soyate, free-standing flexible films were prepared from a blend with MSSP and PCL. Flexible free-standing films are attractive substrate for applications such as drug delivery, tissue engineering, and wound healing. The dimensions and mechanical properties of the films makes them ideal for use around soft tissues or irregular shaped organs. Incorporating MSSP into the PCL formulations resulted in films with enhanced flexibility, higher susceptibility to enzymatic degradation while maintaining the thermal stability. Layer-by-layer coating deposition technique was employed to load anti-cancer drug, doxorubicin, creating multi-layered drug-loaded MSSP composite films. MSSP increased the surface affinity of the composite film resulting in higher loading efficiency than standard PCL films. Drug release from the films was diffusion-controlled which is ideal for applications requiring localized delivery. MSSP is a promising sustainable candidate for preparing two-dimensional valuable biomaterials.

Finally, three-dimensional cross-linked soy-based matrices were formed by crosslinking Epoxidized sucrose Soyate and natural carboxylic acid, citric acid. This soy-based cross-linked matrix was fabricated for applications as a controlled- and extended release depot-type system for water-soluble small molecules. The matrix possesses the potential for application as an extended-release platform demonstrated by the retarded, multi-month, release of an entrapped hydrophilic model substance. Within the matrix, ESS plays a dual role; providing the benefits of having cross-linkable epoxy groups for imparting structural rigidity and hydrolysable ester bonds suitable for biodegradation. Mechanical and physico-chemical properties of these new matrix-

171

forming materials were investigated and correlated to loading capacity and release profile. ESS matrix performs in a similar fashion as a wax-type or solid-lipid matrix evidenced by its release kinetics. Incorporation of release modifiers such as polyethylene glycol (PEG) modulated the diffusion-controlled mechanism for release, without inducing rapid 'burst' release. The ESS cross-linked matrix is a promising technology, which could have a multitude of applications, particularly in extending release and increasing the residence life of notorious water-soluble drugs, which are cleared too quickly from the biological system before achieving adequate therapeutic effect.

Overall, sucrose soyates offer the promise of non-toxicity, biocompatibility, biodegradability, affordability, abundance and tenability of properties, which make them fascinating potential biomaterials to frontier new horizons in modern medicine.

CHAPTER 7. FUTURE DIRECTION

PEGylation of Soysomes

Hydrophobic and charged particles have been reported to be particularly more vulnerable to undergo opsonization, i.e. marked for destruction and elimination by phagocytes. MSSP nanoparticles, Soysomes have a negative zeta potential implying an overall negative surface charge. Therefore, the likelihood for lipid-based nanoparticles to be opsonized needs to be addressed. Researchers have investigated surface modification using hydrophilic polymers as a strategy to prolong the circulation half-life of the hydrophobic nanocarriers via rendering them "stealth". The most frequently employed polymer to produce stealth nanoparticles is PEG. The neutral, flexible, and hydrophilic PEG chains coat the surface of the nanoparticles creating a barrier that reduces the adhesion of opsonins (antibodies or substances that bind to exogenous materials in the body making them more susceptible to phagocytosis).[1-8]

Preparation of PEG-based Nanoparticles

PEGylated Soysomes (MSSP nanoparticles) could achieved by chemical modification of MSSP macromolecule to achieve covalently attached PEG chains or using interactive forces to associate PEG fragments with the Soysomes. The latter is a facile approach and achievable with PEG-fatty acid (PEG-FA) conjugates. PEG-FA conjugates exhibit self-assembling behavior and expected to interact with Soysomes forming hybrid nanostructures.[9, 10] The hydrophobic FA chains will orient towards the core of Soysomes with some interactions with the fatty acid chains of MSSP, while the PEG segments will form the outer shell (Figure 7.1.).
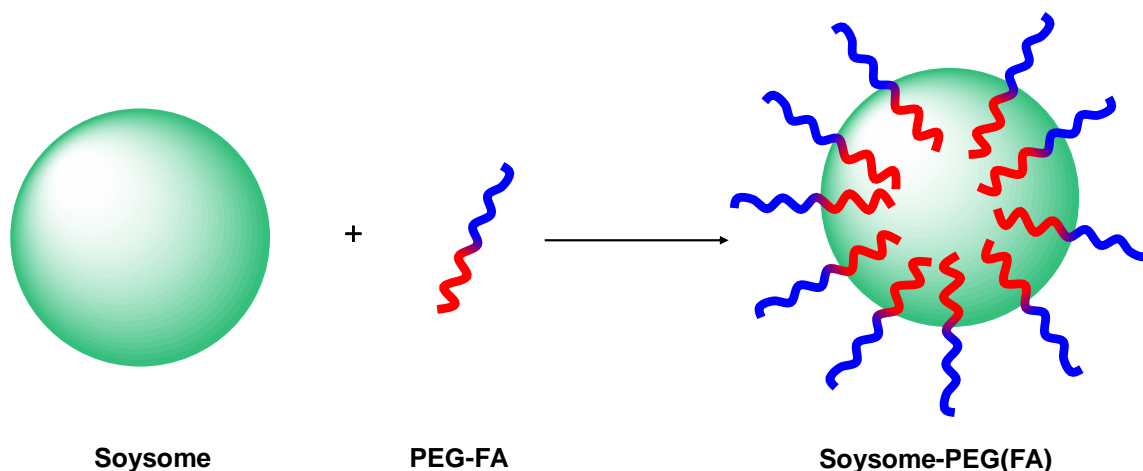
Figure 7.1. Schematic illustration of the idealized interaction between Soysomes and PEG-FA conjugates

Synthesis of PEG-Fatty Acid Conjugates

PEG-fatty acid conjugates will be prepared by conjugating fatty acids of butyric acid (BA), Decanoic acid (DA), palmitic acid (PA) and oleic acid (OA) with amine groups of mPEG-NH$_2$. The fatty acids (FA) will be conjugated using DCC as a coupling agent (Figure 7.2); FA (1.2 mmol), DCC (1.2 mmol), NHS (1.2 mmol) and mPEG-NH$_2$ (1 mmol) will be dissolved separately in chloroform. The DCC-chloroform solution will be added to the FA-chloroform solution and stirred for 30 min at room temperature to activate the FA carboxyl group. The NHS solution will be added to the activated FA solution, and the reaction allowed to stir for 12 h at room temperature. By-product, dicyclohexylurea (DCU) will be formed during the reaction and can be removed from the reaction mixture by filtration. The mPEG-NH$_2$ solution will be added to the FA reaction mixture and stirred for 30 min to complete the conjugation of activated FA and mPEG-NH$_2$. The resulting solution will be dialyzed against distilled water using benzoylated dialysis tubing MWCO 1200 (Sigma-Aldrich) for 3 days. The dialyzed solution will be lyophilized and purified by dissolving the product in THF and dialyzing against

distilled water for 24 h then lyophilizing again. The final PEG-FA conjugate can be stored in at
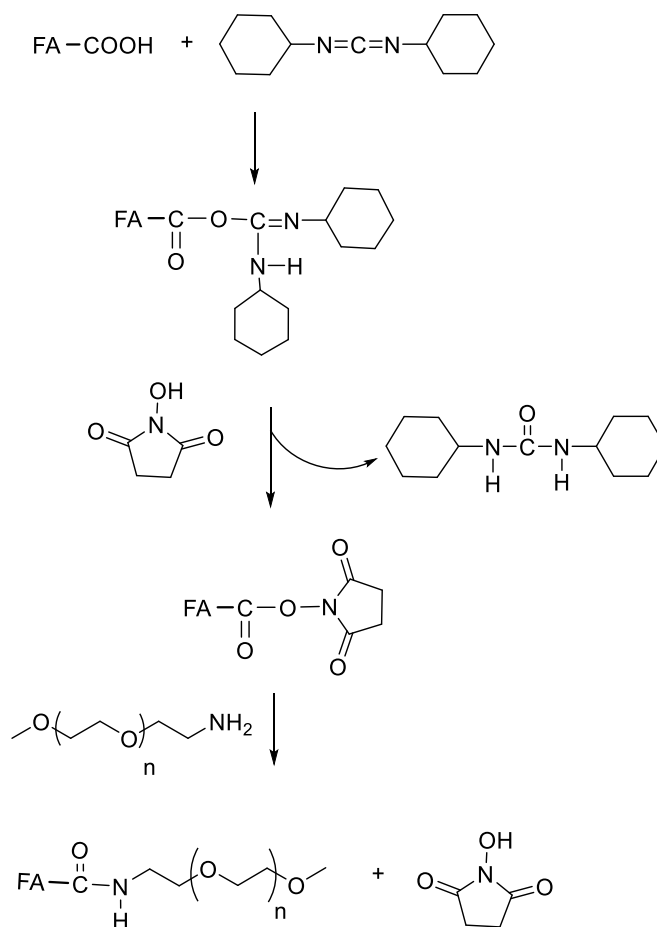
4°C.

Figure 7.2. Reaction scheme for PEG-fatty acid conjugation via DCC coupling

PEGylation of MSSP Nanoparticle using Dock and Lock Approach

PEGylated Soysomes (Soysomes-PEG-FA) will be prepared via dock and lock approach.

Respective PEG-FA will be dissolved separately in DMF to achieve a series of concentrations.

Similarly, MSSP will be dissolved in DMF to achieve 10mg/mL solution. MSSP and PEG-fatty

acid solutions will be mixed together and stirred for 30 min. The mixture will be added dropwise

to water (1:3, organic solvent: water ratio) at a 0.2mL/min addition rate. The resulting

suspension will be dialyzed against DI water for 24 h at room temperature and stored at 4°C for

later use.

Preliminary Data

PEGylated Soysomes were prepared from the conjugates of fatty acids of various chain lengths and mPEG-NH$_2$. Particles were characterized using DLS and TEM.

TEM

TEM micrographs shows a change in particle morphology in the PEGylated soysomes (Figure 7.3 (a)) in comparison to pure Soysomes, which was attributed to the presence to PEG in the hybrid system. Soysomes-PEGs (Figure 7.3. (b) and (c)) formed secondary aggregates (clusters) of particles; similar observation was made in PEG-PLGA particles (Figure 7.3. (d)). Additionally, the nanoparticle shape was altered from spherical in Soysomes, to irregular flattened disc shaped.
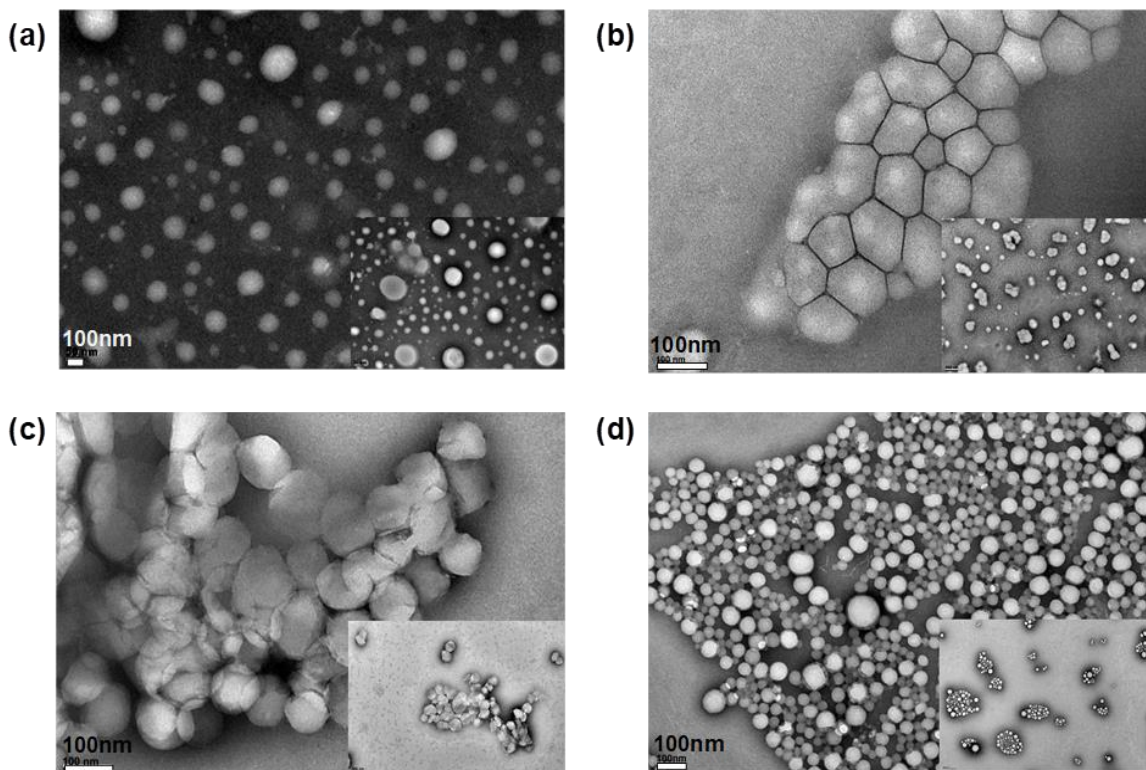

Figure 7.3. TEM micrographs of (a). Soysomes, (b) Soysomes-PEG (PA), (c) Soysomes-PEG (OA) and PEG-PLGA nanoparticles.

DLS analysis shows monomodal distribution profile (Figure 7.4.) as well as narrow distribution as indicated by the low PDI (Table 7.1.) for both pure Soysomes and the PEGylated Soysomes.
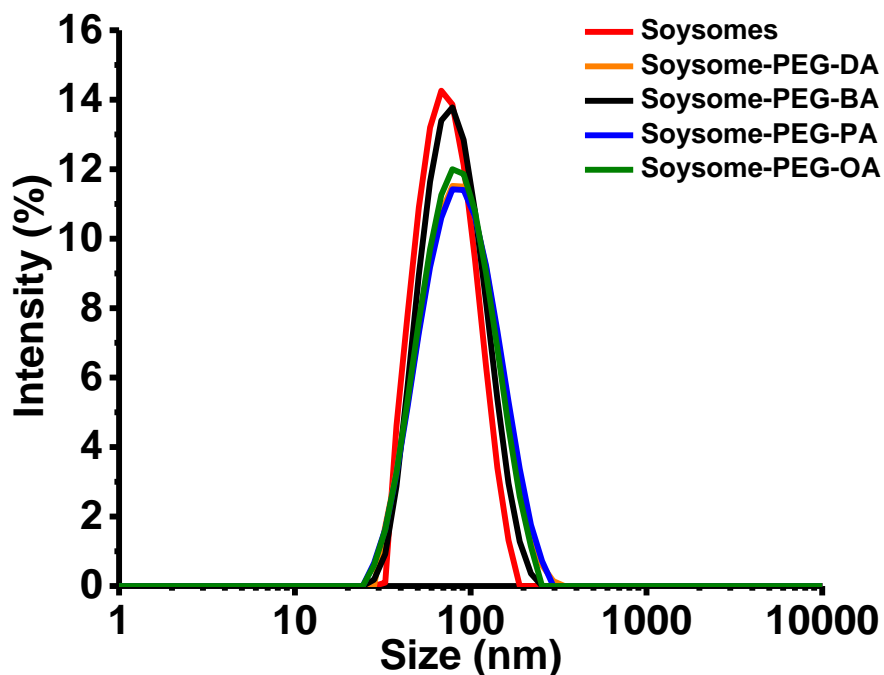

Figure 7.4. Particle size distribution profile of Soysomes and PEGylated Soysomes

The particle size (Table 7.1.) of the hybrid nanoparticles remained within size range ideal for use in biological systems. A marked increase upward of 15 nm was observed from the pure Soysomes size at 75.61 nm ±1.16 nm, to the PEGylated Soysomes. However, particle size was found to be independent of chain length. The difference in size observed did not follow distinct trend.

Table 7.1. Particle Sizes and Polydispersity Indices of Soysomes and PEGylated Soysomes

Nanoparticles Sample	No. Carbons in FA chain	PDI	Size, nm
Soysomes		0.13 ± 0.02	75.6 ± 1.2
Soysomes -PEG-BA	4	0.16 ± 0.02	99.5 ± 25.8
Soysomes -PEG-DA	10	0.19 ± 0.01	94.7 ± 2.4
Soysomes -PEG-PA	16	0.19 ± 0.01	96.2 ± 2.2
Soysomes -PEG-OA	18	0.20 ± 0.01	90.8 ± 0.8

177

Electro Responsive Flexible MSSP Blended Films

A new generation of Biobased biomaterials can be designed to render these platforms "smart" or stimuli-responsive targeted at medical and diagnostic applications. Incorporation of stimuli responsive components into implantable or reservoir type delivery systems is a new pathway for innovations in programmable or on-demand drug release (Figure 7.5).
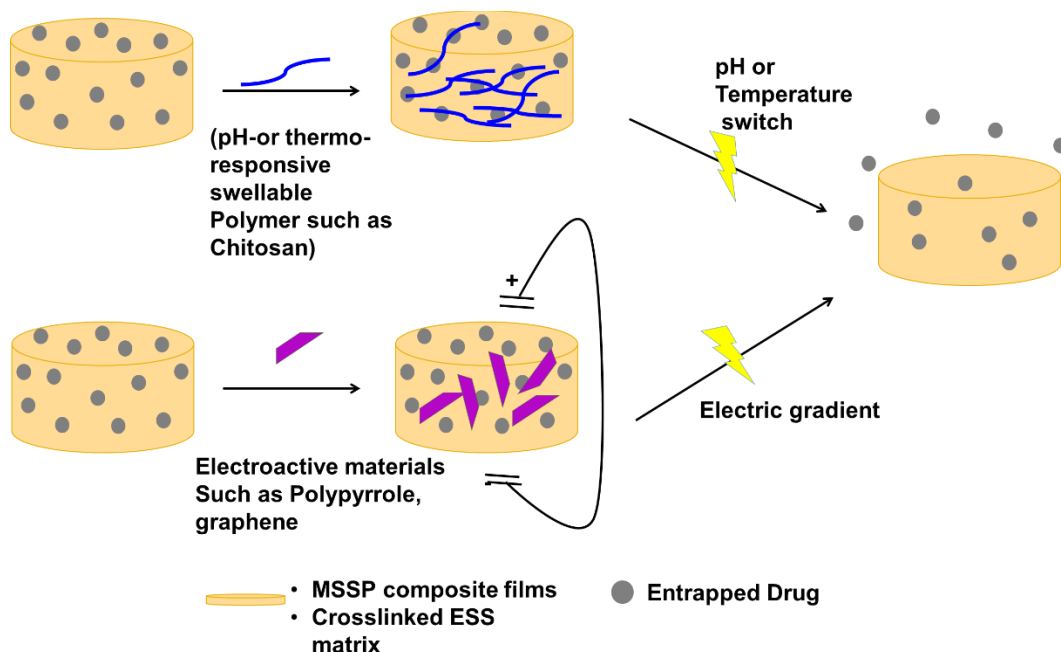

Figure 7.5. Conceptualized illustration of the design and fabrication of stimuli responsive 2D or 3D soy-based delivery platform for on-demand drug delivery

Stimuli responsive delivery systems can be designed to have better-controlled release, programmed dosing, allow repeatability, convenient for both patients and medical providers. Various external stimuli such pH gradient, temperature change, magnetic fields and electric gradient have been studied as means to modulated drug release.[11-23] This is highly important particularly in treatment of complex conditions such as cancer where therapeutic candidates are potent and highly toxic even towards healthy cells in the patient. Modulated release can be programmed to release loaded cargo under specific microenvironment or stimulated conditions.

Fabrication of Electro Conductive MSSP-PCL Blended Films

Electro conductive MSSP composite films incorporating polypyrrole (PPy) into the polymer matrix forming an interpenetrating network according to previously reported protocol.[18, 24] Briefly, a solution of pyrrole (0.084 M) and p-toluene sulfonyl chloride (0.014 M) will be prepared in water. MSSP composite films will be incubated in solution for 1 h at room temperature followed by the addition of ferric chloride (0.228M). The resulting mixture will be incubated at 4 °C for 24 h, after which the MSSP-PPy films will be rinsed with DI water and allowed to air dry prior to subsequent testing. To generate drug-eluting stimuli responsive films, the MSSP-PPy films will be coated with drug-loaded polyelectrolyte solution via layer-by-layer (charge-by-charge) assembly.

Evaluation of On-demand Drug Release

Galvanostatic electrical stimulation will be used to release loaded cargo. An electrochemical analyzer will be set up with two platinum electrodes connected, one serving as both counter and reference electrode and the other as the working electrode. Drug-loaded films of specified dimension will be immersed in a determine volume of release medium (PBS pH 7.4, 10 mM ionic strength); which will also serve as the electrolyte solution. When the electrodes are placed in the electrolyte solution a constant current will be applied for a noted period such as 5 min at every 30 min interval. Aliquots of release medium will be withdrawn after each galvanostatic scan and replaced with fresh media. As a control, a typical diffusion-controlled release experiment will be performed in the absence of electric stimulation.

Preliminary Data

The incorporation of electro conductive polymer polypyrrole via the formation of an interpenetrating network with MSSP composite film was confirmed using XPS and TEM. The

binding energy curve obtained from XPS (Figure 7.6.) shows the presence of a peak

corresponding to 1s nitrogen binding energy (~400eV) in the films containing polypyrrole which
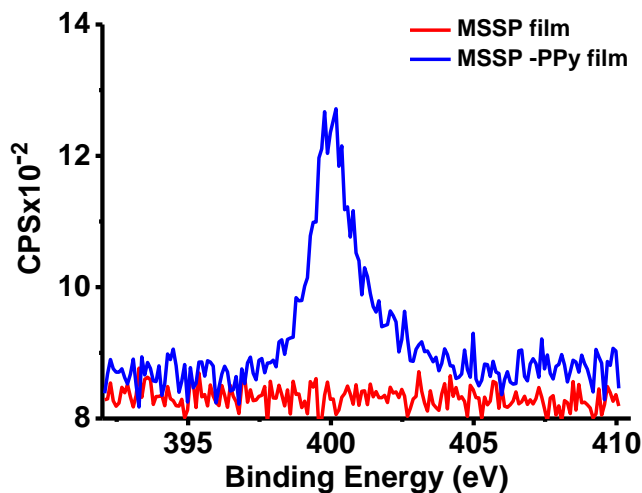
was absent in the neat MSSP composite films.

Figure 7.6. Binding energy curve fits for MSSP composite films and MSSP-PPy composite films using nitrogen excitation

The incorporation of polypyrrole in the films was confirmed by TEM. TEM micrographs

show polypyrrole microstructures within the pores within the MSSP-PPY film (Figure 7.7.),

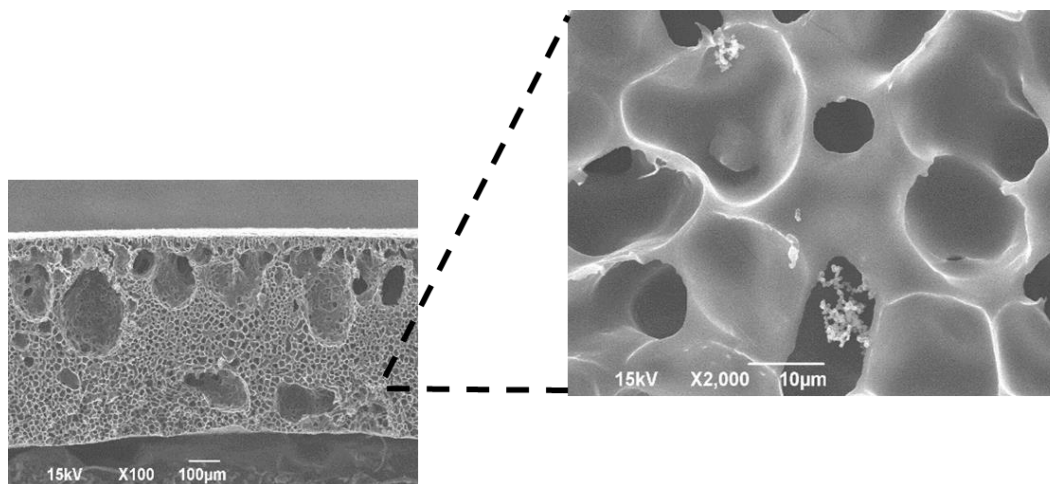which were previous absent in neat MSSP 50% composite films (Figure7.8).

Figure 7.7. Cross-sectional TEM micrograms of incorporation of PPy in the pores of the MSSP-blended films
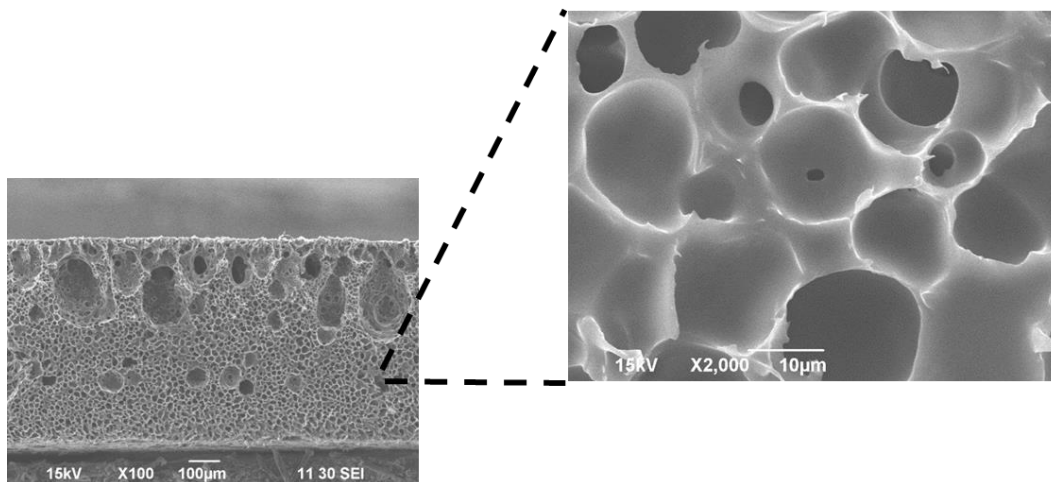
Figure 7.8. Cross-sectional TEM micrograms neat MSSP 50% films without any PPY

Conclusions

Surface modification is a useful strategy to modify and introduce new functionality to a material. Soysomes like other hydrophobic and charged particles, are vulnerable to undergo opsonization. However, PEGylation can be applied to overcome this challenge. PEGylated Soysomes can be prepared via the interaction of PEG-fatty acid conjugates and Soysomes forming new self-assembled structures. . Preliminary results show that incorporation of PEG into the soysomes alters the morphological behavior of the nanoparticles; however, all new nanoassemblies have particles size still within the 70-150nm range. Introducing hydrophilic component to the Soysomes could prolongs the circulation half-life of these hydrophobic nanocarriers. On the other hand, surface modification can be applied to yield new properties. Polymerization of pyrrole on the surface of MSSP-PCL blended films is a way to introduce an electro conductive component into the films. Electro conductivity will render the films 'smart' allowing for controlled 'on-demand' or stimuli-induced response. Preliminary data shows polypyrrole can be successfully incorporated into MSSP and PCL as confirmed by XPS and TEM.

References

1. Pelaz, B.; del Pino, P.; Maffre, P.; Hartmann, R.; Gallego, M.; Rivera-Fernandez, S.; de la Fuente, J. M.; Nienhaus, G. U.; Parak, W. J., Surface functionalization of nanoparticles with polyethylene glycol: effects on protein adsorption and cellular uptake. ACS nano 2015, 9 (7), 6996-7008.

2. Salmaso, S.; Caliceti, P., Stealth properties to improve therapeutic efficacy of drug nanocarriers. J. Drug Delivery 2013, 2013.

3. Moghimi, S. M.; Szebeni, J., Stealth liposomes and long circulating nanoparticles: critical issues in pharmacokinetics, opsonization and protein-binding properties. Prog. Lipid Res. 2003, 42 (6), 463-478.

4. Norman, M.; Williams, P.; Illum, L., Human serum albumin as a probe for surface conditioning (opsonization) of block copolymer-coated microspheres. Biomaterials 1992, 13 (12), 841-849.

5. Roser, M.; Fischer, D.; Kissel, T., Surface-modified biodegradable albumin nano-and microspheres. II: effect of surface charges on in vitro phagocytosis and biodistribution in rats. Eur. J. Pharm. Biopharm. 1998, 46 (3), 255-263.

6. Owens III, D. E.; Peppas, N. A., Opsonization, biodistribution, and pharmacokinetics of polymeric nanoparticles. Int. J. Pharm. 2006, 307 (1), 93-102.

7. Parr, M. J.; Ansell, S. M.; Choi, L. S.; Cullis, P. R., Factors influencing the retention and chemical stability of poly (ethylene glycol)-lipid conjugates incorporated into large unilamellar vesicles. Biochimica et Biophysica Acta (BBA)-Biomembranes 1994, 1195 (1), 21-30.

8. Allen, T. M., Long-circulating (sterically stabilized) liposomes for targeted drug delivery. Trends Pharmacol. Sci. 1994, 15 (7), 215-220.

9. Lee, J.-H.; Jung, S.-W.; Kim, I.-S.; Jeong, Y.-I.; Kim, Y.-H.; Kim, S.-H., Polymeric nanoparticle composed of fatty acids and poly (ethylene glycol) as a drug carrier. Int. J. Pharm. 2003, 251 (1-2), 23-32.

10. Sahu, A.; Bora, U.; Kasoju, N.; Goswami, P., Synthesis of novel biodegradable and self-assembling methoxy poly (ethylene glycol)–palmitate nanocarrier for curcumin delivery to cancer cells. Acta Biomater. 2008, 4 (6), 1752-1761.

11. Yi, Y.; Sun, J.; Lu, Y.; Liao, Y., Programmable and on-demand drug release using electrical stimulation. Biomicrofluidics 2015, 9 (2), 022401.

12. Qiu, Y.; Park, K., Environment-sensitive hydrogels for drug delivery. Adv. Drug Delivery Rev. 2001, 53 (3), 321-339.

13. Okano, T.; Bae, Y.; Jacobs, H.; Kim, S., Thermally on-off switching polymers for drug permeation and release. J. Controlled Release 1990, 11 (1-3), 255-265.

14. Derfus, A. M.; von Maltzahn, G.; Harris, T. J.; Duza, T.; Vecchio, K. S.; Ruoslahti, E.; Bhatia, S. N., Remotely triggered release from magnetic nanoparticles. Adv. Mater. 2007, 19 (22), 3932-3936.

15. Zachkani, P.; Jackson, J.; Pirmoradi, F.; Chiao, M., A cylindrical magnetically-actuated drug delivery device proposed for minimally invasive treatment of prostate cancer. RSC Adv. 2015, 5 (119), 98087-98096.

16. Pirmoradi, F. N.; Jackson, J. K.; Burt, H. M.; Chiao, M., A magnetically controlled MEMS device for drug delivery: design, fabrication, and testing. Lab on a Chip 2011, 11 (18), 3072-3080.

17. Pirmoradi, F. N.; Jackson, J. K.; Burt, H. M.; Chiao, M., On-demand controlled release of docetaxel from a battery-less MEMS drug delivery device. Lab on a Chip 2011, 11 (16), 2744-2752.

18. Spearman, B. S.; Hodge, A. J.; Porter, J. L.; Hardy, J. G.; Davis, Z. D.; Xu, T.; Zhang, X.; Schmidt, C. E.; Hamilton, M. C.; Lipke, E. A., Conductive interpenetrating networks of polypyrrole and polycaprolactone encourage electrophysiological development of cardiac cells. Acta Biomater. 2015, 28, 109-120.

19. Schmidt, D. J.; Moskowitz, J. S.; Hammond, P. T., Electrically triggered release of a small molecule drug from a polyelectrolyte multilayer coating. Chem. Mater. 2010, 22 (23), 6416-6425.

20. Wood, K. C.; Zacharia, N. S.; Schmidt, D. J.; Wrightman, S. N.; Andaya, B. J.; Hammond, P. T., Electroactive controlled release thin films. Proc. Natl. Acad. Sci. U. S. A.2008, 105 (7), 2280-2285.

21. Maloney, J. M.; Uhland, S. A.; Polito, B. F.; Sheppard Jr, N. F.; Pelta, C. M.; Santini Jr, J. T., Electrothermally activated microchips for implantable drug delivery and biosensing. J. Controlled Release 2005, 109 (1-3), 244-255.

22. Boulmedais, F.; Tang, C. S.; Keller, B.; Vörös, J., Controlled electrodissolution of polyelectrolyte multilayers: a platform technology towards the surface-initiated delivery of drugs. Adv. Funct. Mater. 2006, 16 (1), 63-70.

23. Pavlukhina, S.; Lu, Y.; Patimetha, A.; Libera, M.; Sukhishvili, S., Polymer multilayers with pH-triggered release of antibacterial agents. Biomacromolecules 2010, 11 (12), 3448-3456.

24. Lee, J. Y.; Bashur, C. A.; Goldstein, A. S.; Schmidt, C. E., Polypyrrole-coated electrospun PLGA nanofibers for neural tissue applications. Biomaterials 2009, 30 (26), 4325-4335.